AIR ENTRAINMENT IN VERTICAL SHAFTS

by
Dayantha S. Wijeyesekera,
D.E.C., A.M.I.C.E., M.I.A.H.R.

A THESIS SUBMITTED
FOR THE DEGREE OF
DOCTOR OF PHILOSOPHY
UNIVERSITY OF EDINBURGH
1969.

Typical Drop Shaft Intake Scheme.

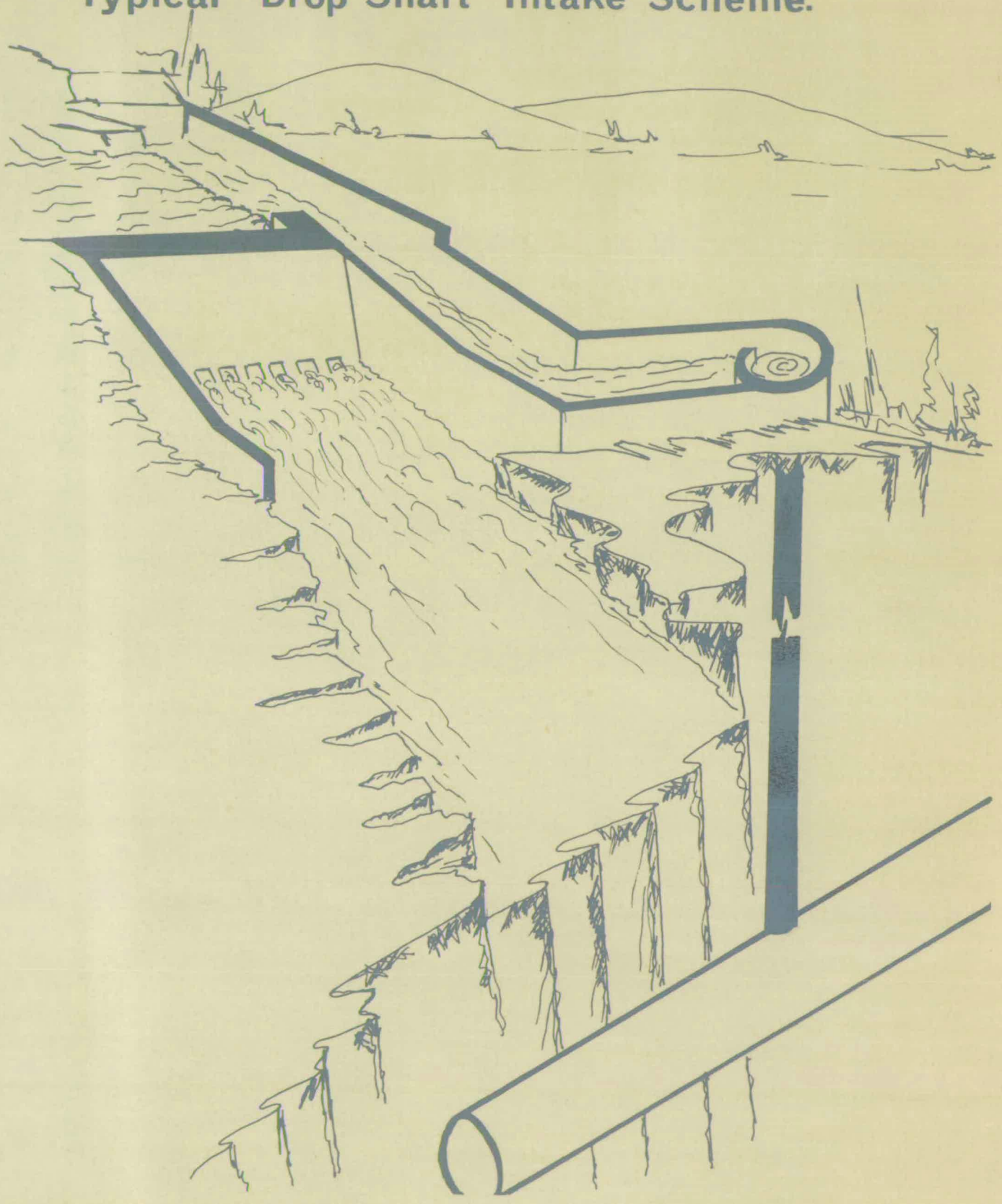

ACKNOWLEDGEMENTS

The Author is deeply indebted to Professor A. W. Hendry for granting the opportunity to undertake the research project and for his supervision and encouragement which led to the fruition of this study. Sincere thanks are due to Mr. D. Simpson for his guidance and for the review of the thesis. Valuable suggestions and assitance received from Dr. S. Soundranayagam and Dr. J. Morgan are appreciated.

Acknowledgement is made to Sir Alexander Gibb and Partners, Consulting Engineers, for the permission to adopt their prototype design for the model investigations.

The Author wishes to express his thanks to those members of the Technical Staff of the Department of Civil Engineering and Building Science, for their skilful attempts in the Model fabrication and for their assistance in the experimentation. Thanks are extended to Miss Elizabeth Turner for the photographic work.

The Author's warm gratitude is due to those who have shown a keen interest in his work, by way of help or otherwise, as this interest lent a strong impetus toward the completion of this study.

Finally, the Author conveys his grateful appreciation to all those who assisted with the Secreterial work, especially to Miss Gina Gillerlane for skilfully typing and duplicating the thesis, and also to Mrs. Nelun Wijeyesekera for checking the manuscripts and for constant encouragement.

C O N T E N T S

C H A P T E R I

I N T R O D U C T I O N

CHAPTER II

THEORETICAL ANALYSES

CHAPTER III

DESCRIPTION OF APPARATUS

CHAPTER IV

EXPERIMENTAL TECHNIQUES

CHAPTER V

EXPERIMENTAL ANALYSES

CHAPTER VI

CORRELATION OF ANALYSES THEORETICAL AND EXPERIMENTAL

CHAPTER VII

SCALE EFFECTS AND PROTOTYPE PREDICTIONS

CHAPTER VIII

CONCLUSIONS

APPENDICES

LIST OF FIGURES

Chapter VII

Appendix B

LIST OF PLATES

S Y N O P S I S

The growing concern of Air Entrainment in Vertical Shafts led to this investigation.

Vertical shafts, under two specific Hydraulic conditions, were considered in the study; firstly, shafts with free flow in them and secondly those with an Annular Hydraulic Jump.

A theoretical analysis as to the actual mechanism of Air Entrainment is postulated in Chapter II. The theory established for the case of free flow in the shaft, elucidates the cause of Air Entrainment as being due to Suction effects resulting from an increased air core within the Shaft. The semi-empirical theory developed in the case with an Annular Hydraulic jump, demonstrates that the process of Air Entrainment is solely due to the spread of the Annular jet; which envelopes air along its path of travel and engulfs the air so entrapped, at the jump. The magnitude of the Air Entrainment under the latter condition is very much less than the former.

The Experimental Analyses support the theoretical approach and also illustrate the phenomenon of different flow regimes beyond the Annular jump. These flow regimes are classified with respect to Froude Number and yield useful design information.

The empirical analysis presented in Chapter VII, to predict prototype and other model size performances, indicates that the air-water ratio increases with decrease of model scale. The Nomogram provided for the purpose of this prediction is applicable to model tests/

model tests conducted on Froude's criterian.

Since a panacea for Air Entrainment in Vertical Shafts may not be available in the near future; the fruits of this study while offering a clear understanding of the underlying mechanisms, would also provide useful data for the use of Vertical Shafts with Air Entrainment.

CHAPTER 1

INTRODUCTION

1.00 GENERAL INTRODUCTION

Water has one thing in common with fire; while it is a splendid servant, it is also a treacherous master. Its service has been mainly to provide the necessities of life, the ancients with little or no knowledge of the basic physics of fluid flow, developed water supply and irrigation systems which still exist as Engineering wonders of the world.

As some of the masterful tendencies of water, it is worth mentioning, a few but serious effects, such as erosion, flooding and cavitation. The detrimental effects resulting, have been well recognised in the recent years and have been of much concern for the research workers in those fields.

What does the future hold? It is impossible and presumptuous to predict the forthcoming fruits of research. However, there is much that can be learnt from a study of the past, for it enables the present to be viewed in its true perspective and is the basis for speculation as to the future. Although the fundamentals may have been discovered, their application to complex problems still affords much scope for the exercise of human intellect.

Just as importance is laid on knowledge to utilize water more effectively; in irrigation, Hydro-electric schemes etc., it is economically just as important that research/

research is done to find the cause and remedy the damage done, because of the very utilization.

The present study is focused on a particular adverse effect of water i.e. Air Entrainment which leads to Cavitation. The Air Entrainment in Vertical Shafts which would normally intercept water to an underground feeder tunnel; that would be either under pressure or otherwise, is investigated. Assimilation is also attempted to the circumstances when the Vertical Shaft would either feed directly on to a turbine or to the atmosphere as in the case of an outfall. The Frontispiece displays an artist's impression of a typical river intake scheme, with a vortex entry conveying water to an underground feeder tunnel, through a drop shaft.

The widespread interest in Air Entrainment has led to a variety of research including the question of Air Entrainment in Vertical Shafts. The Author, however, feels that in most of the research concerned with Air Entrainment in Vertical Shafts there is a dearth of knowledge on two important aspects. which are as mentioned below.

A clear understanding of the underlying theory involved, in the phenomenon of Air Entrainment appears hardly sufficient. This is due to the fact that most of the investigations in this field are on a purely empirical basis and the results which have been postulated depend a great deal on the experimental techniques, for their validity. However, an attempt is made in the present study to establish a plausible and a consistent theory, to illustrate/

to illustrate the mechanism of Air Entrainment in drop shafts.

At a time when Hydraulic Engineers are becoming increasingly aware of the "Scale Effects", that constantly persist in model analysis and thereby hinder precise prototype predictions, the need for a method of evaluating such discrepancies and to advocate requisite allowances is a matter of growing concern to the designer. An intensive study of five different model scales has been incorporated in this project with a view to elucidating the magnitude of such scale effects and to vouch-safe prototype predictions.

1.10 Cavitation.

Cavities occur in almost every liquid of interest to man as well as in man himself. It is this ubiquitous occurrence that demands a thorough scientific understanding of not only the phenomenon itself but also the factors aggravating it. An infinite liquid velocity in close conduits is impossible, since there is an inter-relationship between pressure and velocity. Cavitation will therefore, as a rule, occur in a liquid when the dynamic conditions cause the pressure to fall below the vapour pressure of the liquid. These cavities thus formed will collapse when the pressure rises above the vapour pressure.

If the collapse occurs against a boundary or solid object, small particles of material may be removed from the boundary or solid object which, over a period of time may result in serious damage which is termed Cavitation Pitting or Cavitation Erosion.

The incipient/

The incipience of Cavitation as occurring on ship propellers or on turbine blades is due to the collapse of air bubbles in the microscopic range. Air Entrainment as referred to in this study, would not however cause major detrimental effects but would promote its occurrence

1.20 A REVIEW OF PAST LITERATURE

In this section a brief review of some of the investigations carried out by others is made. Reference is also made concisely to theories which have been incorporated in the subsequent chapter, wherein a detailed review is made.

1.21 Laushey L.M. and Mavis F.T.

Laushey and Mavis (1) conducted their investigations at the Carnegie Institute of Technology, United States. They carried out measurements of the quantities of air entrained by water flowing down vertical shafts 30 ft. in length. The shafts were made of Lucite, 2·8 in. and 5·6 in. in diameter. They reported that the Volumes of Air depended on the following;

(a) The type of entry to the top of the shaft.

(b) The distance from the inlet to the hydraulic grade line in the shaft.

(c) The diameter of the shaft.

(d) The amount of Sub-atmospheric pressure.

For spiral flow in these two shafts, the ratio of air to water depended primarily on the distance of free fall to the hydraulic grade line. In their experiments, the air measurements were made at the exit.

The variation of the Air-Water ratio with the free fall were as follows.

Small shaft/

Results of Laushey & Mavis's Experiments

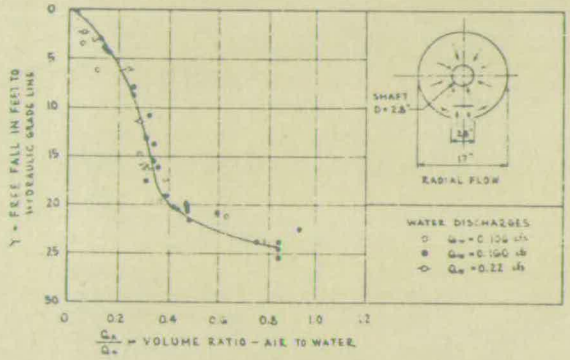

Fig. **a** - Air entrained in the small shaft by radial flow.

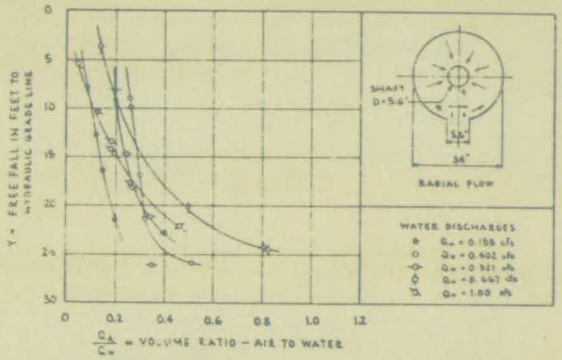

Fig. **b** - Air entrained in the large shaft by radial flow.

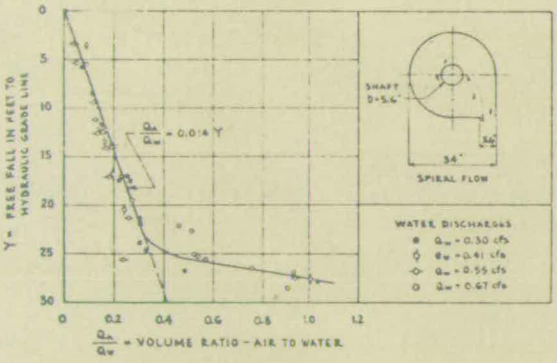

Fig. **c** - Air entrained in the large shaft by spiral flow.

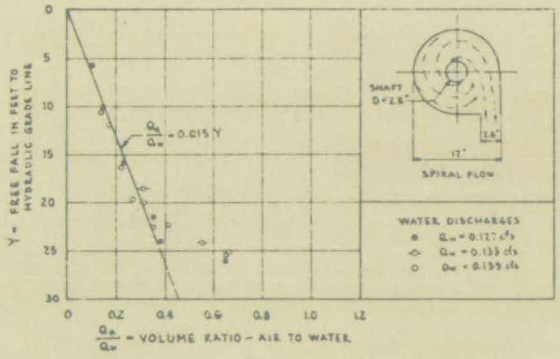

Fig. **d** - Air entrained in the small shaft by spiral flow.

FIG. 1-1

Small Shaft $Q_a/Q_w = 0{\cdot}15\ Y$

and for Large Shaft $Q_a/Q_w = 0{\cdot}14\ Y$

where Qa and Qw are Air and Water discharges and Y is the free fall. They observed that the entrainment of air was due to reasons other than suction. A comparison of Radial motion to spiral motion is made, indicating the preference to spiral motion. Some of the results of their findings are as shown in Figures 1.1 (A-D).

1.22 Viparelli M.

The invesigations Viparelli conducted at the University of Naples, are reported in his paper (2) "Les Courants d'air et d'eau dans les puits verticaux".

He concluded that when the shaft inlet and outlet pressures are equal, the water falls freely along the walls; at low discharges a central core forms, surrounded by an Annular flow of water; at high discharges, the air core breaks up into large bubbles or air pockets. In these cases, the air velocity tends more and more towards the water velocity as the length of the shaft increases.

He also stated that when the pressure at the outlet exceeds that at the inlet, a hydraulic jump usually forms in the lowest portion of the shaft. If the jump is complete the Air Entrainment rate depends both on the free falling distance of the water above and the flow downstream. If the jump is incomplete, the air flow depends on the water velocities before they are damped out by the very turbulent conditions in the jump.

An empirical relationship derived for conditions with a jump is as follows:

$$\frac{Q_a}{Q_w} = 0{\cdot}022 \left(\frac{f}{d}\right)^{3/5} \qquad \text{.....1.22}$$

where Qa and Qw are Air and Water discharges and f & d are the free fall and shaft diameter./

Viparelli's Experimental Analysis

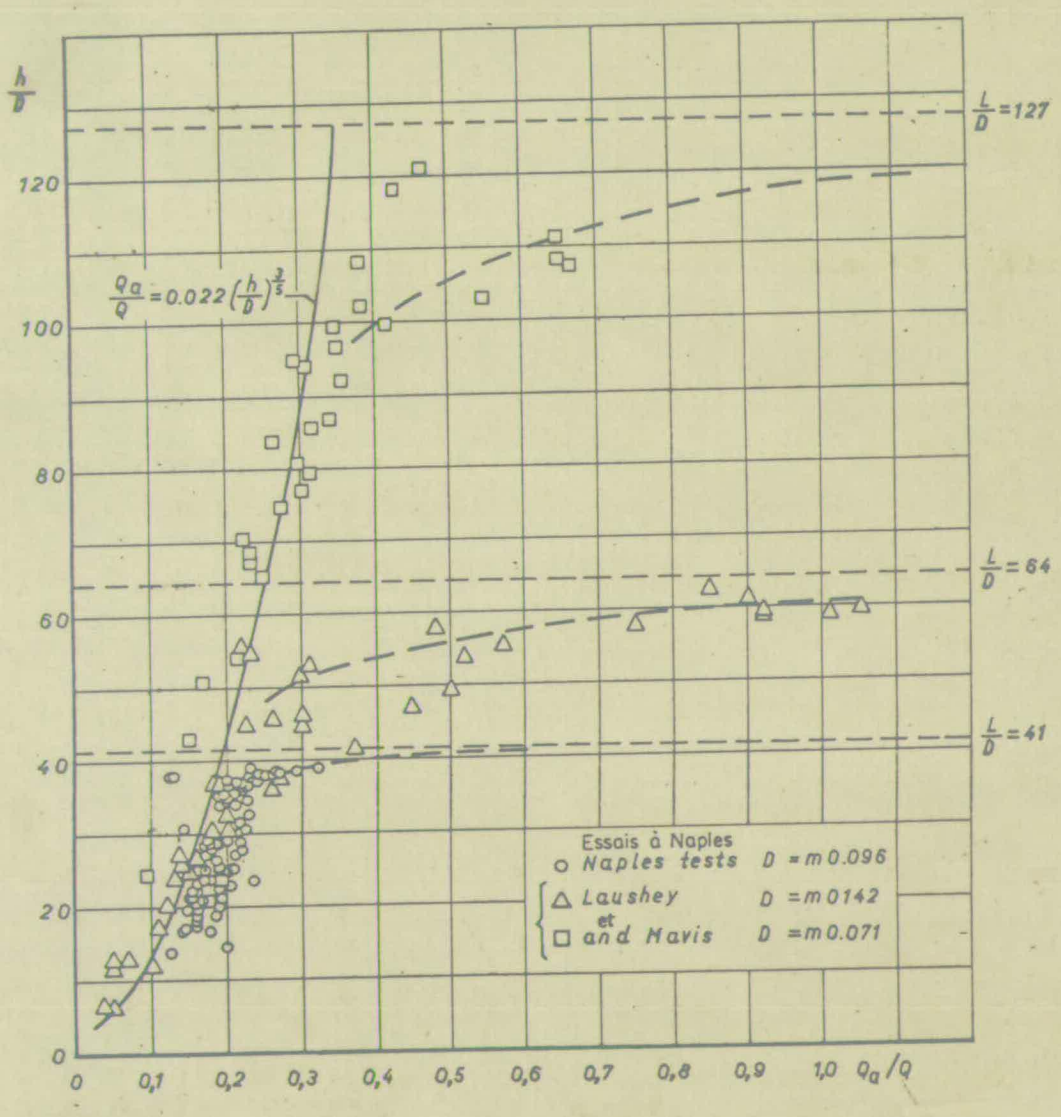

Fig. a

Courbe [Q_a/Q, h/D] avec ressaut hydraulique dans le puits.

Curve [Q_a/Q, h/D] *with jump in the shaft.*

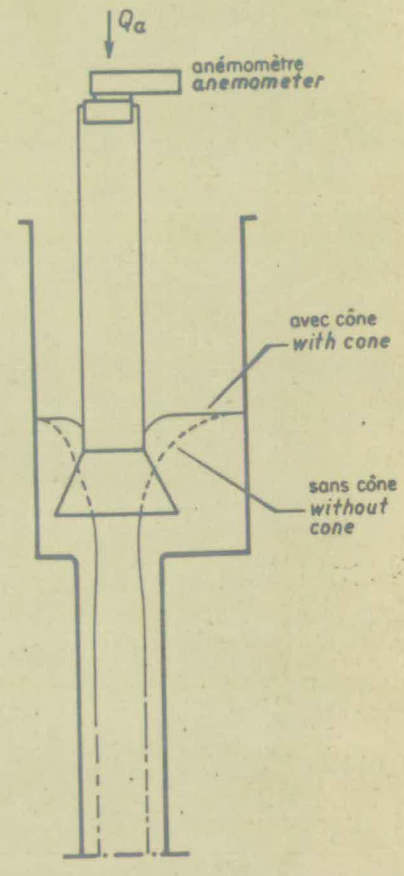

Fig. b

Dispositifs de mesure.

Arrangement used for measuring.

FIG. 1·2

fall and shaft diameter. The results of his experimentation in establishing the above relationship are as shown in figure 1·2 A. The air measurements were made in the experiments at the entry into the shaft; the arrangement of the measuring instrument and its effect on the water surface profile is as illustrated in figure 1·2 B.

1·23 Kalinske A.A.

Kalinske in his investigations; on "Hydraulics of Vertical drain and Overflow pipes" carried out at the Iowa Instiute of Hydraulic Research reported the following in his publications (3).

The maximum velocity of the falling water is reached witin a few feet of the entrance. The total rate of air flow down the pipe depends on the pipe size, water discharge and length of pipe. The maximum rate of air flow is obtained at a relatively low water discharge and this air discharge may be in excess of the water flow. In his endeavour to ascertain the head required for pipe full flow, he observed that the head at which the pipes begin to flow full, depended on their length and that the longer the pipe the greater was the head required.

He stated the following relationship which would enable the head H to be determined for a pipe of length L.

$$H + L = CeV^2/2g + (fL/D)V^2/2g + V^2/2g$$

where C_e is entrance loss coefficient.

f is ordinary pipe friction factor.

1·24 Hydraulic Research Station.

In the report on Hydraulic Model Investigation of a typical drop shaft and de-aeration Chamber, the results were found to be of great interest. The model investigations were conducted on a drop shaft in the Plover Cove Water Supply Scheme in Hong Kong.

The report/

The report (4) stated that the effect of the vortex chamber decreases with decreasing flow. It was mentioned that large quantities of air were entrained at the transition from the annular jet to pipe-full flow, or annular hydraulic jump (5). The volume of air carried down the drop shaft has been found to be greater with a radial inlet, since the water tended to fall haphazardly down the drop shaft causing a larger exposed area, which resulted in an increased volume of air being entrained. Indication was also made that the air-water ratio decreased with increasing scale and this was explained by the increased Centipetal movement of the air bubbles.

1·25 Quick M.C.

Quick made known from his investigations that when an Annular film of water flows down a vertical pipe leaving the centre of the pipe filled with air, there are certain circumstances under which a sudden transition to the pipe-full condition can occur. In his theory (8) he explained the mechanism of the jump, especially the central tongue of fluid which stands on the jump. The occurrence of the jump is discussed by considering energy losses through the system. It is shown qualitatively that the jump position is determined by these losses.

1·26 Ackers P. and Crump E.S.

The investigations conducted by these two authors are described in their paper "The Vortex Drop" (6). They explained how a drop shaft with its inlet in the form of a vortex chamber may be used for transferring fluid flowing in an open channel to a lower level. They combined the hydraulic properties of a free vortex with the Bernoulli equation and by applying the principle of maximum discharge, the relationship of Head to Discharge was obtained.

They forwarded/

They forwarded a theory which illustrates the behaviour of the Air-Core with varying water discharge. Details of this theory are presented in the next chapter.

1·27 Dawson and Kalinske.

The above mentioned authors published a report (7) on Hydraulics and Pneumatics of Plumbing drainage systems. The main purpose of the investigation was to determine how water flows down partially full vertical pipes, the velocity it attains at different heights and how that velocity varies with rate of discharge and size of pipe. They derived a relationship to determine the maximum terminating velocity and to determine the position of its occurrence. Their analytical approach is described in the next chapter.

1·28 General Comments on the Literature.

There appears to be a correlation between the results of Laushey and Mavis with those of Viparelli as seen on figure 1·2. The relationships derived by Laushey and Mavis do not consider the shaft diameter; hence there is a necessity for different relationships, when different diameters are considered.

The results on Fig. 1·2A produced by Viparelli, indicate a group of experimental points, which deviate from his general equation. This suggests a possibility of scale effects which has not been accounted for.

Results of the Plover Cove scheme though largely empirical, produced a variety of information, useful to a research worker in this field. The extensive study of the de-aeration characteristics is unique. The hydraulic theories developed by Ackers and Crump as to the effect of air/

of air-core variation and also the theory developed by Dawson and Kalinske with respect to the velocity variation in a vertical shaft, have been the ground on which, the author's theoretical analysis is based. Therefore these theories are dealt with in greater detail in the next chapter.

1·30 The Scope of the Present Investigation.

With reference to the literature mentioned in the preceeding section, it is apparent that a great deal is yet to be known about the mechanism of Air Entrainment. The cause for Air Entrainment in the absence of an annular jump is not evident. Though it has been mentioned (4) that in the case where a jump is present, large amounts of air are entrained (at the impact), a quantitative analysis of the air entrainment at the jump needs further investigation.

The ubiquitous use of model analysis would not vouchsafe confident prototype predictions unless the scale effects are accounted for. To elucidate the disparity of predictions a clear understanding of the underlying phenomenon of Air Entrainment, occurring in several scale sizes, is necessary. This would facilitate a semi-empirical relationship to be developed.

In the present study it is envisaged that a theoretical analysis would be produced wherever possible. Also from the experimental results a theoretical procedure may be justified, where available, if not the experimental results would be utilised to develop empirical relationships.

CHAPTER II

THEORETICAL ANALYSES

2·0 INTRODUCTION

The theoretical analysis of Air Entrainment in Vertical Shafts will be considered under two main categories namely air entrainment occurring under free flow conditions and, with a jump in the shaft.

In the analysis of the free flow condition an ideal flow state is first considered, ignoring the spread of the water surface, as it falls along the shaft axis. The reason for such a consideration is to evaluate the surface profile of the water discharge ignoring the aeration of the surface.

When a column of water falls under gravity, it tends to increase its vertical component of the Axial Velocity until it reaches a certain maximum terminating velocity at a section which shall be herein after referred to as the "Terminating Section". Investigations into the velocity variation along a vertical shaft have been conducted by Dawson and Kalinske (7). The finite velocity at which a raindrop reaches the earth, illustrates the above phenomenon.

The increase in the vertical component of the axial velocity of the water, from the throat section to the terminating section, gives rise to a decrease in the area of cross-section of the flow in that region. At any section this decrease in water area causes an increase in the air core. In the ideal state considered, the shape of the air core will be similar to that of an elongated bottle, with its neck as the region where the vertical velocity is increasing. These effects in the surface profile are as shown in figures 2·1, 2·2 and 2·3.

The volumetric increase of the air core with the fall, gives rise to a vacuum effect within the shaft which in turn draws air from the atmosphere/

atmosphere to counterbalance the negative pressure. It is this quantity of air which could be measured at the entry into the shaft. A portion of this air will be enveloped on the surface of the water profile and the rest will be dragged with the water, due to the effect of the principle of exchange of momentum at the air-water interface.

The effect of a jump in the shaft is to prevent the flow of air in the central core. The only quantity of air which could be carried beyond the jump is that amount which is already enveloped due to the spread of the water surface. Even this air could be rejected if the velocity beyond the jump is low enough. The latter aspect will be dealt with, in detail in Section 5·4.

2.01 Air Entrainment without a jump.

To establish a plausible and consistent theory as to the air entrained without a jump, it is necessary to evaluate this excess supply of air by considering the difference in volume of the air core under two specific conditions. Primarily, the volume of the air core in the state already described in the earlier section and secondly under a further ideal condition where there could be no vacuum effects. This latter condition could be obtained only if there is no increase in the air-core diameter beyond the throat. Hence, by assuming no increase in the vertical component of the velocity and therefore no increase in the air-core diameter, a state which causes no vacuum effect could be visualised, having a core diameter of a cylindrical shape with a constant diameter as that at the throat. The length of this cylinder will be equal to the entire shaft length. These volumes are as seen in figure 2·3; considering vacuum effects the volume is (A + A2); without vacuum effects volume of air core is A2.

The diameter/

The diameter of the air core at the throat is controlled by the geometry of the vortex chamber and the discharge through it. The method of evaluating the variation of this diameter with the discharge, for a particular geometry of chamber has been put forward by Ackers and Crump (6), which is utilised to determine the volumes of the air cores under both conditions.

Computation of this difference in volume entails the evaluation of the surface profiles from the throat downwards and this is facilitated by the use of a Computer Program (No. CIE/018/0018) a flow diagram, of which is shown in figure 2·4 and described in detail under section 2·14.

2.02 Air Entrainment with an Annular Hydraulic Jump.

The effect of the jump is to disrupt the free flow of air in the core, leaving the entrapped air in the water surface to be engulfed and carried beyond the jump. The presence of an annular jump in a vertical shaft is due to the transition of the flow from an annular jet to pipe-full flow, analagous to the change from super critical flow to sub critical flow in an open channel (5). When a drop shaft feeds a tunnel under pressure, the pressure in the tunnel causes a column of water to occupy the lower end of the shaft., equivalent to the pressure in the tunnel. Even when there is no flow in the drop shaft a column of water would represent the pressure in the tunnel. Due to the advantages of having a cushion of water various methods are adopted to create a standing column, even when the tunnel is not under pressure.

A commonly practised method is to have a constricted shaft exit in the form/

the form of an orifice or a nozzle so that a reasonable head above the opening would persist at all discharges. This head could be varied, by altering the size of opening for the particular discharge. The presence of an annular hydraulic jump causes a large proportion of air rejection at the point of impact. Although air entrainment would occur for reasons similar to the conditions prevailing without a jump, the air rejection which takes place at the jump reduces the net quantity of entrainment.

In the present study the analysis of air entrainment with a jump is not purely theoretical. The relationship for the air-water ratio derived by Viparelli (2) as mentioned in 1·22 appears to be in fair accordance with the Author's experimental results (see figure 6·30) except for possible discrepancies due to Scale Effect. By understanding the underlying phenomenon responsible for the entrainment under this condition, which is the spread of the annular jet, a semi empirical relationship could be derived to predict the magnitude of the spread for a particular discharge and shaft diameter. The growth of such a jet could be established as a straight line and therefore the air entrainment would depend on the difference in the cross-sectional area due to the spread, considered at the point of impact.

2·10 HYDRAULIC THEORY FOR FREE FLOW CONDITIONS.

2·11 Variation of Air-Core diameter at the Throat.

With reference to figures 2·1 (a and b) a free vortex is considered at the entry to the shaft.

Hence, by considering the properties of a free vortex the method of analysis for the conditions both at the inlet and at the throat of the vortex chamber, are conducted.

With the notation/

The Vortex Drop

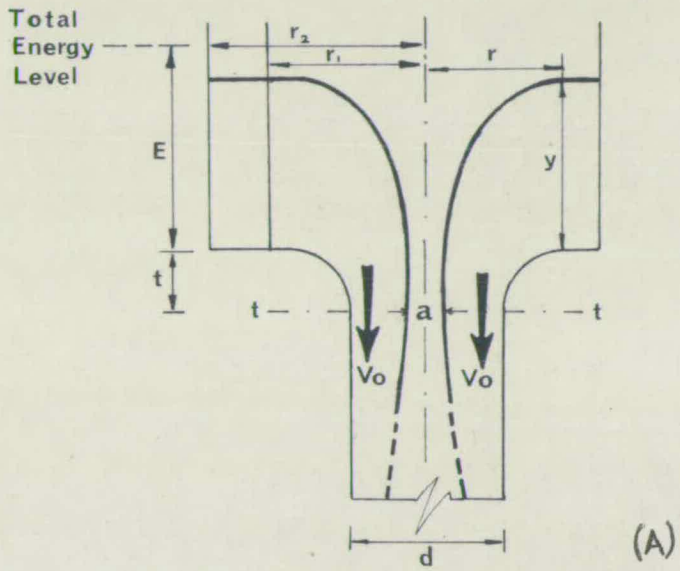

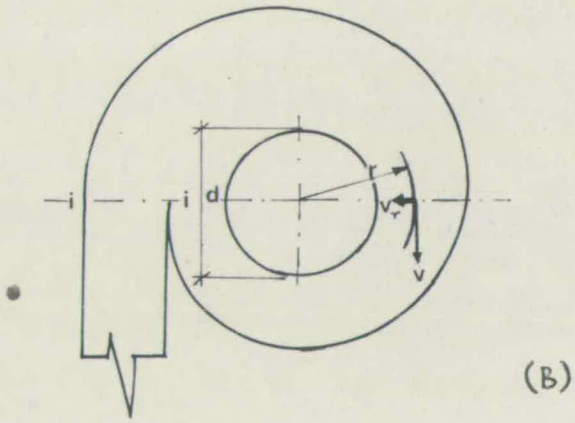

FIG. 2.1

Notation [1]

C = Circulation.

v = Whirling component of the velocity.

E = Total Head (relative to chamber floor).

V = Vertical component of Velocity at the throat.

p = Static pressure.

a = Air core diameter at the throat.

d = Internal diameter of shaft.

f = Fractional air core at the throat.

r_1 and r_2 = minimum and maximum radii of vortex chamber.

t = Distance between throat and floor of vortex chamber.

Q = Water discharge.

With notation [1],

At any general section

$$\text{Circulation } C = v.r \qquad \ldots\ldots\ldots 2\cdot11A$$

By Bernouilli's Theorem

$$E = y + \frac{v^2}{2g} = y + \frac{C^2}{2gr^2} \qquad \ldots\ldots\ldots 2\cdot11B$$

With the assumption of zero energy loss in the chamber, the velocity distribution of the fluid entering the chamber is as shown in equation 2·11A and the total energy will be constant as in 2·11B.

Across section ii in figure 2·1A

the discharge $Q = \int_{r_1}^{r_2} v.y\,dr$

$$= \int_{r_1}^{r_2} \frac{C}{r}\left(E - \frac{C^2}{2gr^2}\right) dr$$

$$= \left[E.C.\log_e r + C^3/4gr^2\right]_{r_1}^{r_2}$$

i.e. $$Q = E.C.\log_e \frac{r_2}{r_1} - \frac{C^3}{4g}\left\{1/r_1^2 - 1/r_2^2\right\} \qquad \ldots\ldots\ldots 2{:}11C$$

Consider the throat section tt in figure 2·1B. Since the shaft is considered to be open to the atmosphere, the static pressure in the core at the throat will be atmospheric and from Bernoulli's equation, its energy with the throat as datum is as follows:

$$E + t = \frac{v^2}{2g} + \frac{V^2}{2g} + \frac{p}{w} \qquad \ldots\ldots\ldots 2\cdot11D$$

Now at the air-water interface at the throat section p = 0, r = a/2

Substituting in equation 2·11D

$$E + t = 2C^2/ga^2 + V^2/2g \qquad \ldots\ldots\ldots 2\cdot11E$$

Since by the equation of Continuity

the discharge/

the discharge $Q = \frac{\pi}{4}(d^2 - a^2)V$

and by introducing $a^2/d^2 = f$, the fractional air core, it is possible to combine with equation 2·11E to give

$$Q = \pi/4\ d^2(1-f)\ \{2g(E + t) - 4C^2/d^2 f\} \quad \ldots\ldots\ldots 2\cdot 11F$$

The above equation was first derived by Bi.. ie and Hookings (8). By partially differentiating, it is possible to apply the principle of 'Maximum discharge' to determine the size of Air Core which for a known gemetry will permit the greatest discharge for a particular energy.

i.e. $$\frac{\partial q}{\partial f} = 0 = -\{2g(E + t) - 4C^2/d^2 f\}^{\frac{1}{2}}$$

$$+ \tfrac{1}{2}(1 - f)\frac{4C^2}{d^2 f^2}\{2g(E + t) - 4C^2/d^2 f\}^{-\frac{1}{2}}$$

$$2g(E + t) - 4C^2/d^2 f = 2(1 - f)C^2/d^2 f^2$$

$$g(E + t) = 2C^2 f/d^2 f^2 + C^2(1 - f)/d^2 f^2$$

$$g(E + t) = \frac{C^2}{d^2 f^2}(1 + f) \quad \ldots\ldots\ldots 2\cdot 11G$$

inserting in equation 2·11F

$$Q = \frac{\pi}{4} d^2(1 - f)\sqrt{\left\{\frac{2C^2(1 + f)}{d^2 f^2} - \frac{4C^2 f}{d^2 f^2}\right\}}$$

$$Q = \frac{\pi}{4} dC(1 - f)\sqrt{\left\{\frac{2(1 + f) - 4f}{f^2}\right\}}$$

$$Q = \frac{\pi}{4} dC\sqrt{\left\{\frac{2(1 - f)^3}{f^2}\right\}} \quad \ldots\ldots\ldots 2\cdot 11H$$

In this equation, C the vorticity is not readily measurable. Considering the three equations already derived for the inlet condition, throat condition and the maximum discharge and re-writing them in a non-dimensional form.

$$Q/dC = E/d \log_e\left\{\frac{r_2}{r_1}\right\} - C^2/4gd^3\left\{\frac{d^2}{r_1^2} - \frac{d^2}{r_2^2}\right\} \quad \ldots\ldots\ldots 2\cdot 11I$$

$$Q/dC = \frac{\pi}{4}\left\{\frac{2(1 - f)^3}{f^2}\right\} \quad \ldots\ldots\ldots 2\cdot 11J$$

$$(E + t)/d = \frac{C^2 (1 + f)}{gd^3 f^2} \qquad \text{.....2·11K}$$

Substituting for Q/dC from equation 2·11J in equation 2·11I and also for C^2/gd^3 from equation 2·11K in equation 2·11I.

$$\pi/4 \sqrt{\left\{\frac{2(1 - f)^3}{f^2}\right\}} = E/d \log_e \left\{\frac{r_2}{r_1}\right\} - \frac{1}{4} \frac{(E + t)}{d} \frac{f^2}{(1 + f)} \left\{\frac{d^2}{r_1^2} - \frac{d^2}{r_2^2}\right\} \qquad \text{.....2·11L}$$

Collecting terms

$$\frac{E}{d} \left[\log_e \left(\frac{r_2}{r_1}\right) - \frac{f^2}{4(1 + f)} \left\{\frac{d^2}{r_1^2} - \frac{d^2}{r_2^2}\right\}\right] = \frac{\pi}{4} \sqrt{\left\{\frac{2(1 - f)^3}{f^2}\right\}} + \frac{tf^2}{4d(1 + f)} \left\{\frac{d^2}{r_1^2} - \frac{d^2}{r_2^2}\right\} \qquad \text{.....2·11M}$$

To simplify the algebra

let $F1 = f^2/4(1 + f)$ .....2·11N

$F2 = \pi/4 \left(1/f - 1\right) \sqrt{2(1 - f)}$ .....2·11V

$G1 = \log_e (r_2/r_1)$ .....2·11P

$G2 = d^2/r_2^2 (r_2^2/r_1^2 - 1)$ .....2·11Q

and substituting in equation 2·11M

$$\frac{E}{d} [G1 - F1 \cdot G2] = F2 + \frac{t}{d} G2 \cdot F1 \qquad \text{.....2·11R}$$

G1 & G2 are geometric properties of the vortex chamber;

F1 & F2 are parameters depending solely on the fractional air core.

Ackers and Crump suggested the following procedure to evaluate the variation of discharge with the fractional air core.

(i) Calculate G1 & G2 for the given geometry.

(ii) For a series of values of f, calculate F1 & F2.

(iii) Insert in equation 2·11R and evaluate E/d.

(iv) Evaluate C^2/gd^3 from $4F1 \left(\frac{E}{d} + \frac{t}{d}\right) = \frac{C^2}{gd^3}$

hence $\frac{c^2 d^2}{gd^3 d^2} = \left\{4F1 \frac{(E + t)}{d}\right\}$

i.e. $dC = \sqrt{g}d^{5/2} \{4F1 \frac{(E + t)}{d}\}$

Substituting value of dC from above equation in equation 2·11H

$$Q = \pi/4\sqrt{g}d^{5/2} F2 \sqrt{\{4F1 (E + t)/d} \quad \ldots\ldots\ldots\ldots 2\cdot11S$$

(v) Evaluate Q from equation 2·11S.

(vi) Interpolate values of f for given (regular) values of Q.

2·12 Variation of Air-Core diameter along the Shaft.

(from the throat to Terminating Section)

With reference to figure 2·2 and notation [2]. Let Δh be an accelerating elemental annular ring of water at a distance h below the throat.

mass of water $m = (\Delta h)\ A.\frac{w}{g}$

then $mS = mg - K'.\pi d\ (\Delta h)\ w.V^2$ ..... 2·12A

Since the shaft is not flowing full, the area A can be best expressed as $\frac{Qw}{V}$

Also to use the frictional resistance as dimensionless K^1 is replaced by $\frac{K}{g}$ dividing equation 2·12A by m.

$$S = g - \frac{(K/g)\pi d(\Delta h).wV^2}{(\Delta h)(Qw/V)(w/g)}$$

i.e. $S = g - \frac{K\pi dV^3}{Qw}$ ..... 2·12B

For any particular discharge $\frac{K\pi d}{Qw}$ is a constant

let $Z = (\frac{K\pi d}{Qw})$ and since $S = \frac{V.dV}{dh}$

$$dh = \frac{V.dV}{S} = \frac{V.dV}{g - ZV^3}$$

i.e. $$dh = \frac{V.dV}{g - ZV^3}$$ ..... 2·12C

Hydraulic Conditions

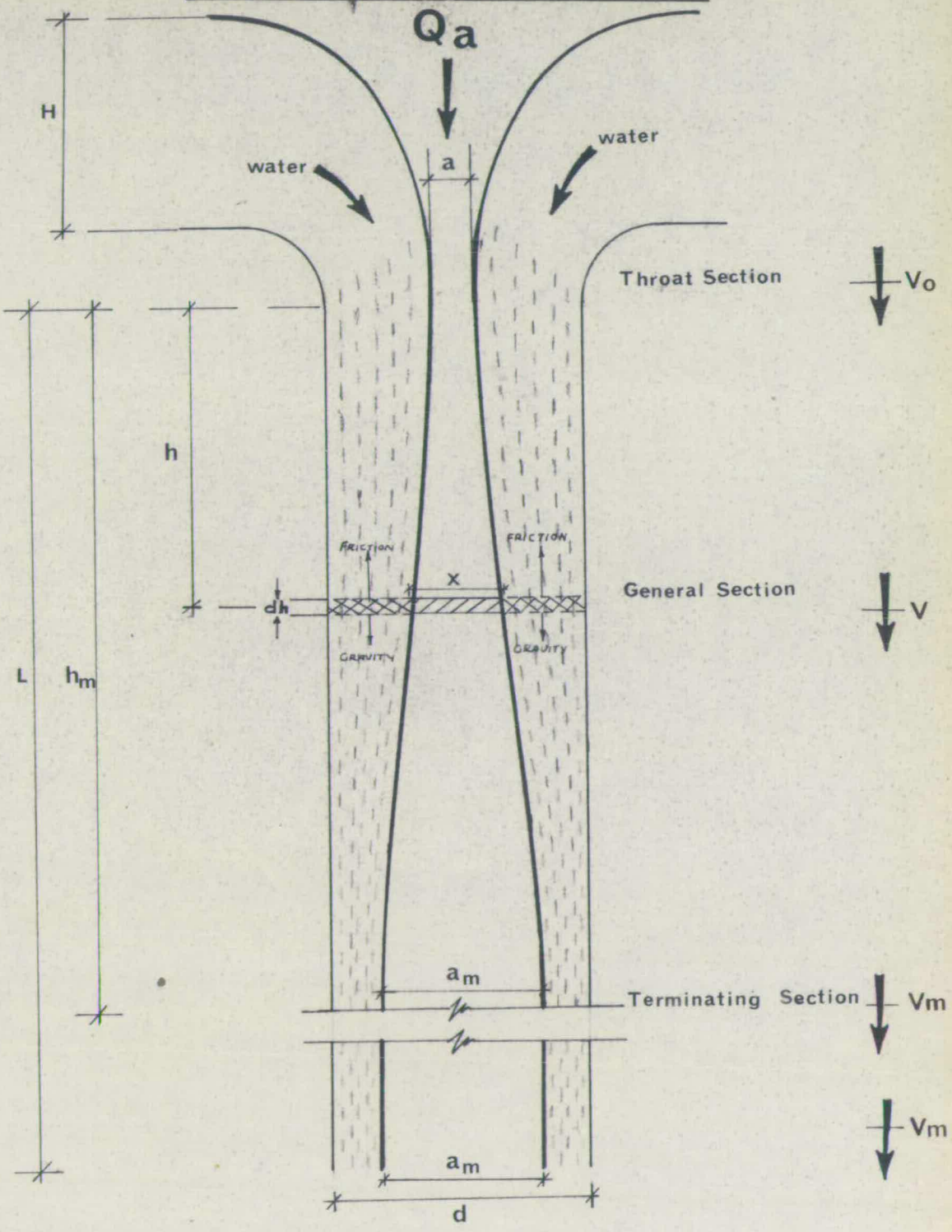

FIG. 2.2

Notation (2)

Δh = accelerating elemental annular ring.

h = distance of the annular ring from the throat.

hm = depth of the terminating section.

L = length of shaft.

d = diameter of shaft.

K' = frictional resistance expressed in force/unit area/unit density/unit velocity.

V = average velocity of water (friction varies approximately as square of velocity.

w = unit weight of water.

g = gravitational constant.

S = acceleration of water at any point.

A = area of flow in shaft.

Qw = Water discharge.

Vm = maximum terminating velocity.

Vo = throat velocity.

x = air core diameter at depth h.

Qa = air discharge.

Maximum Terminating Velocity.

At the maximum terminating velocity, acceleration is zero.

i.e. $0 = g - \frac{K_m d . V_m^3}{Q_w}$

therefore $V_m = \left\{\frac{Q_w . g}{K_m d}\right\}^{1/3}$ .....2·12D

Variation of Velocity with height.

Velocity V = Vo at the throat section.

also V = Vm at the terminating section.

Using equation 2·12C $dh = \frac{V dV}{g - ZV^3}$

integrating for the limits of V from Vo to V

$$h = \int_0^{h_m} dh = \int_{V_o}^{V} \frac{V dV}{g - ZV^3} \qquad \text{.....2·12E}^1$$

$$h = \frac{1}{6\sqrt{3}Vm} \left[\log_e \left\{1 + \frac{3VmV}{(Vm - V)^2}\right\} - \log_e \left\{1 + \frac{3VmVo}{(Vm - Vo)^2}\right\}\right]$$

$$- \frac{1}{\sqrt{3}ZVm} \left(\text{arc tan} \frac{2V + Vm}{Vm.\sqrt{3}} - \text{arc tan} \frac{2Vo + Vm}{Vm.\sqrt{3}}\right)$$

.....2·12E

(Derivation from 2·12E^1 to 2·12E is presented in Appendix (c).

This equation relating the velocity variation with depth of fall was first derived by Dawson and Kalinske (7)

Determination of frictional resistance K.

From equation 2·12D

$$Vm = \left(\frac{Q_w g}{K_m d}\right)^{1/3}$$

but K the frictional resistance varies with the square of the velocity.

Using Manning's formula to find Vm

$$V = \frac{1.486}{n} R^{2/3} i^{1/2}$$

where n is the roughness coefficient

R/

R the Hydraulic Radius

i the gradient

$$R = \frac{Qw}{V} \frac{1}{\pi . d} = \frac{Qw}{V\pi d}$$

$i = \sin 90^{\circ} = 1$

$$\text{Therefore } Vm = \frac{1 \cdot 486}{n} \cdot \left(\frac{Qw}{\pi Vmd}\right)^{2/3} \cdot 1$$

$$\text{i.e. } Vm^{5/3} = \left(\frac{1 \cdot 486}{n}\right) \left(\frac{Qw}{\pi . d}\right)^{2/3}$$

$$Vm = \left(\frac{1 \cdot 486}{n}\right)^{3/5} \left(\frac{Qw}{\pi . d}\right)^{2/5} \qquad \ldots\ldots\ldots 2 \cdot 12F$$

Equating 2·11D and 2·11F

$$\left(\frac{Qwg}{K\pi d}\right)^{1/3} = Vm = \left(\frac{1 \cdot 486}{n}\right)^{3/5} \left(\frac{Qw}{\pi d}\right)^{2/5}$$

$$\left(\frac{Qwg}{K\pi d}\right) = \left(\frac{1 \cdot 486}{n}\right)^{9/5} \left(\frac{Qw}{\pi d}\right)^{6/5}$$

$$K\pi d \left(\frac{1 \cdot 486}{n}\right)^{9/5} \left(\frac{Qw}{\pi d}\right)^{6/5} \frac{1}{Qw} = g$$

$$K = \frac{g}{\left(\frac{1 \cdot 486}{n}\right)^{9/5} \left(\frac{Qw}{\pi d}\right)^{1/5}} \qquad \ldots\ldots\ldots 2 \cdot 12G$$

From equation 2·12E, the height at which different values of V (from Vo to Vm) could be evaluated. From these results an interpolation could be made to obtain the variation of V for given (regular) values of h.

Hence the air core diameter at any height h could be evaluated as follows:

$$Qw = \frac{\pi}{4} (d^2 - x^2) V$$

where x = air core diameter at a general section.

$$x^2 = d^2 - \frac{Qw.4}{\pi V}$$

$$x = \sqrt{d^2 - \frac{4.Qw}{\pi V}} \qquad \ldots\ldots\ldots 2 \cdot 12H$$

where $V = f(h, Z, Vo, Vm)$

2·13 Volumetric Analysis of Air Core.

With reference to figure 2·2. Consider the general section, h units below the throat and having an air core diameter of x units.

Area of cross-section of the annular ring of water

$$= \frac{\pi}{4}(d^2 - x^2)$$

i.e. $$Qw = \frac{\pi}{4}(d^2 - x^2)\, V \qquad \text{.....2·13A}$$

at the throat section

$$Qw = \frac{\pi}{4}(d^2 - a^2)Vo \qquad \text{.....2·13B}$$

and at the terminating section and beyond it

$$Qw = \frac{\pi}{4}(d^2 - x_m)^2 V_m \qquad \text{.....2·13C}$$

Consider the shaft in two sections:-

(i) From throat to the terminating section,

and (ii) From terminating section to the end of the shaft.

Let q_A = total volume of air core. (under normal conditions)

q_1 = volume of air core in the 1st section of shaft.

q_2 = volume of air core in the 2nd section of shaft.

q_B = total volume of air core (with no vacuum effects)

(Section 2·00 describes conditions necessary to produce q_A and q_B).

In the first section of the shaft;

Volume of an elemental disc of the air core

$$dq_1 = \frac{\pi x^2}{4}\, dh$$

Since $$\frac{Qw}{V} = \frac{\pi}{4}(d^2 - x^2)$$

and also $V = f(h, Vo, Vm)$

$$q_1 = \int_0^{hm} \left\{\frac{\pi}{4} d^2 - \frac{Qw}{f(h,Vo,Vm)}\right\} dh \qquad \text{.....2·13D}$$

In the second section of the shaft

$$Qw = \frac{\pi}{4}(d^2 - x_m^2)\, Vm$$

$$\frac{\pi}{4} x_m^2 = (\frac{\pi d^2}{4} \cdot Vm - Qw)\frac{1}{Vm}$$

$$q_2 = \frac{\pi}{4} x_m^2 (L - hm)$$

Therefore $q_2 = (\frac{\pi}{4} \cdot d^2 \cdot Vm - Qw)\frac{(L - hm)}{Vm}$ .....2·13E

Hence the total volume of air core q_A

$$q_A = q_1 + q_2$$

$$= \int_0^{hm} \{\frac{\pi d^2}{4} - \frac{Qw}{f(h,Vo,Vm)}\}\, dh + \frac{(L - hm)}{Vm}(\frac{\pi}{4} \cdot d^2 Vm - Qw)$$

.....2·13F

The above equation evaluates the total volume of air core under normal conditions.

To evaluate q_B the total volume under the idealised condition, having no vacuum effect, variation of the air core at the throat with the water discharge is used as derived in 2·11.

Air core diameter $a = f(Qw, G)$

where G is the geometry of vortex chamber.

However $q_B = \frac{\pi}{4} \cdot a^2 \cdot L$ .....2·13G

Substituting for a in 2·13G

$$q_B = \frac{\pi}{4} \cdot L \cdot [f(Qw, G)]^2$$ 2.13H

The scope of this analysis is to correlate the volumetric differennce of q_A/

of q_a and q_B to QA the rate of air discharge into the shaft. In doing so, a period of time should be considered over which the volumetric difference of occurs. This period of time is the corresponding time taken by water to fill the remaining volume (shaft volume - total air volume) of the shaft at the particular rate of flow Qw.

It is probably evident at this stage, that with the increase of water flow there is a volumetric increase in the difference of q_A and q_B. However, it is evident that with the increase of water discharge there is a decrease of the fractional air core which results with an increase in the throat velocity of the air. But, from the principle of the exchange of momentum it is clear that the air velocity cannot be greater than the water velocity at the air-water interface or any where else in the core. Hence a controlling factor of the air flow would occur when the air core diameter is comparatively smaller and when the throat air velocity reaches the maximum terminating velocity of the water.

2·14 Method of Computation.

To elucidate the two latter aspects in this analyses and also to curtail rigorous mathematical analysis, the following procedure with the aid of a Computer Program is incorporated.

The computer program (No. CIE 018/0018) enables the air flow to be evaluated for a dropshaft having a vortex entry, for different values of water discharges and shaft lengths.

Referring to figure 2·3, flow diagram in figure 2·4 and the notation [3] a brief outline of the steps in the evaluation is shown below.

(1) For a/

Classification of Volumes

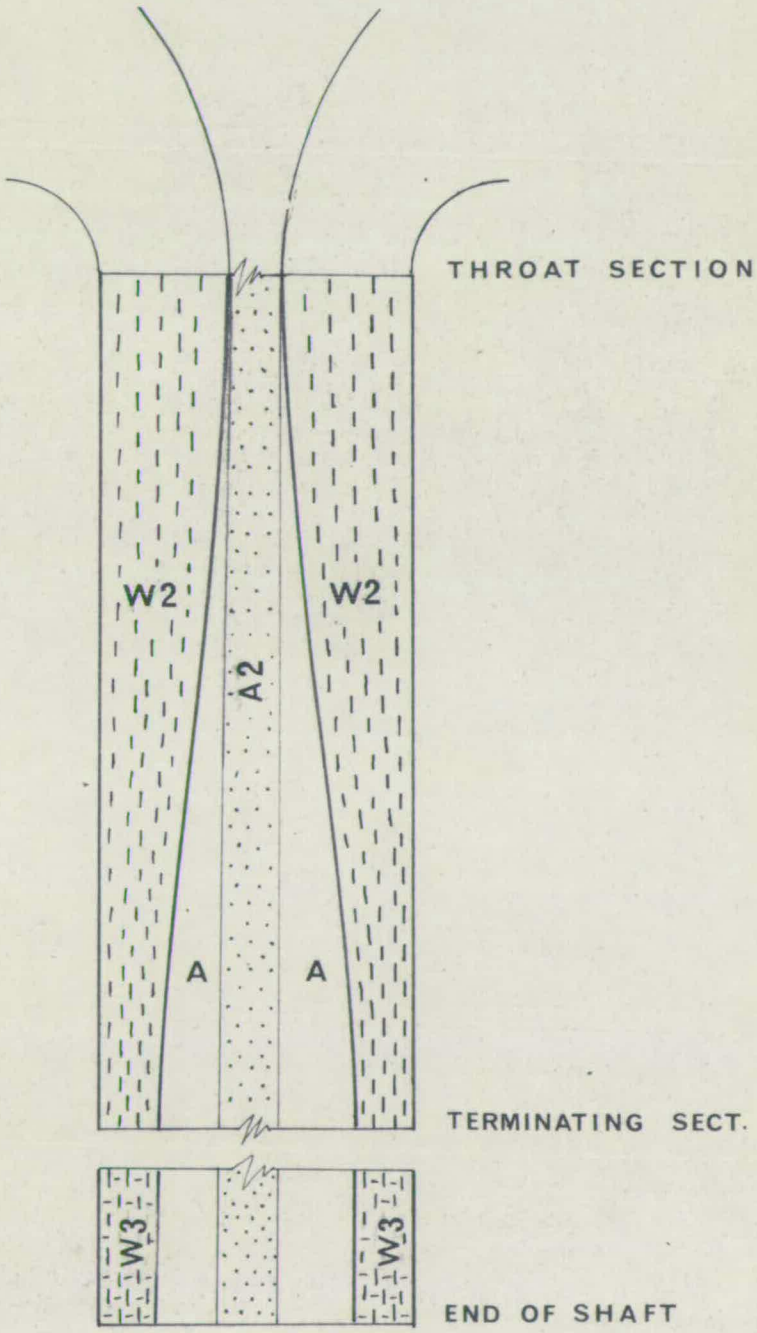

FIG. 2.3

FLOW DIAGRAM FOR COMPUTER PROGRAMME No.CIE 018/0018
AIR ENTRAINMENT WITH FREE FLOW CONDITIONS

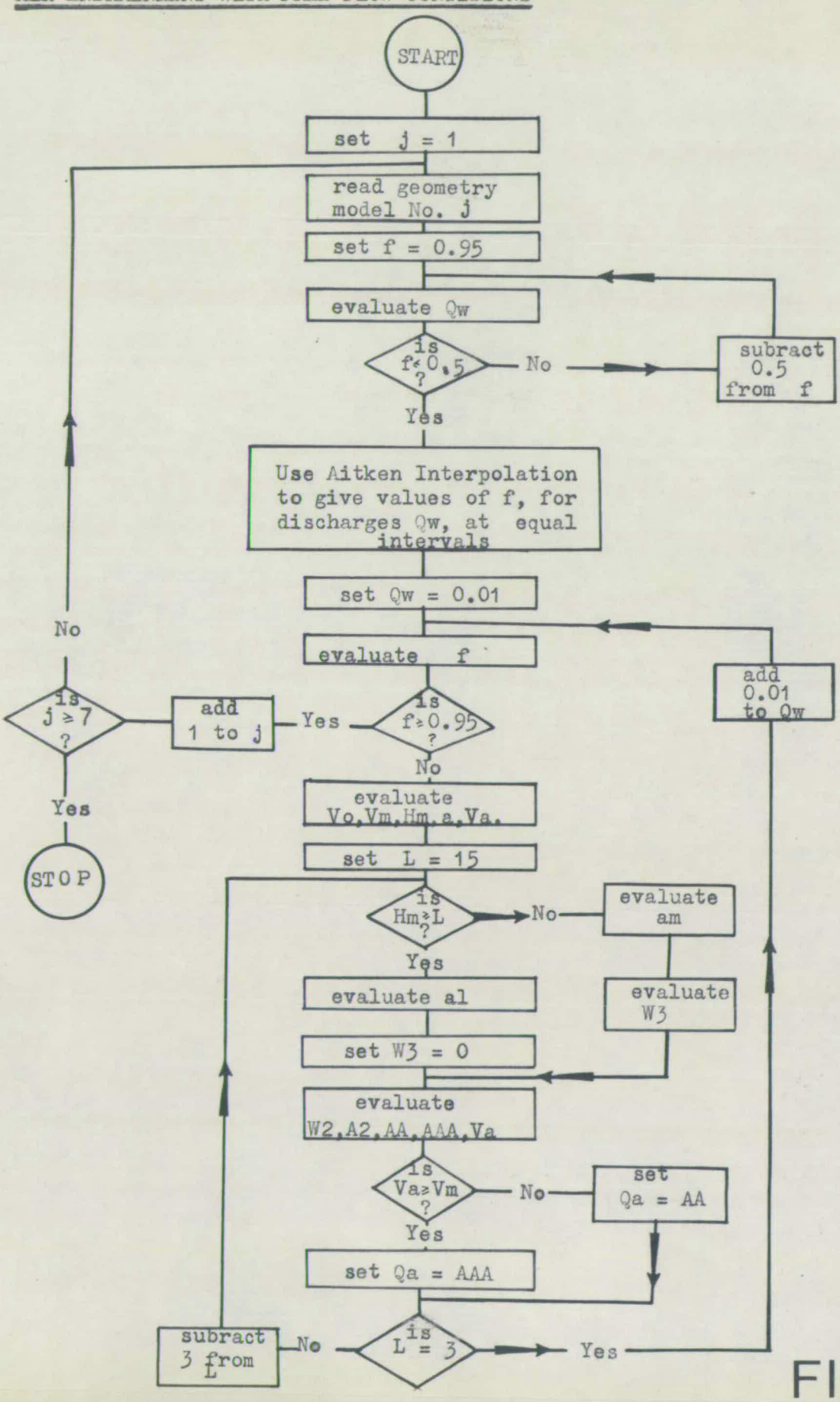

FIG. 2.4

Notation [3]

j = Model number (1 to 6).

f = Fractional air core.

Qw = Water discharge (Cusecs).

Vo = Throat velocity of water (ft. per sec.)

Vm = Maximum terminating velocity of water (ft. per sec.).

Hm = Length of terminating section from the throat (ft.).

a = Air core diameter at the throat (ft.).

Va = Air velocity at the throat (Ft/s).

am = Air core diameter at terminating section (ft.).

L = length of shaft (ft.).

W2, A2, W3 and A = Volumes (cu.ft.) as illustrated in figure 2·14A.

AA = Air flowwhen $Va \leq Vm$.

AAA = Apparent air flow when $Va > Vm$.

Qa = Air entrained in cusecs.

Special for program considering jump.

h = Fall height.

C = Growth constant.

ah = Air core diameter at fall height (without considering spread).

aa = Air core diameter at fall height (considering spread).

(i) For a particular geometry of vortex chamber evaluate the rate of water discharge Qw for values of fractional air core from 0·95 to 0·5 in steps of 0·5.

(ii) Using Aitken interpolation evaluate values of f for values of Qw from 0·01 to a maximum of 0·60 in steps of 0·01 (Cusecs).

(iii) Use values of Qw and determine terminating values Vm and Hm.

(iv) For the values of Qw, determine water volumes W2 & W3.

(v) Also for values of Qw determine air core volumes A2 and (A + A2)

(vi) Determine time taken to fill volume (W2 + W3) at the rate Qw i.e. $T = (W2 + W3)/Qw$.

(vii) Determine air flow rate $\frac{A}{T}$.

(viii) Determine throat velocity of the air considering air core diameter a.

(ix) If the throat air velocity is less than Vm then the air entrained into the shaft is as determined by step (vii).

(x) If throat velocity of the air is greater than Vm, then air entrained into the shaft is determined by the product of the area of air core and Vm.

The above procedure is repeated for several water discharges and shaft lengths varying from 15 feet to 3 feet in steps of 3 feet. The results of this theoretical analysis are presented in figures 6·21-6·25 alongside the experimental results.

2·20 HYDRAULIC THEORY WITH AN ANNULAR JUMP

The process of air entrainment with an Annular Hydraulic Jump is greatly dependent on the surface area, (mainly the length) of the jet exposed/

jet exposed to the air or atmosphere. This fact can be demonstrated by placing a container at different distances, from the exit of a domestic water tap. It will be evident that, with the rate of water flow from the tap maintaned constant, more air bubbles will be engulfed into the container with the increase of fall. This illustrates that more air was enveloped in the jet when it had a longer path of travel before impact. This phenomenon is evident in plates 2·1 (A, B and C).

Hence the criteria required to be investigated is the spread of the Annular jet. Abramovich (9) describes the growth of a circular jet to be linear.

As mentioned in Section 1·22 Viparelli derived an empirical relationship for the air-water ratio with the ratio of Fall to Diameter, as follows:-

$$\frac{Qa}{Qw} = 0{\cdot}022 \left(\frac{h}{d}\right)^{3/5} \qquad \ldots\ldots\ldots 1{\cdot}22$$

where d is the shaft diameter and h is the free fall of the annular jet. It will be seen later as in 5·30 and figure 6·30 that the experimental results from the present study with a jump in the shaft, shows accordance with Viparelli's relationship except for discrepancies due to possible scale effects.

Hence using Viparelli's relationship, a study is made with a view to evaluate the spread of the annular jet for different flows and shaft sizes.

To establish a plausible theory as to the spread of an annular jet the procedure adopted by Abramovich (9) for a circular jet is closely followed.

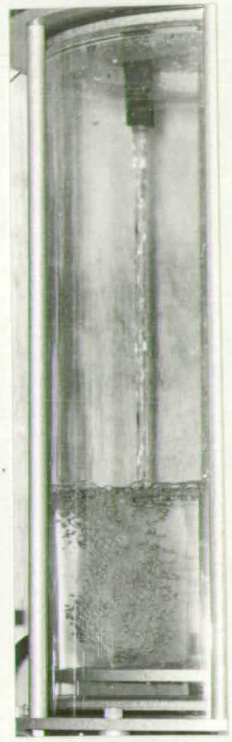

(A)

Long

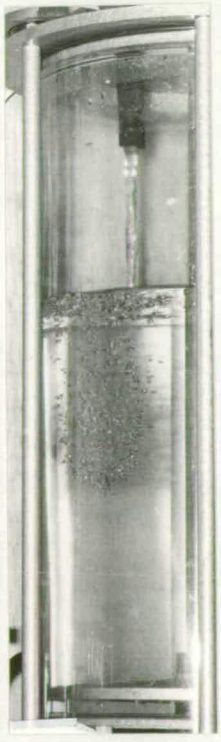

(B)

Medium

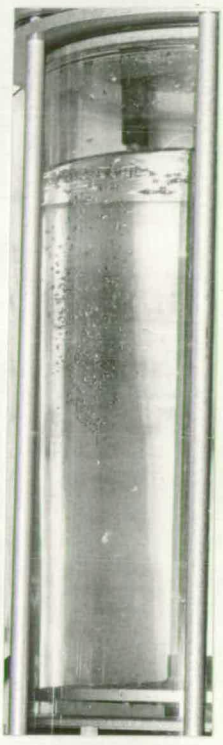

(C)

Short

Plate 2·1 EFFECT OF JET LENGTH ON AIR ENTRAINMENT.

2·21 Spread of an annular jet.

Considering the turbulent annular jet, the components of velocity at any point can be divided into a time averaged value and a randomly varying peturbation.

Let the x direction be that parallel to the axis of the shaft and hence to the axis of the jet; y and z directions are those perpendicular to the x axis.

Let U and V be the velocity components in x and y directions.

Then due to the random variation in velocity which occurs about a mean

$$U = \bar{u} + u'$$

and $$V = \bar{V} + V'$$

If the "mixing length" is equal to L then

$$\Delta\bar{u}' = L\frac{\partial\bar{u}}{\partial y}$$

It then follows that

$$u' \propto L\frac{\partial\bar{u}}{\partial y}$$

By considering the rate of mass flow it may be assumed that

$$-V' \propto u'$$

Hence $$-V' \propto L\frac{\partial\bar{u}}{\partial y}$$

Due to the experimental results shown by Abramovich in which the velocity profiles indicate the similarity of boundary layers in different cross-sections of a free stream, it is possible to write the following

$$\frac{L_1}{(d - a_1)} = \frac{L_2}{(d - a_2)} = \text{Constant} \quad \ldots\ldots\ldots 2\cdot21A$$

where L is the length of the jet considered

d/

d is the diameter of shaft

and a is the diameter of the air core

Let (d - a) the thickness of the annular ring be equal to r.

From 2·21A it is possible to establish a law for the growth of the jet as a function of distance along the axis of the jet, in order to determine the way in which the mixing lengths increase. Prandtl assumed that the rate of increase of thickness of the jet boundary is dependent on the peturbation velocity.

So that $\frac{dr}{dt} \propto V'$

Since the velocity profiles at different cross-sections are similar, it is evident that

$$\frac{\partial \bar{u}}{\partial y} \propto \frac{\bar{u}}{r}$$

So $$\frac{\partial r}{\partial t} \propto \frac{l\partial \bar{u}}{\partial y} \propto \frac{l\bar{u}}{r} \qquad \text{.....2·21B}$$

But from the rate of growth

$$\frac{dr}{dt} = \frac{dr}{dx} \cdot \frac{dx}{dt} \propto \frac{dr}{dx} \cdot \bar{u} \qquad \text{.....2·21C}$$

By comparing 2·21B and 2·21C it is evident that

$$\frac{dr}{dx} = \text{constant} \qquad \text{.....2·21D}$$

which indicates the outer profile of the jet is a straight line.

With reference to figure 2·5A

am = diameter of air core at terminating section assuming no spread.

ah = dieameter of air core at fall h assuming no spread.

aa = diameter at air core at fall h making allowance for spread.

Hence the net/

Spread of Annular Jet

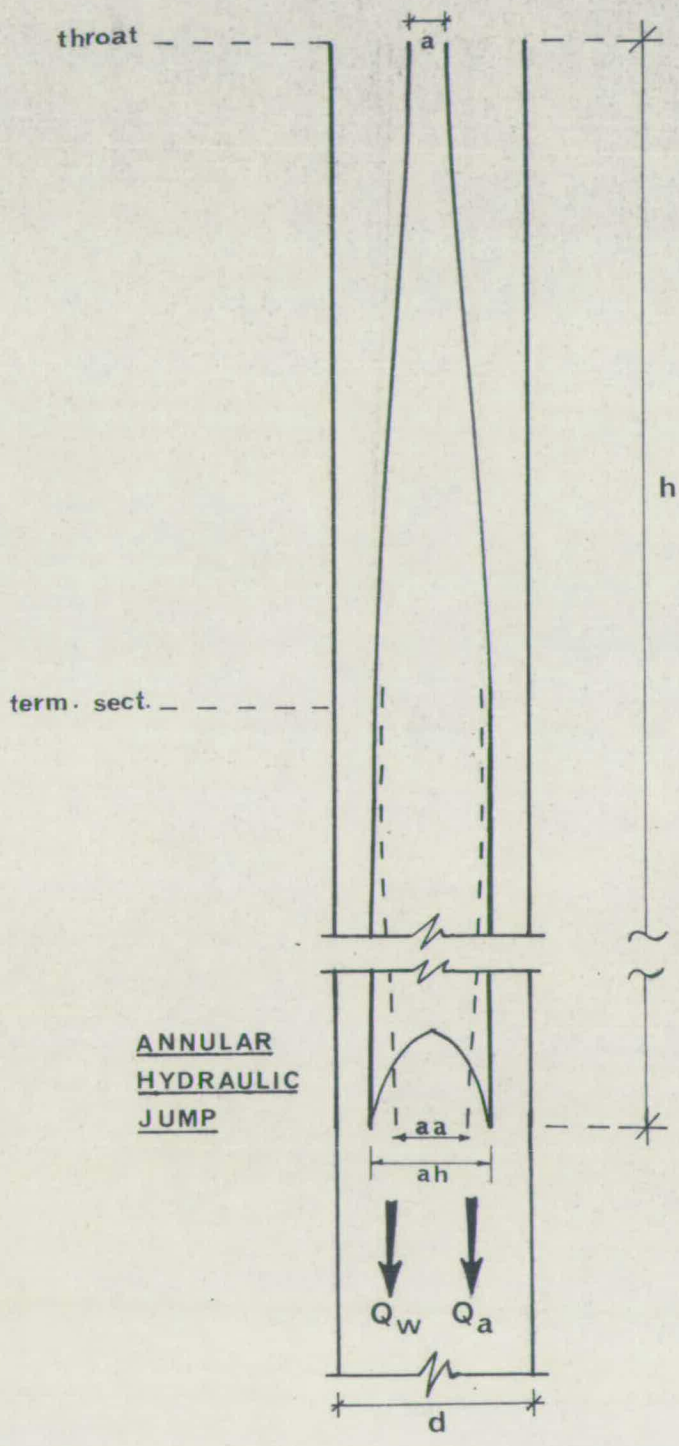

FIG. 2.5

Hence the net spread in the thickness of the annular jet is $(ah - aa)/2$.

However the water discharge $Qw = \frac{\pi}{4} (d^2 - ah^2) \times Vm$

Therefore the air enveloped due to the spread of the jet could be evaluated as, (with reference to figure 2·5)

$$Qa = \frac{\pi}{4} (d^2 - aa^2) Vm - Qw$$

i.e. $$Qa = \frac{\pi}{4} (ah^2 - aa^2) Vm \qquad \ldots\ldots\ldots\ldots 2\cdot21E$$

In the above equation the value of ah is obtained by considering the spread of the jet. By assuming the preceeding theory, that the growth of the jet is linear (from 2·21D) it can be written that

$$\frac{ah - aa}{2 \cdot h} = C \quad \text{constant} \qquad \ldots\ldots\ldots 2\cdot21F$$

where C is the linear constant of growth.

At this stage it is necessary to utilise the experimental results in section 5·31 to evaluate the value of the constant C. The results of a computer program (No. CIE 018/0026) which produced the values of C are plotted in figure 2·6.

The family of curves in figure 2·6 indicates the variation of the growth constant C with various water discharges in the five shafts. It is evident that a linear relationship exists between C and Qw for values of water discharge higher than about 20% of the maximum flow of each model tested.

From Figure 2·6 the variation of water discharge Qw with linear growth of jet C is very nearly in the form $Qw = M.C$

Values of m are as shown in table 2·1..

Variation of Water flow with Jet Growth

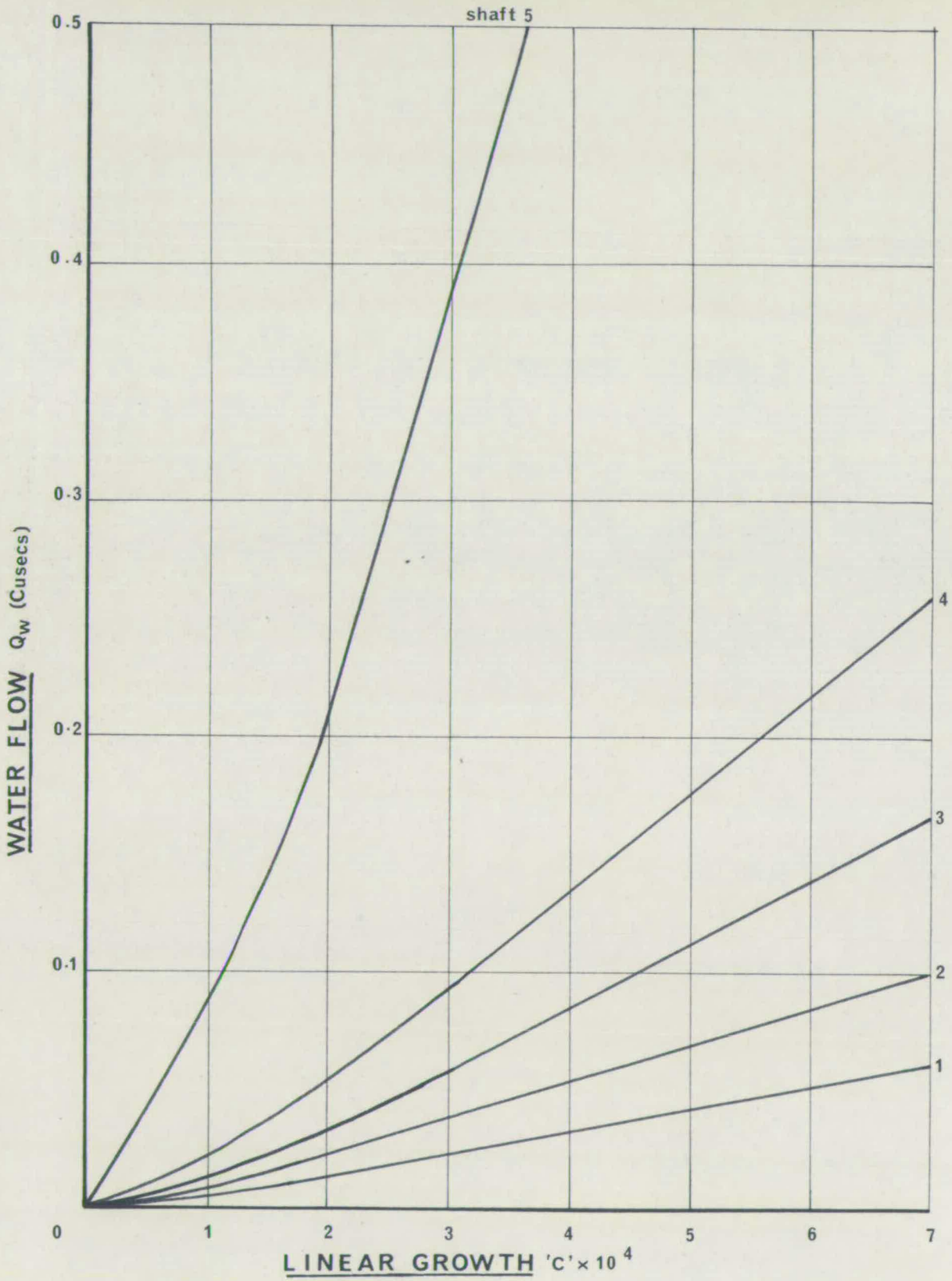

FIG.2.6

Shaft Number	Shaft Diameter (ins.)	gradient m
1	1·375	96
2	1·750	125
3	2·250	200
4	2·750	292
5	5·750	1630

From figure 2·7 the variation of m (as defined above) with shaft diameter D in indies is as follows:-

$$m = 46D^{1\cdot93}$$

Therefore $C = Q_w/46D^{1.93}$

Table 2·1

Effect of Geometry on the Growth

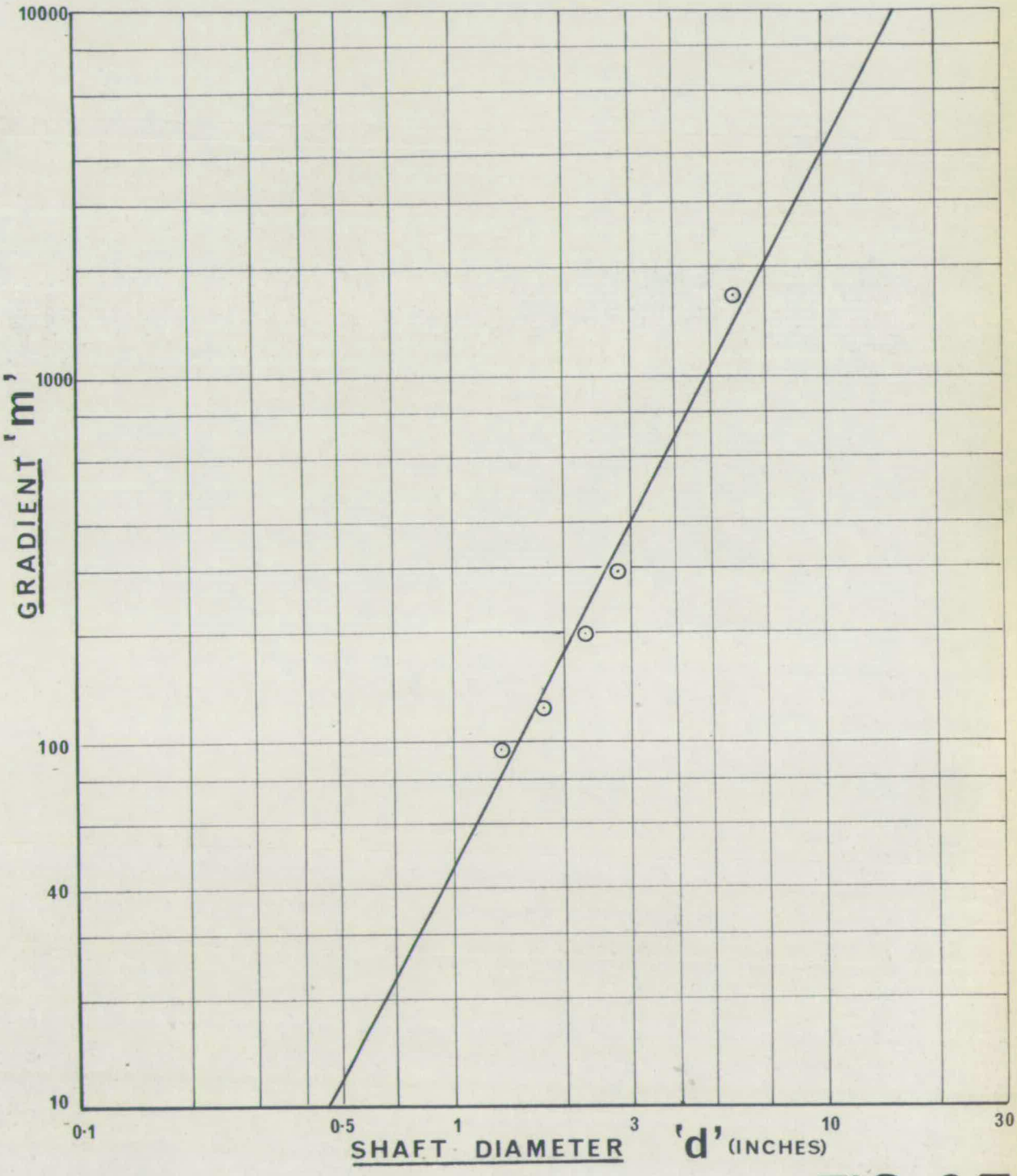

FIG. 2.7

Hence, it can be written, for a particular shaft

$$Q_w = m.C \qquad \text{.....2·21G}$$

where $m = f(D)$ D = shaft diameter in inches

d = shaft diameter in feet

From figure 2·7 it is evident that

$$m = 46(12d)^{1·93}$$

From 2·21G $C = \frac{Q_w}{m}$

therefore $C = \frac{Q_w}{46.(12d)^{1·93}}$ .....2·21H

Substituting for C in equation 2·21F

$$\frac{ah - aa}{2h} = \frac{Q_w}{46.(12d)^{1·93}}$$

i.e. $aa = ah - \frac{2h \times Q_w}{46 \times (12d)^{1·93}}$ .....2·21I

From 2·21E $Q_a = \frac{\pi}{4}(ah^2 - aa^2) V_m$

which can be evaluated by substituting for aa and determining ah and V_m as described earlier in section 2·12.

2·22 Method of Computation.

The method of computation of the rate of air entrainment with a jump does not yield to rigorous analysis as much as for the case with free flow. Never-the-less repetitive computation of the terminating velocity and the growth of the annular boundary involves considerable mathematical manipulation. To facilitate such a procedure a computer program (CIE 018/0026) has been developed. With reference to Notation [3] and flow diagram in figure 2;8, the steps of the computer program are outlined as follows:

(i) For a particular geometry of the vortex chamber evaluate Q_w and f.

(ii) Using Aitken interpolation evaluate values of f for given (regular) values of Q_w.

(iii)/

FLOW DIAGRAM FOR COMPUTER PROGRAMME No.CIE 018/0026

AIR ENTRAINMENT WITH AN ANNULAR HYDRAULIC JUMP

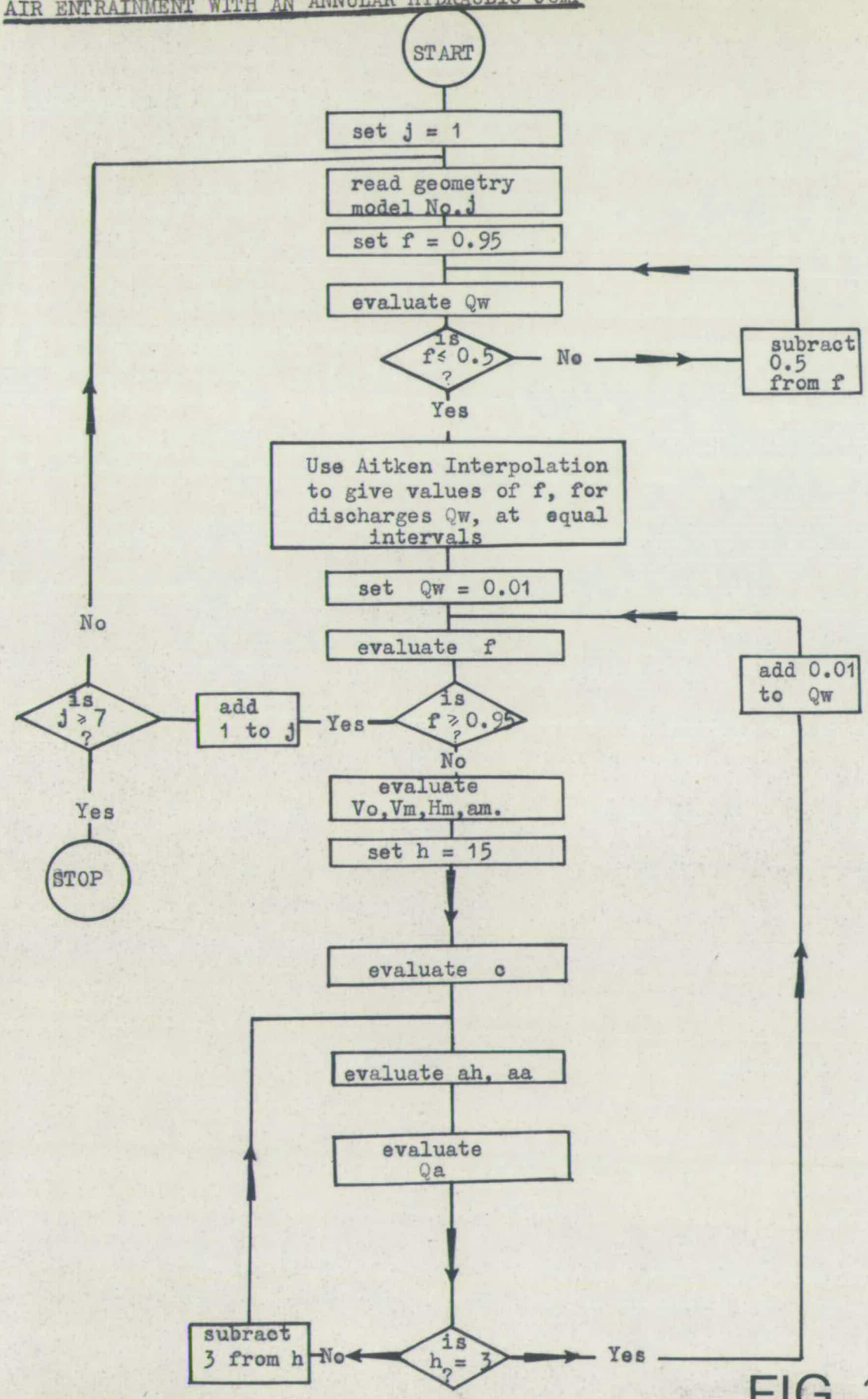

FIG. 2.8

(iii) Use values of Qw and determine terminating values of Vm and Hm.

(iv) For the particular Qw evaluate growth constant C.

(v) Evaluate air core areas ah (assuming no spread) and aa (assuming spread).

(vi) Evaluate Qa air entrainment.

2·30 CONCLUSIONS.

It is clearly evident from the theoretical analyses that air entrainment in vertical shafts is dependent upon the parameters constituting the entire air core. The length of the shaft has the greatest effect, which in turn is reduced in the case of a shaft, containing an annular hydraulic jump. In such cases the free fall has a considerable effect.

The underlying mechanism of air entrainment in vertical shafts as expressed in this chapter could be concluded as (i) Suction effects due to increase in the volumetric air core in the shaft and (ii) the spread of the annular water jet as it falls, thus enveloping air, and engulfing it on impact. The first case predominates when the free flow condition exists and the second case when the jump is present.

The theory which has been developed in this chapter is compared in Chapter 5 with the experimental results. Although the first theory has been purely analytical the second theory for the spread of the water surface is semi-empirical.

In this analysis a vortex entry with the shaft is assumed, which affords an orderly manner of flow in the shaft and facilitates its analysis. However, the process of Air Entrainment due to any other form of entry would be the same though its method of analysis would differ.

CHAPTER III

DESCRIPTION OF APPARATUS

3·00 INTRODUCTION

It is generally accepted that very great importance is now attached to the use of scale models, as an aid, not only to Hydraulic Engineering design, but also to its research. Although for economic reasons it is desirable to utilize models of small size, the scale effects which constantly persist, demand the need for the model size as close to the prototype as possible.

In the present study, the main features of the apparatus are the five scale models of a proposed drop shaft and intake. Of these five, the smallest model has been the basis for previous investigations[13] which on the execution of certain modifications, rendered satisfactory results for its performance. A report of these investigations is as attached in Appendix B.

3·10 CHOICE OF SCALE

The two limits of the model scale were determined by the availability of shaft sizes; smallest as mentioned in 3·00 and the largest by the use of the main tunnel (see Figure B.1). These scales were 1 in 15·25 and 1 in 3·65. The remaining three intermediate scales were determined by an even distribution and by the availability of shaft sizes in the market. These scales were 1 in 12, 1 in 9·34 and 1 in 7·65. The models were named as Numbers 1 to 5 with 1 being the smallest.

3·20 DETAILS OF THE MODEL

The dimensions of each model are as shown in Table 3·1. The overall length/

Dimensions of Vortex Chambers and Shafts

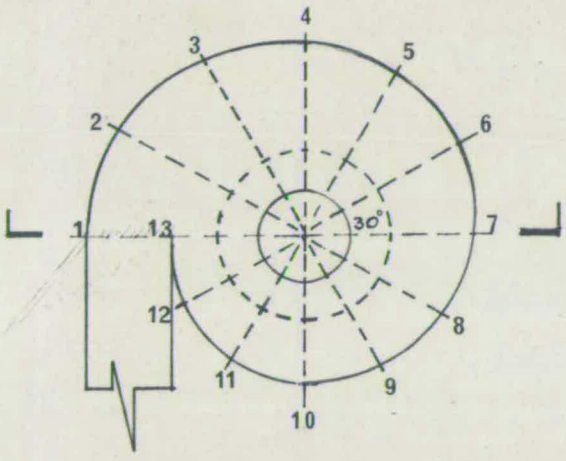

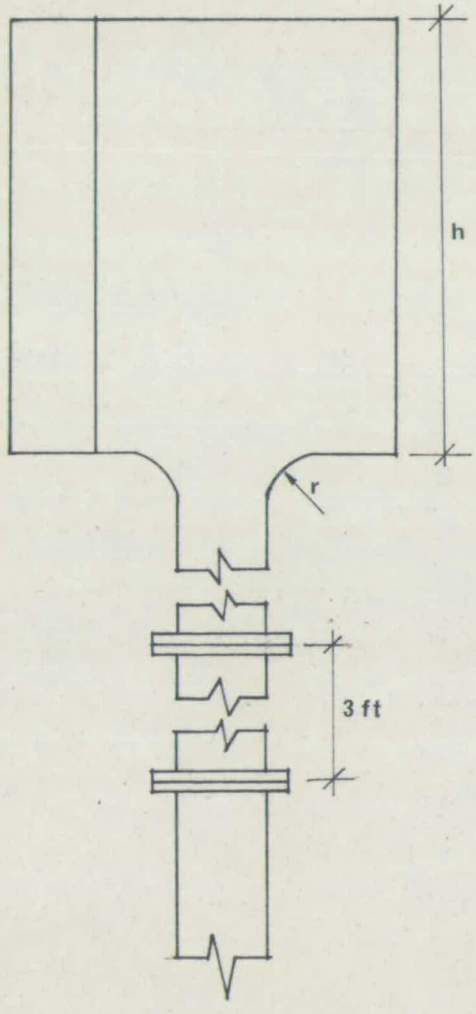

Mod. No	1	2	3	4	5
Scale	1:15.25	1:12.00	1:9.34	1:7.65	1:3.65
Dia.(d)	1·375	1·750	2·250	2·750	5·750
Rad.(r)	1·18	1·50	1·93	2·36	4·93
Ht. (h)	6	10	13	16	33
Sect.1	3·93	5·00	6·42	7·85	16·42
2	3·80	4·84	6·20	7·59	15·90
3	3·67	4·66	6·00	7·31	15·45
4	3·45	4·50	5·78	7·05	14·80
5	3·41	4·34	5·56	6·80	14·30
6	3·28	4·16	5·45	6·54	13·70
7	3·14	4·00	5·14	6·26	13·15
8	3·02	3·83	4·93	6.01	12·60
9	2·88	3·67	4·67	5·75	12·05
10	2·75	3·50	4·50	5·50	11·50
11	2·62	3·34	4·28	5·25	11·00
12	2·49	3·17	4·06	4·95	10·40
13	2·36	3·00	3·85	4·75	9·85

All dimensions are in inches;

Tabulated dimensions for each Section are from the Centre of shaft to edge of Vortex Chamber.

FIG. 3·1

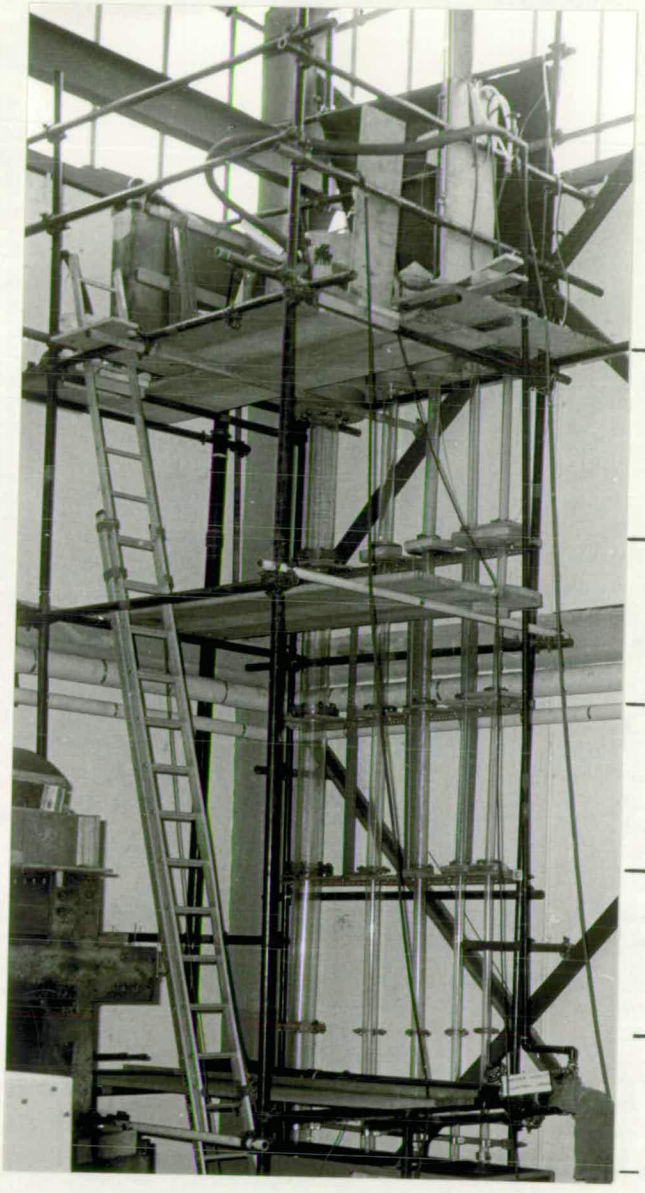

Plate 3•1A GENERAL ARRANGEMENT OF MODEL.

length of each shaft is 15 feet and their effective lengths with respect to the appropriate scale are as established in the Table 3·1. Each shaft comprised of 3 feet lengths of shaft, fixed together by standard flanges.

The spiral form of each vortex chamber is as shown in Figure 3·1. The approach channels for all the chambers except for No. 5 were 3 feet in length, so as to avoid unreal hydraulic conditions in the channels. The approach length for chamber No. 5 constituted of an extra 2 feet length and, in addition, all the channels were provided with baffles to reduce undue turbulence.

3·30 CONSTRUCTION AND GENERAL ARRANGEMENT OF MODEL

The materials used in the construction of the model were sheet metal, wood and perspex. Perspex being a material increasingly adopted because of its transparency, is often of immense value as an aid to visual and photographic study. The four larger vortex chambers were made of sheet metal, while the other was made of wood.

The joints of the intakes were welded to ensure water tightness. The throats were made of glued laminated strips of wood, smoothened to produce a radius as illustrated in Figure 3·1. The gap between the metal edge and the top of the wood surface was smoothened further by a coating of polyfilla, as seen in Plate 3·2.

The general arrangement of the model is shown in Plate 3·1A and figure 3·2. The positioning of four small vortex chambers is as in Plate 3·1B. The five shafts were placed alongside one another, with their exits positioned on the upstream side of a 'V' notch tank./

General Arrangement of Model

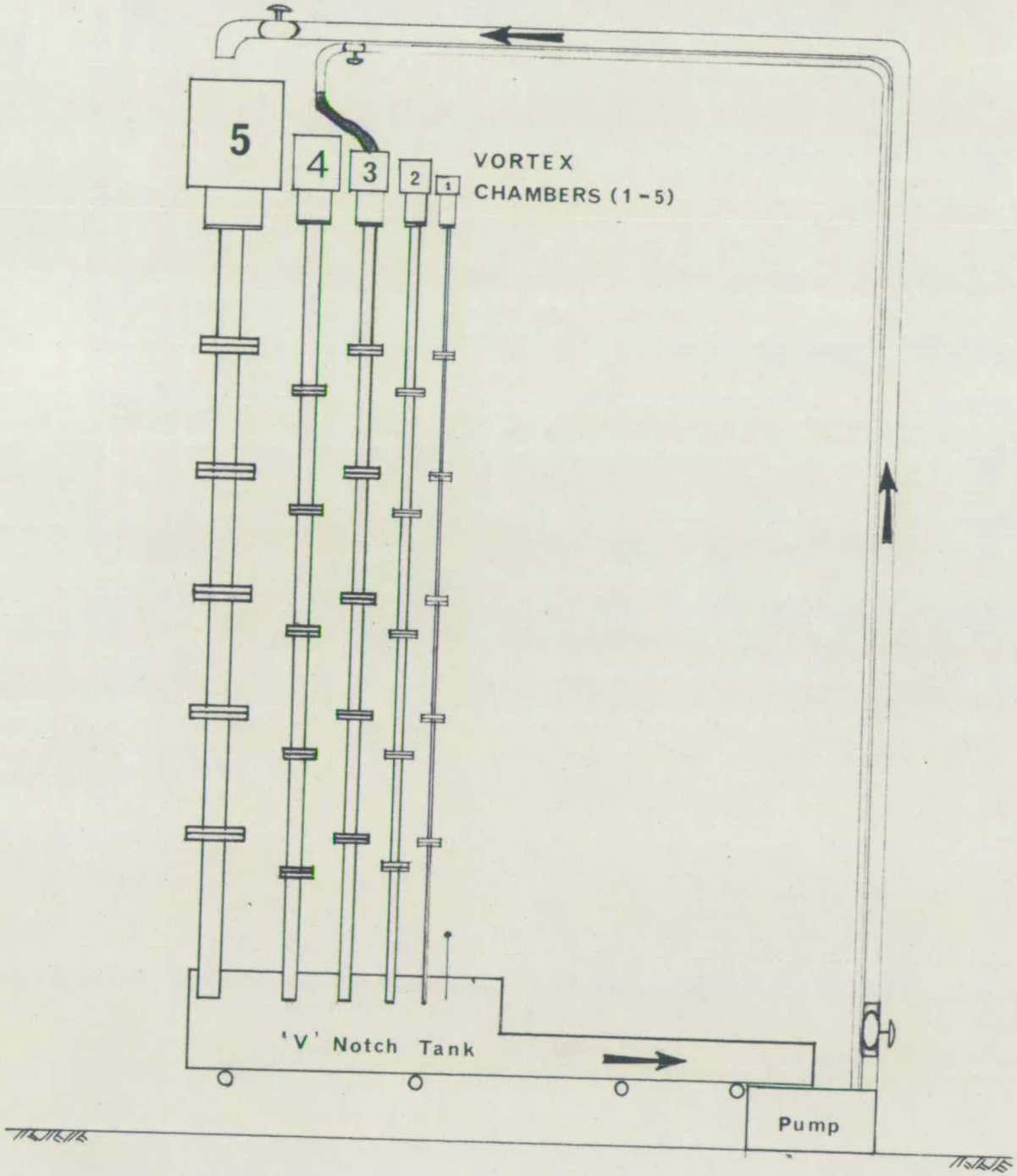

FIG. 3.2

General Arrangement of Model

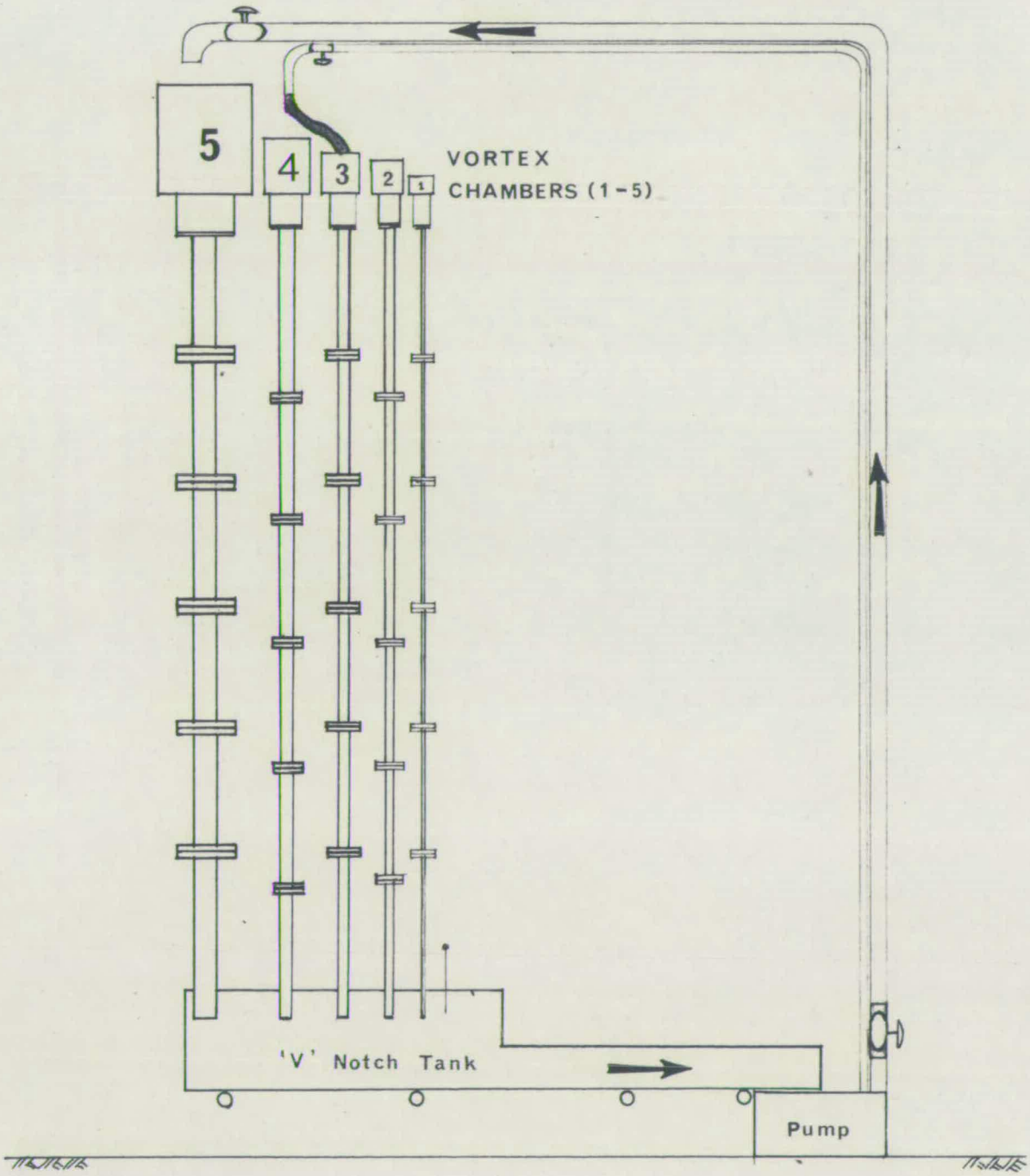

FIG. 3.2

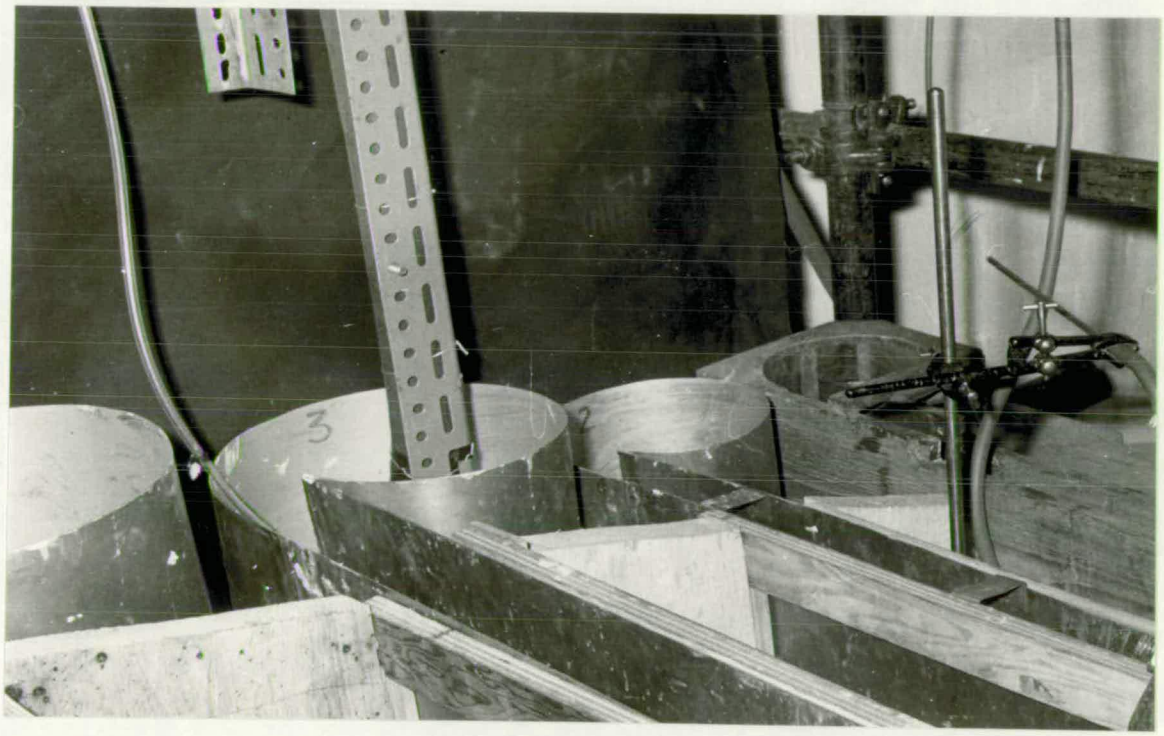

Plate 3·1B ARRANGEMENT OF VORTEX CHAMBERS.

Plate 3·2 SMOOTH ENTRY INTO THE SHAFT.

EDINBURGH UNIV. TEIL EX

MODEL DETAILS

Model Number	Model Scale	Inside diameter	Effective length	Chamber height
1	15·25	1·375 ins.	2·88 ft.	6 ins.
2	12·00	1·750 ins.	3·66 ft.	10 ins.
3	9·34	2·250 ins.	4·70 ft.	13 ins.
4	7·65	2·750 ins.	5·75 ft.	16 ins.
5	3·65	5·750 ins.	12·00 ft.	33 ins.

Table 3·1.

tank. The tank, shafts and the chambers were mounted on a rig having overall dimensions of about 20 ft. × 8 ft. × 8 ft. At the downstream end of the 'V' notch tank, was the supply tank in which an immersible pump circulated the water.

3·31 Air-flow meter.

The air flow meter is as shown in plate 3·3 and figure 3·3. It consists of an air blower as the supply, which is controlled by a Variac. Two perspex lengths of pipe of about 3 feet and 4 feet in length having an internal diameter of 1·375 ins. are flanged together. At the junction of the pipes, the orifice plate or the Davimeter is placed. At the end of the air flow meter a funnel enclosed the air demand into the shaft. Two funnels were necessary due to the variation in chamber size and from the funnel a pressure tapping was made. Plate 3·4 shows the pressure tapping.

3·40 DESCRIPTION OF EXPERIMENTAL STAGES

The experimental stages are divided into five series and dealt with, in detail in Chapter 5. Since it is necessary to discuss the special/

Air–Flowmeter

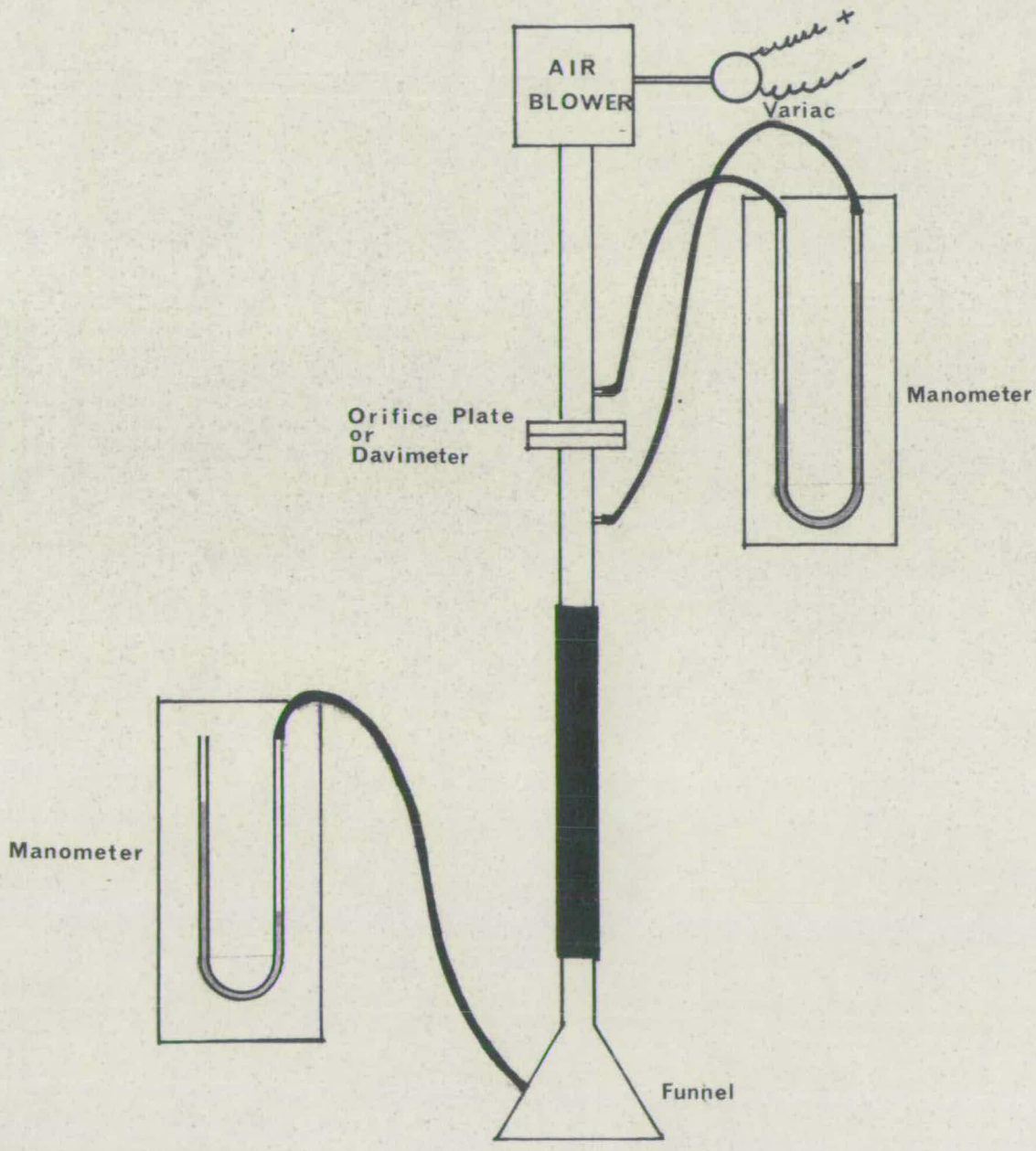

FIG. 3.3

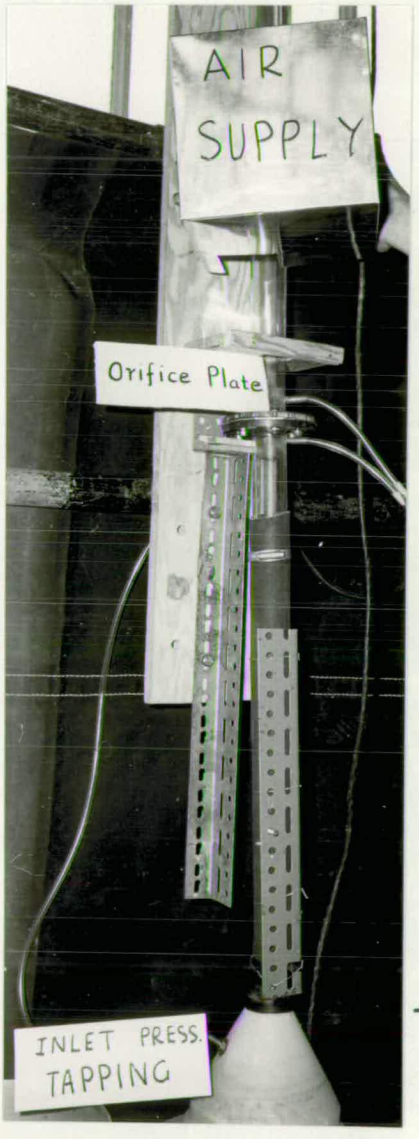

Plate 3·3 AIR-FLOW METER.

Plate 3·4 THE INLET PRESSURE TAPPING.

the special provisions required for the individual series of tests, brief descriptions of the stages will be given in this chapter.

3·41 Series I Tests.

The first series of tests involve the study of the Air Entrainment in Vertical Shafts with free flow in it. Full lengths of the shafts are considered which in fact, in some cases would be in excess of their effective lengths respective to the scale.

3·42 Series II Tests.

Series II tests are an extension of the former tests. In this series of tests the effect of shaft length on air entrainment is investigated.

3·43 Series III Tests.

The presence of an Annular Hydraulic jump is the main characteristic feature of this series of tests. The effect of the free fall of the water flow is studied.

3·44 Series IV Tests.

An investigation of the air bubble and air pocket motion is made in this series of tests. A detailed study is made on the 3rd shaft for this purpose.

3·45 Series V Tests.

Series V tests entail experimental verifications of two theories incorporated in the theoretical analysis. Air core variation with water discharge and velocity variation with height, is carried out on the 2nd shaft.

Special Provisions

Series I tests

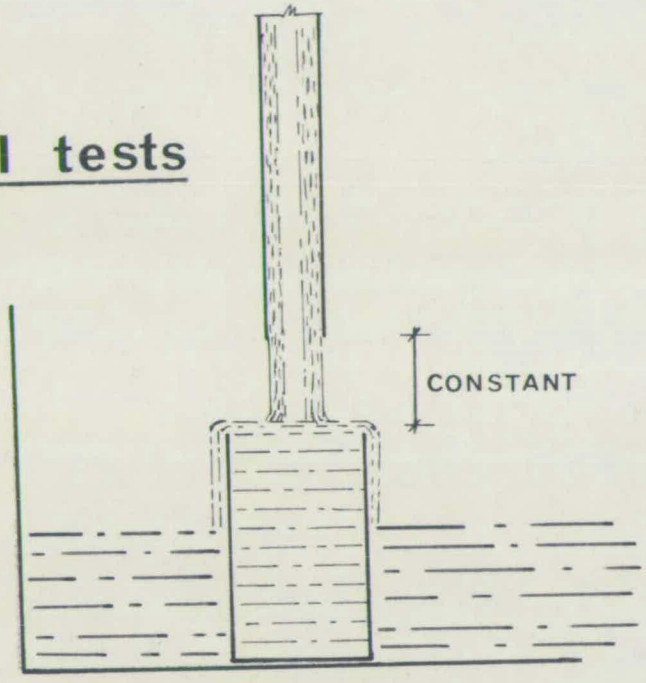

FIG. 3.4

Series II tests

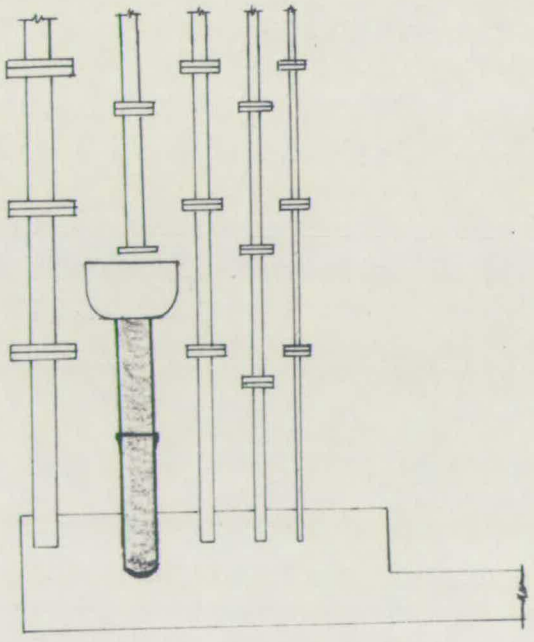

FIG. 3.5

3·50 SPECIAL PROVISIONS FOR INDIVIDUAL STAGES

3·51 Series I Tests.

Since the exit from each shaft is directed to the 'V' notch tank which is made use of to determine the water discharge, it is necessary to allow for the rise of the water level in the tank. The rise of water level in the tank with increase of water discharge reduced the length of air core in the shaft. Hence it was necessary to make a provision as in figure 3·4. The water from the shaft was made to fall into a larger diameter container which is taller than the maximum depth of water in the tank. Water which dropped into the container overflowed into the tank, maintaining the distance between the bottom of the shaft and the top of the container virtually constant.

3·52 Series II Tests.

To facilitate the effect of shaft length to be studied, it was necessary to carry out a series of air and water measurement with the removal of each 3 foot length from each shaft. This entailed the collection of water at each of these new exits. A collector with an adjustable length of 3 inch hosing was made available at each exit position of the shaft under test. The arrangement is illustrated in figure 3·5 and plate 3·5.

3·53 Series III Tests.

To demonstrate the drop shaft feeding a tunnel under pressure and thereby causing a column of water in the shaft, a pressure box is fixed at the end of each shaft as shown in fig. 3·6 and plate 3·6. The box has two main openings; one to connect the shaft and the other to release the water to the required height by means of the adjustable p.v.c. tube./

Series III tests

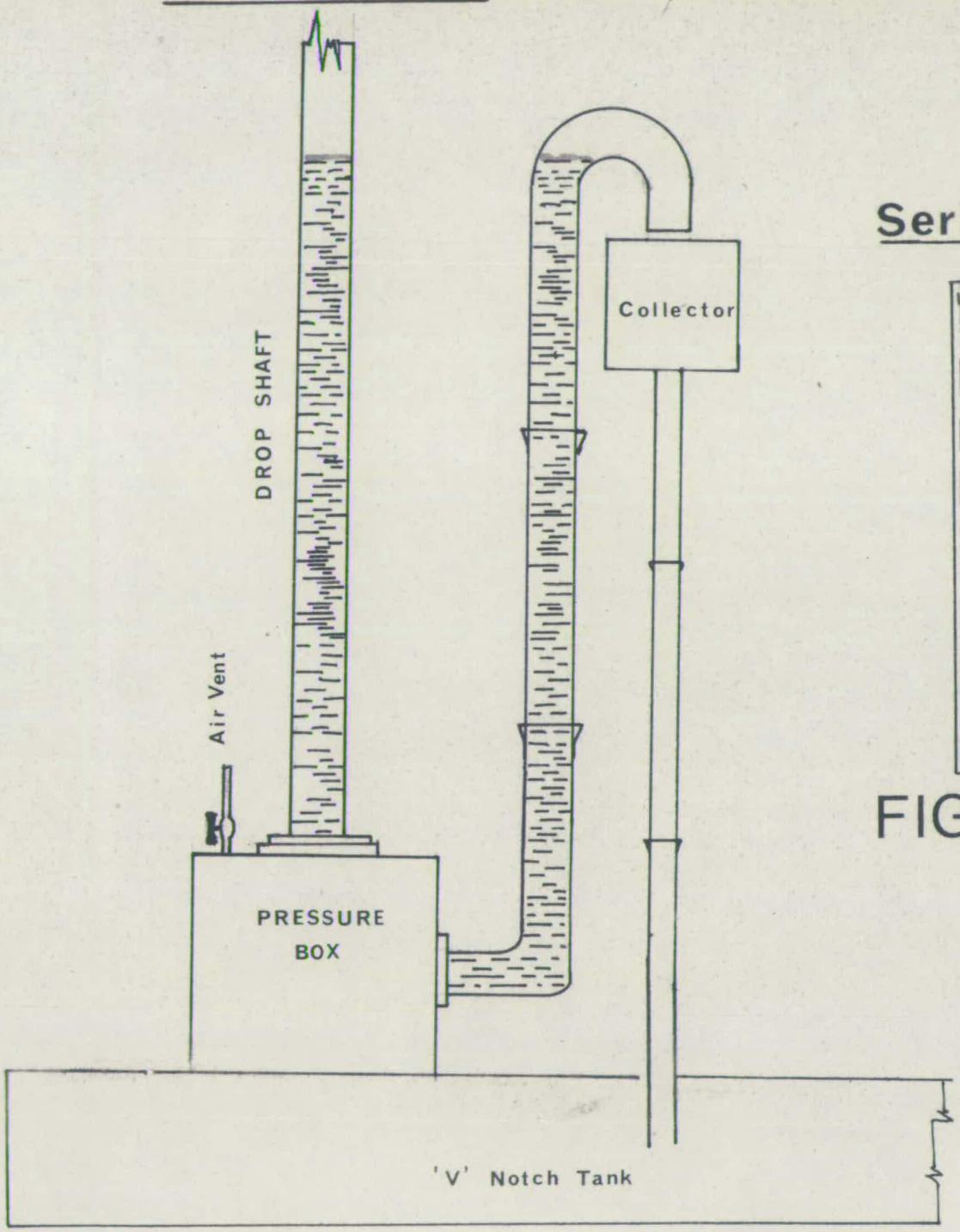

FIG. 3.6

Series V tests

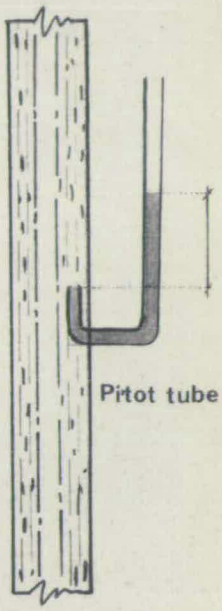

FIG. 3.7

Plate 3·5

Series II tests

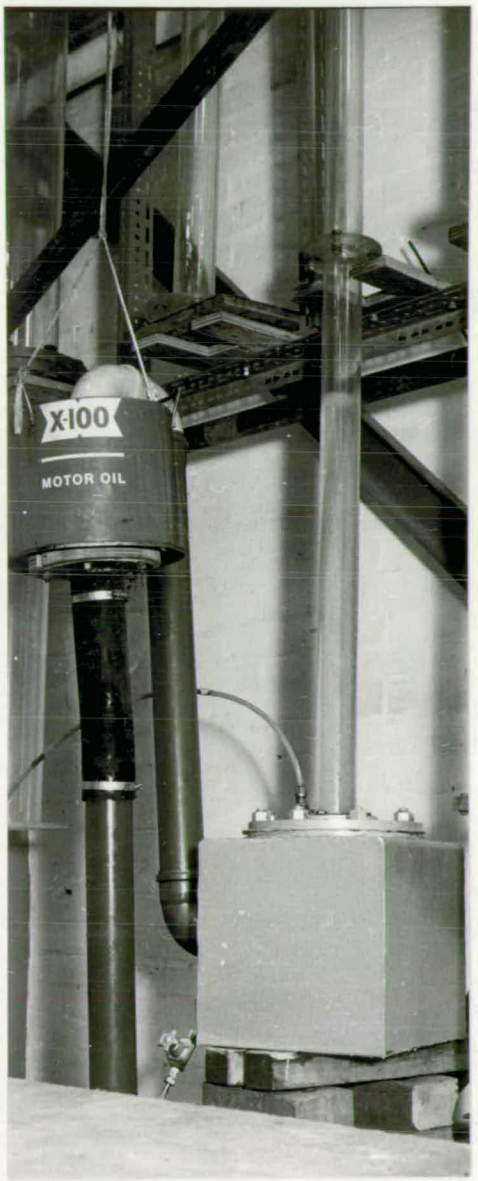

Plate 3·6

Series III tests

SPECIAL PROVISIONS

adjustable p.v.c. tubes. The tubes are available in 3 feet lengths which enables the standing column to be varied in 3 feet intervals. Water is returned to th 'V' notch tank via the collector used in the former series of tests.

3·54 Series IV Tests.

To determine the velocity of air bubbles rising upwards, no elaborate measuring instruments were used. By means of a stop watch the time taken for a bubble to rise was determined. By obtaining repetitive measurements, the results were found to be reasonably consistent.

3·55 Series V Tests.

This series of tests involved the measurement of the air core diameter at the throat of the vortex drop, and this was carried out by using a pair of Callipers.

The tests also required the measurement of velocity along the length of the shaft. Being a vertical flow, the standard N.P.L. type of pitot tube could not be used. Instead a bent tube as displayed in Fig. 3·7 was necessary.

3·60 CONCLUSIONS

Elaborate instruments were not utilised in the apparatus except for the measurements of the two important quantities i.e. air flow and water flow, where the apparatus was selected to ensure accurate results.

CHAPTER IV

EXPERIMENTAL TECHNIQUES

4·00 INTRODUCTION

Fundametntal considerations in model technique were based on the information provided by various authors (10), (11) on the subject. Geometric Similarity was maintained, except for the shaft lengths, which were all retained equal and their individual effective lengths taken into consideration.

The two main experimental measurements were that of air flow and water flow. Due to the wide range of flow, reliance on a single system, lacked confidence. However, collaboration was maintained between the systems employed.

Elaborate techniques were not adopted in the measurements of air bubble and pocket motion but the consistency of the experimental results yielded much scope for investigation. This was also the case in the experimental verifications of the two theories co-ordinated in the theoretical analysis.

4·10 CALIBRATIONS

The flow measuring instruments were calibrated against standardised instruments. Calibrations were conducted in accordance with British Standards 1042 and 3680 Part 4a of 1965. The results of the calibrations were re checked wherever possible.

4·11 Calibration of Water flow meter.

The water discharge through each drop shaft was determined by measuring the head over a 'V' notch.

The 90°/

Experimental Set Up for 'V' Notch Calibration

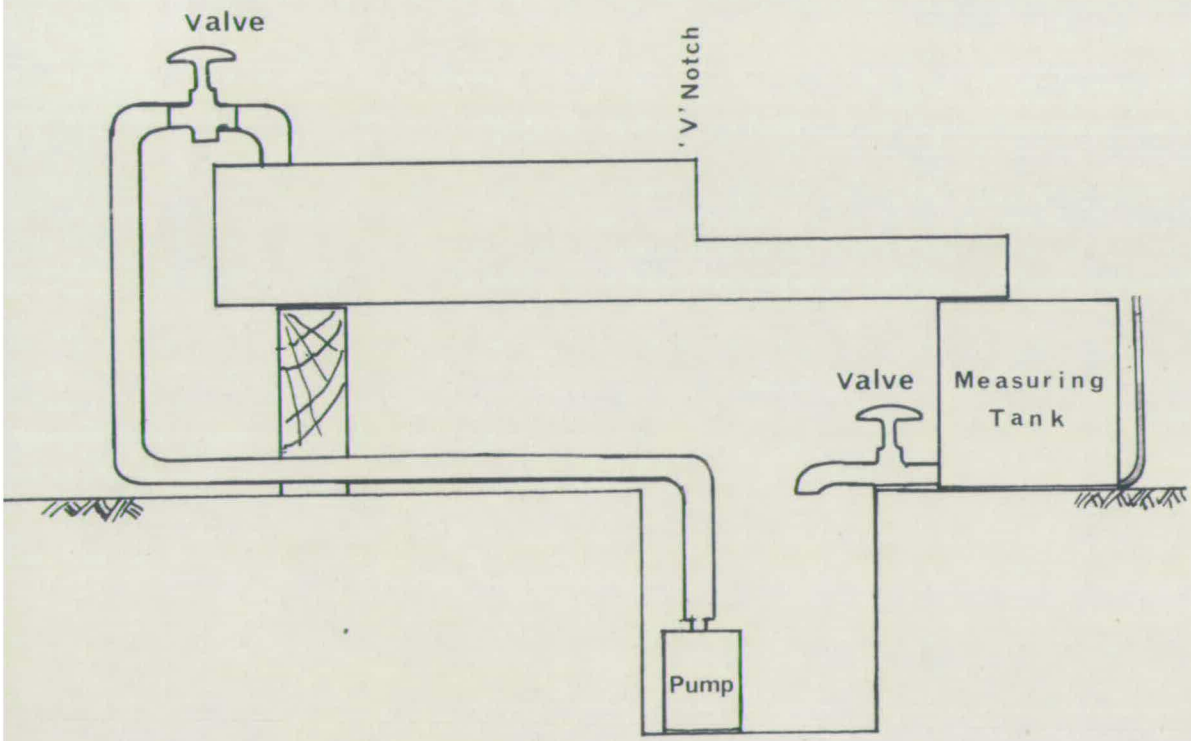

FIG. 4.1

The 90° triangular weir was capable of measuring a maximum head of 0·6 feet, which corresponded to a maximum discharge of 0·662 cusecs. The needle gauge measuring the head in decimals of a foot, was capable of measuring up to a thousandth of a foot and was situated 3 feet away from the notch.

The calibration of the Vee notch was carried out by placing the 'V' notch tank horizontally over a second tank as shown in fig. 4·1. The calibration tank was 2' × 3' × 4' having the facility to measure the depth of water, through a glass tube, thus enabling the discharge into the tank to be determined.

During the calibration, water was pumped from the sump into the 'V' notch tank, from where the water returned through the calibration tank into the sump. When steady conditions were observed at the needle gauge the outlet valve of the calibration tank was closed, noting time taken for the water level to rise a known height. The rise of level of one foot in the tank was equivalent to six cubic feet, hence the discharge.

This simple method of collecting and measuring the quantity, though rather elementary, affords confident results. This method was directly used in the case of very small water discharges and also for some of the flows through the first drop shaft. This enabled the accuracy of the water discharge over the notch to be checked specially at very low heads. The results of the calibration are as presented in Table 4·1 and plotted as in fig. 4·2. The results processed in the computer program (No. CIE 018/0011) gave the following relationship and also values of discharge, for head increases of 0·001 ft. up to a maximum head of 0·600 feet.

'V' Notch Calibration

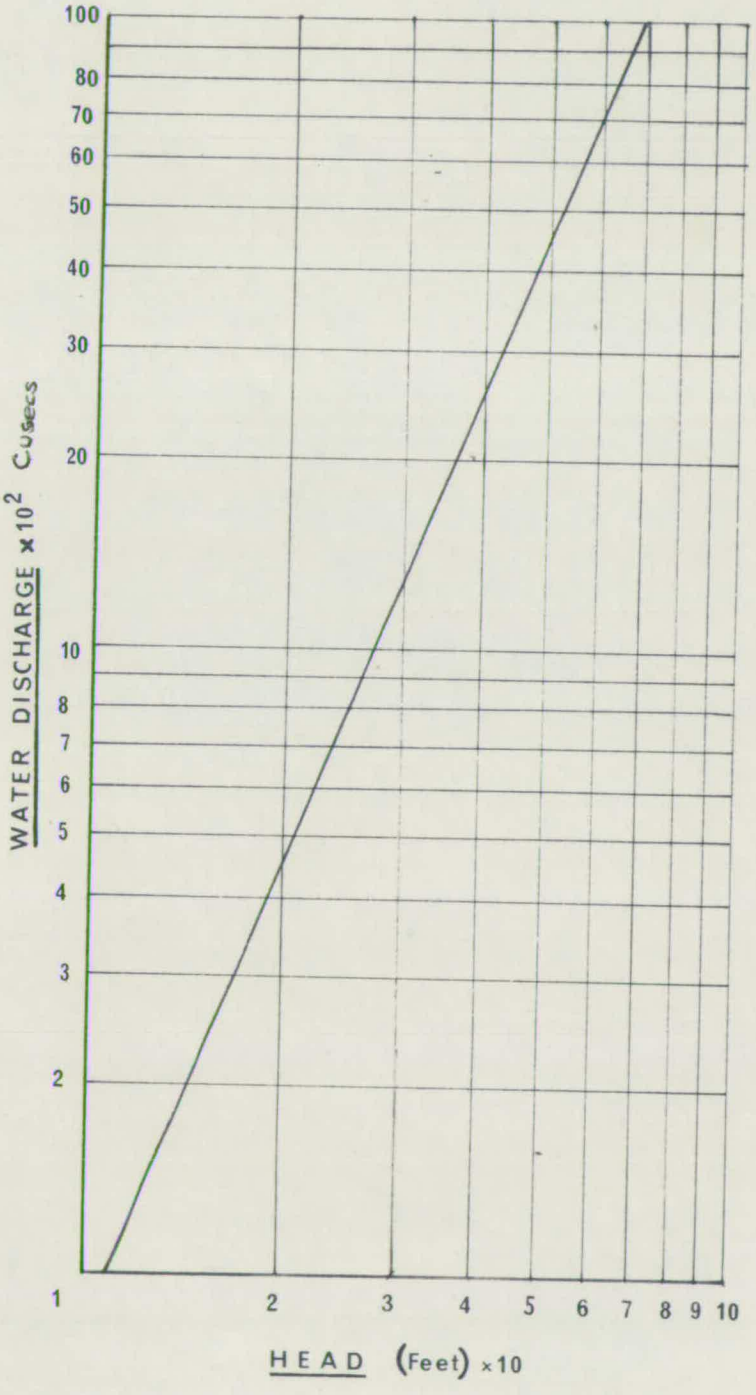

FIG. 4·2

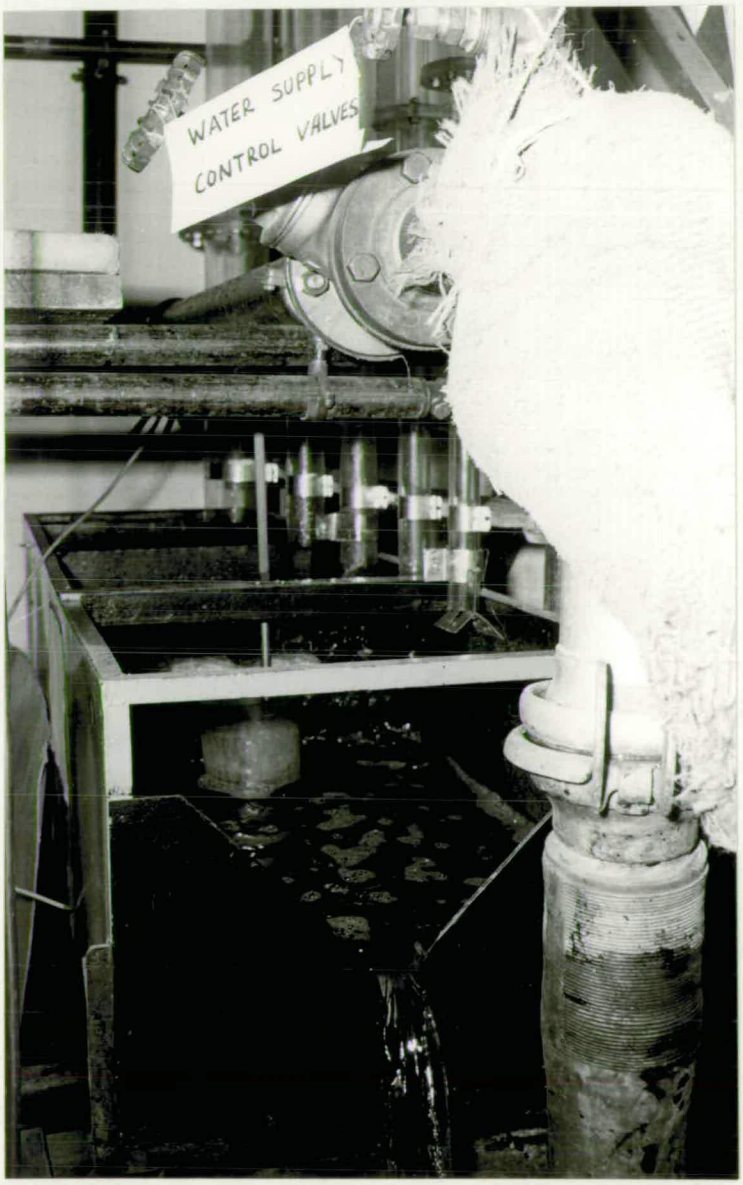

Plate 4.1 POSITIONS OF DROP SHAFT EXITS AND 'V' NOTCH.

$Q = 2{\cdot}317\, H^{2{\cdot}44}$

where Q = discharge in cusecs

H = head in feet.

Gauge Reading (ft.)	Head (ft.)	Discharge (Cusecs).
0·523	0·353	0·1918
0·433	0·263	0·0950
0·340	0·170	0·0320
0·446	0·276	0·1159
0·390	0·220	0·0630
0·493	0·323	0·1595

Table 4·1.

Plate 4·1 illustrates the positioning of the drop shaft exits and the flow over the notch.

4·12 Calibration of Air flow meter.

The measurement of air into the shaft varied a great deal, so much that a single specific method was not sufficient. The principle adopted in general was the same in all cases which was to supply air into the funnel at the intake so that the atmospheric pressure was maintained at the entry. This supply of air was to be measured and the description of the components incorporated in the air flow meter are as given below.

Calibration of Orifice plates.

Orifice plates were designed in accordance with B.S.1042. Each orifice plate was placed in position as shown in figure 3·3. The orifices/

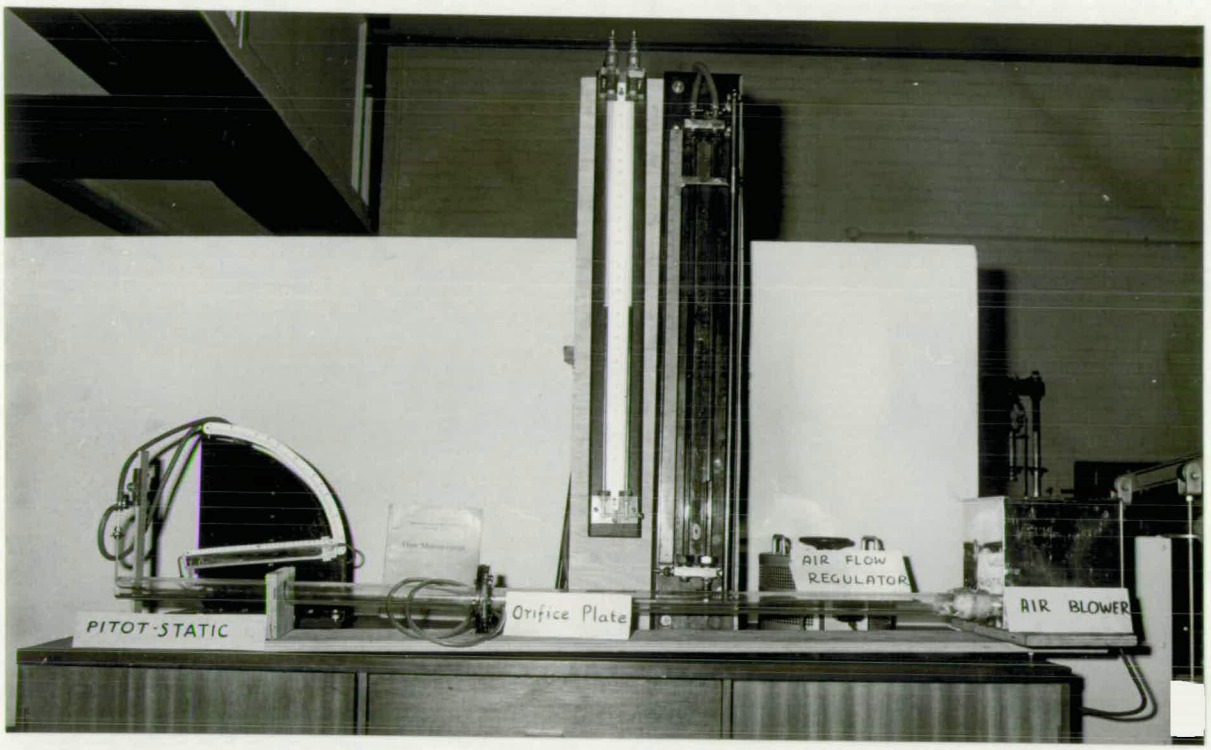

Plate 4•2

Plate 4•3 CALIBRATION OF AIR-FLOW METER.

orifices were calibrated against a pitot static tube and the experimental set up of the calibration is as presented in plates 4·2 and 4·3. An air blower was made use of to supply the air and was controlled by a variac. A pitot static tube at the end of the shaft indicated the velocity distribution across the shaft. The difference in pressure across the orifice plate was recorded on two manometers: methanol for low pressure differences and mercury for high pressure differences. The orifice plates and the manometers are illustrated in Plate 4·4.

For the range of air flows required i.e. 0·0025 cusecs to 0·3250 cusecs it was apparent that at least four orifice plates were necessary. Their design conformed to the B.S. except the small orifice whose diameter was 0·20 ins. The limits specified in the code are from 0·25 inches to 0·707 D inches where D is the internal diameter of the shaft. The flow rate with the smallest orifice required a further calibration against a more sensitive instrument, for which a hot wire anemometer was used. The calibration curve of the hot wire anemometer is as shown in figure 4·3.

The results of the calibrations are plotted on a logarithmic base as in figure 4·4. They gave the following relationships for the discharge through the orifices.

Qa = air flow in cusecs

hw = head difference in ft. of water

$$Qa = mhw^{n}$$

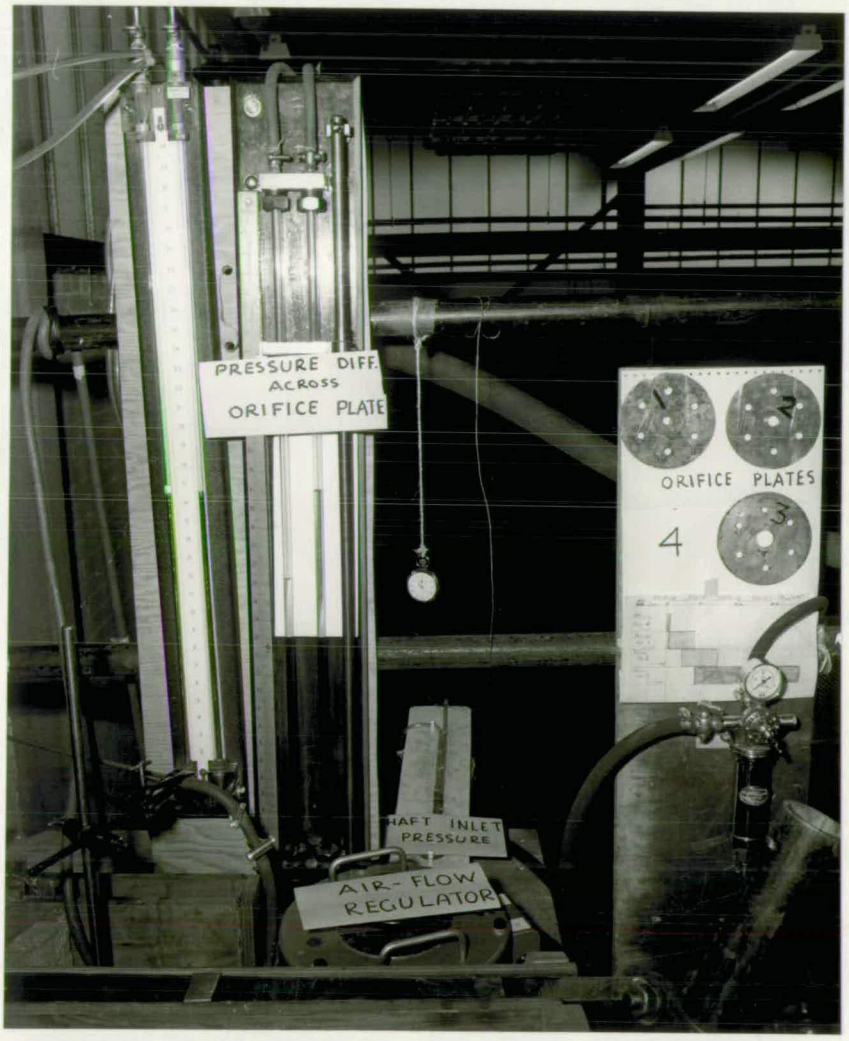

Plate 4.4. THE ORIFICE PLATES AND MANOMETERS.

Hot wire Anemometer Calibration

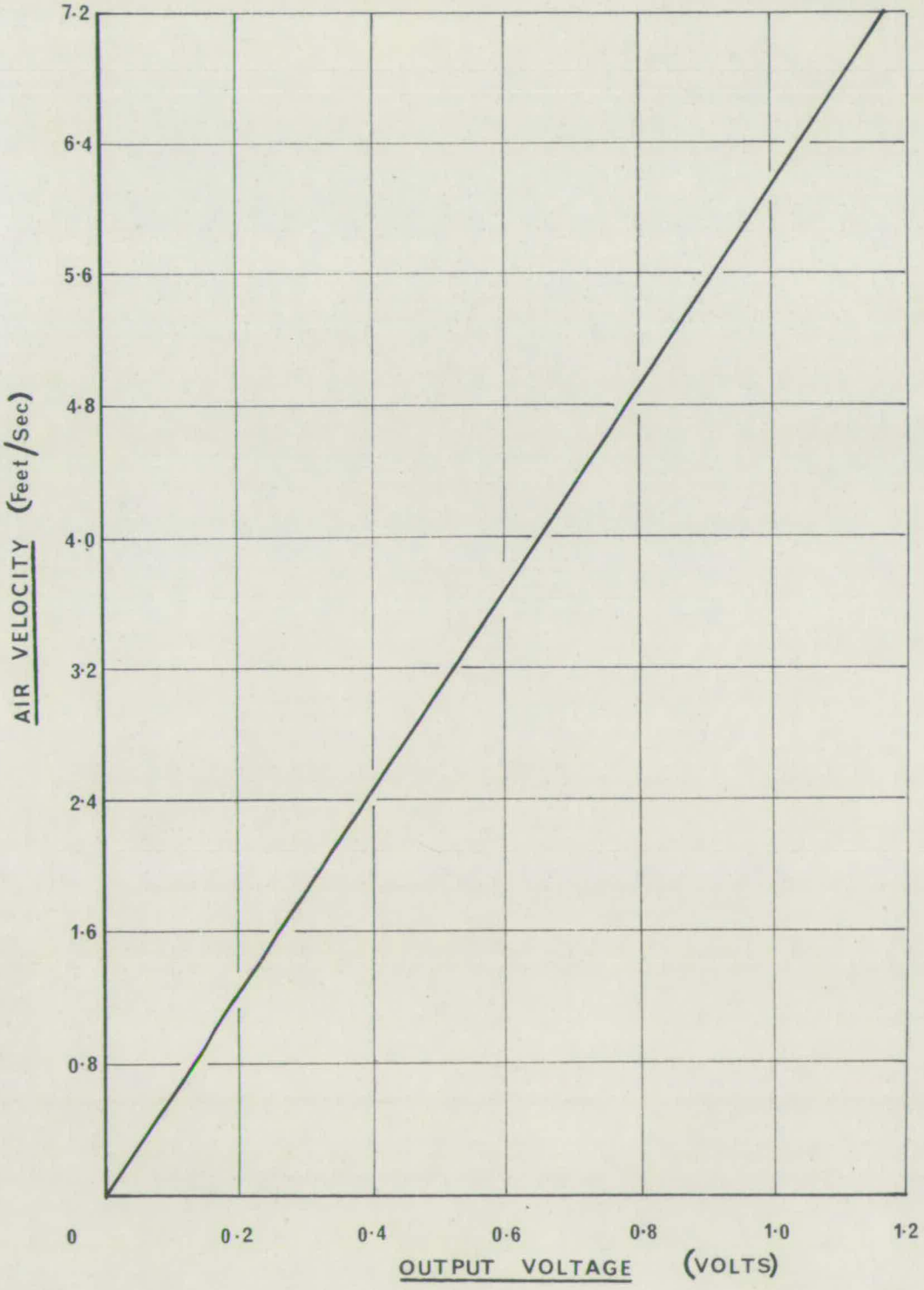

FIG. 4·3

Calbration Curves for Orifice Plates

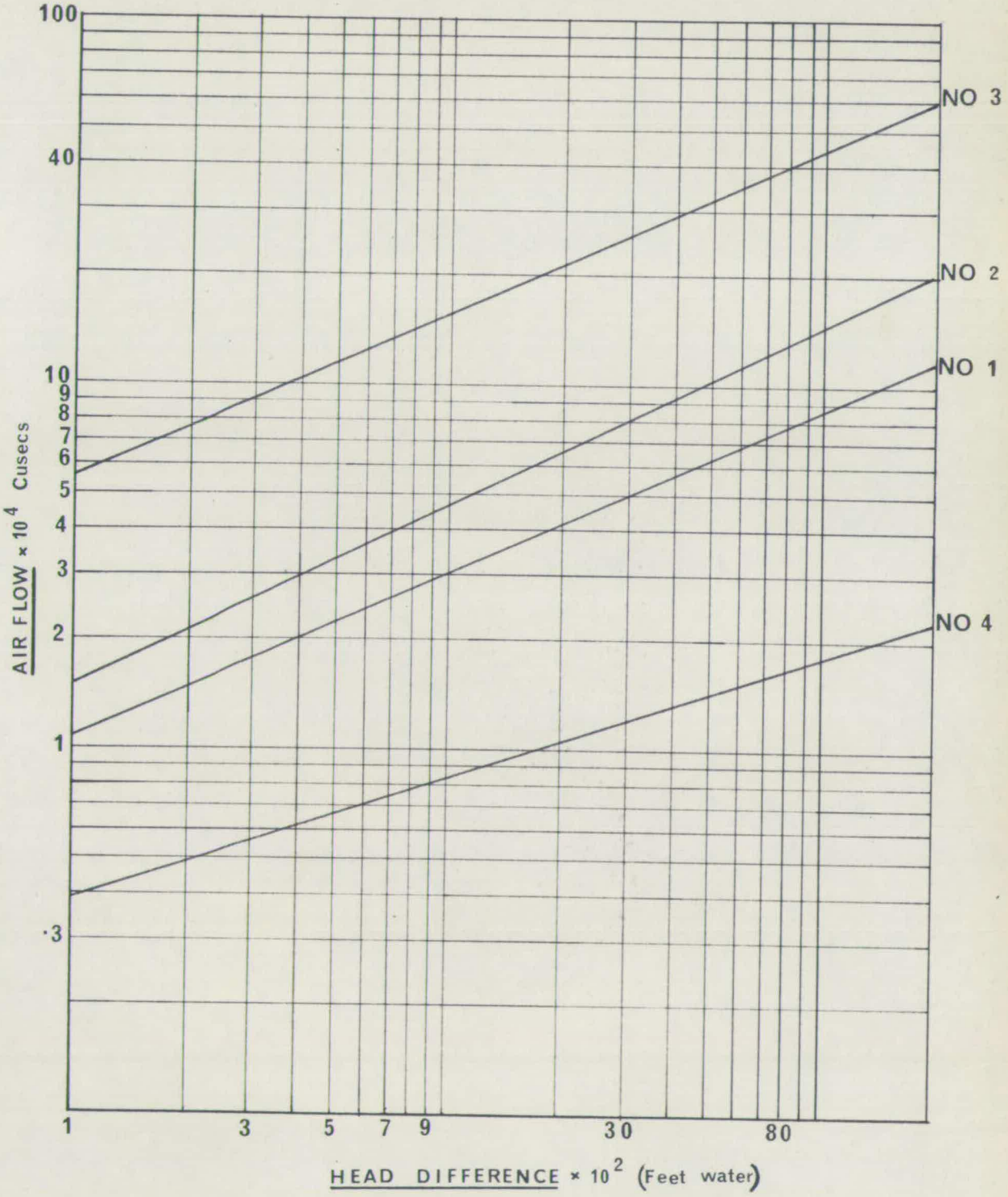

FIG. 4.4

Orifice Plate Number	Diameter in inches	Working range cusecs	Constants M	C
4	0·200	0·0042-0·0178	0·0178	0·333
1	0·370	0·0122-0·0851	0·0851	0·450
2	0·534	0·0156-0·1445	0·1445	0·505
3	0·922	0·0625-0·4365	0·4365	0·450

Table 4·2.

From the above table of results it is apparent that in spite of the deviation from the British Standards (i.e. diameter less than 0·25 inches) the minimum flow possible to be measured is not within the required range. Hence to be more precise on the small air flows and also to facilitate the measurement of such flows an additional method as described below was adopted.

Calibration of Davimeter.

The Davimeter is as shown in Plate 4·5 and works on the principle of the hot wire anemometer. The scale which is divided in to a logarithmic form reads a maximum of 6000 feet per minute. The great advantage of the instrument is its ability to read low velocities very accurately, when the reliance on the orifice plates decreases. Up to an air flow of 0·01 cusecs the accuracy is within 2·5%, and the accuracy is 10% at a flow of 0·1 cusecs and greater. The meter is calibrated against the standardized hot wire anemometer (whose calibration curve is in figure 4·3) and the scale readings were observed to be very accurate.

The Davimeter was then placed in the air flow meter instead of the orifice plates. The position of maximum velocity was determined

by/

Plate 4·5 THE DAVIMETER

by traversing the Davimeter across a diameter of the shaft.

4·20 EXPERIMENTAL PROCEDURES

The experimental procedures adopted in the air flow measurement were the same in shaft nos. 1-3, for which the Davimeter was used. For shafts 4 and 5 the orifice plates were used to ascertain sensitive readings of the davimeter.

The measurement of water flow was conducted solely by observing the head over the 'V' notch in the case of shafts 2 to 5, but in the case of shaft no. 1 actual discharge over the notch was collected for a known time. This procedure not only checked the notch calibration, but also ensured accurate values of flow from the 1st shaft which was situated rather too close to the notch.

4·30 CONCLUSIONS

The measurement of water discharge was made by determining the head over a 'V' notch. During low discharges direct measurement of the flow was obtained by collecting a quantity of water for a known duration.

Air flow measurements were obtained by observing the pressure difference across an orifice plate. There were four orifice plates with openings of different sizes. Low air discharges were measured by the use of a Davimeter which worked on the principle of a hot wire anemometer. The accuracy of the davimeter was specially high during low air velocities.

Though elementary methods were used in the less important experimental investigations the consistency of the observation was ensured wherever possible.

Although on the whole/

Although on the whole, the techniques adopted could have been more advanced, the sensitivity of the instrumentation was justified by the experimental performance.

C H A P T E R V

E X P E R I M E N T A L A N A L Y S E S

5·00 INTRODUCTION

In a previous chapter the theoretical analysis of the air entrainment phenomenon has been postulated. Owing to the complexities associated with the air flow mechanism a precise mathematical analysis is not possible for all cases. Therefore, experimentation is necessary to solve flow problems either by pure experimentation or by making certain simplifying assumptions to facilitate a theoretical approach and above all to justify the hypothetical analysis.

The scope of the present chapter is to facilitate a correlation (in the next chapter) between theory and practice, by means of the three considerations mentioned above.

The test code is in the form X·Y where X = series No.; and Y = shaft no.

5·10 SERIES I TESTS

With reference to the section 3·40, the aim of these tests was to obtain the relationship of air flow to water flow under free flow condition. A theoretical analysis of this state is presented in section 2·10.

5·11 Experimental Observations.

There were not many visual observations apparent in this series of tests. Air bubbles or any air entrainment were not visible due to the annular water surface covering the full length of shaft. The only/

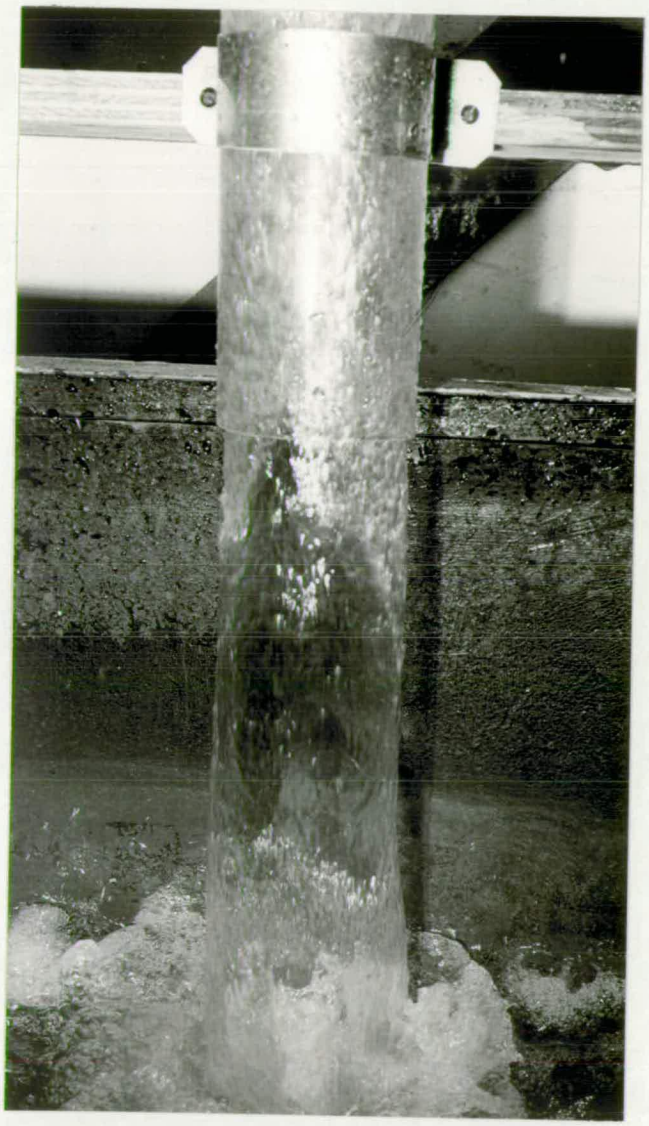

Plate 5·1 VARIABLE LENGTH OF AIR CORE BEYOND SHAFT.

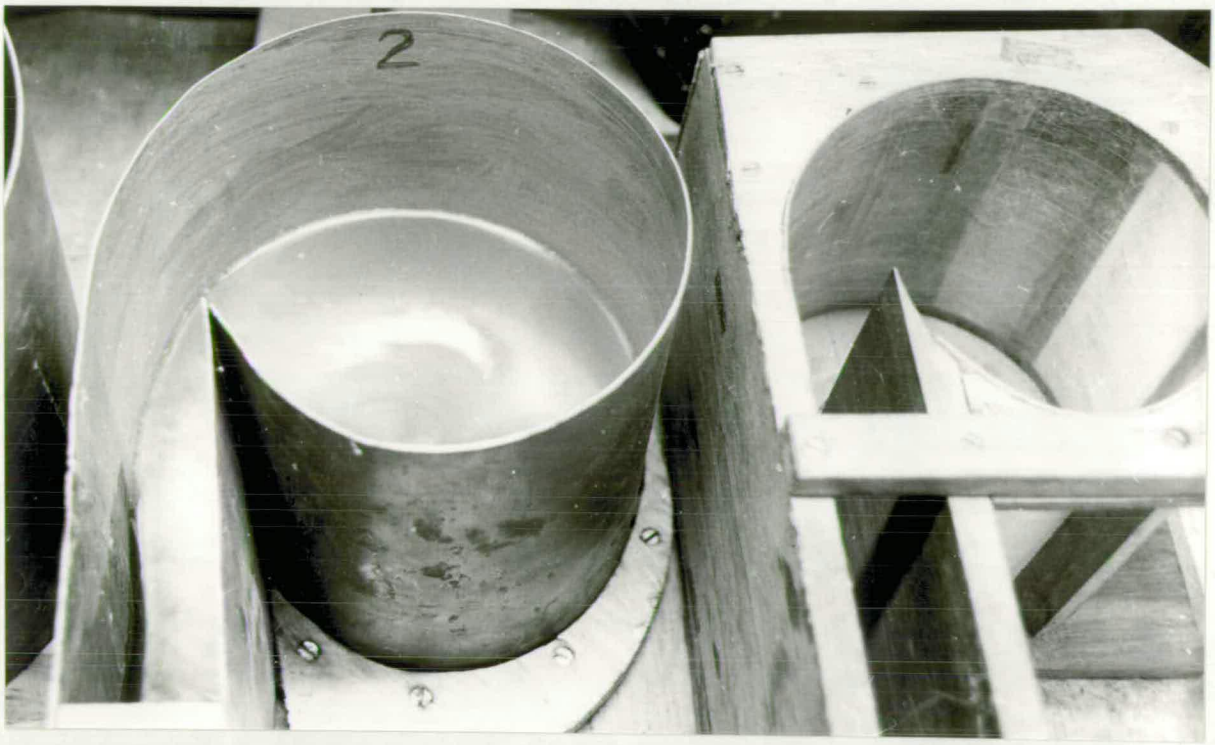

Plate 5·2A

Plate 5·2B FLOW IN VORTEX CHAMBERS.

The only apparent observation was that of air bubbles being engulfed and eventually drawn to the water surface at the exit. The effect when the container was placed, as in figure 3·4, was very significant. The rise in the level of the water in the 'V' notch tank, with increase of water discharge, caused a reduction in the volumetric estimation in the absence of the container. The length of shaft was considered to be from the throat to the top of the container which was about 5 inches below the end of the shaft.

The results of the tests are as presented in Table 5·10 and are plotted in Figs. 6·21-6·25 alongside the theoretical results. Plate 5·1 shows the effect at the shaft exit without the container, regulating the length of air core beyond the shaft, and plates 5·2 (A and B) illustrate the flow in the chamber.

5·12 Analysis of Results.

Tests 1·1-1·5 indicate an increase in air flow with increase in water flow, but the tests on 1·1 and 1·2 signify the reduction in air flow beyond a particular water discharge in the shaft. This is due to the effect as elucidated in section 2·13, where the decrease of the throat air core area reduces the air flow in to the shaft with increase of water discharge. This phenomenon is not evident experimentally in the larger shafts due to the maximum water discharge into them being insufficient.

5·20 SERIES II TESTS

Referring to section 3·40, the aim of the tests is to determine the effect of shaft length on the air entrainment. The theoretical analysis of the effect is described in Section 2·10.

SERIES I TEST RESULTS

Test Code	Head in ft. over notch	Water flow Cusecs	Maximum Air Velocity ft. per min.	Air flow Cusecs
1·1	0·345	0·033	338	0·0301
	0·320	0·023	310	0·0275
	0·307	0·018	300	0·0261
	0·302	0·016	250	0·0235
	0·277	0·010	200	0·0172
1·2	0·369	0·045	500	0·0449
	0·350	0·035	475	0·0423
	0·338	0·030	425	0·0380
	0·321	0·023	375	0·0333
	0·288	0·013	335	0·0298
1·3	0·300.	0·016	395	0·0352
	0·349	0·035	620	0·0551
	0·379	0·051	700	0·0625
	0·406	0·068	800	0·0710
	0·439	0·094	870	0·0776
1·4	0·307	0·018	490	0·0438
	0·340	0·031	675	0·0601
	0·386	0·055	933	0·0932
	0·415	0·075	1010	0·0901
	0·441	0·096	1125	0·1005
1·5	0·0386	0·055	1555	0·139
	0·438	0·093	2020	0·180
	0·493	0·147	2450	0·218
	0·591	0·281	3000	0·268
	0·653	0·392	3375	0·301
	0·672	0·431	3550	0·316

Table 5.10

5·21 Experimental Observations.

The observations made in this series of tests were comparable with the former tests. The collector at the end of each length of shaft enabled the water to be re-circulated to the supply and some of the air was rejected at the collector, while the remainder was carried to the tank. The arrangement of the collector is as illustrated in Figure 3·5 and Plate 3·5.

Tables 5·21-5·25 represent the results of series II tests which are plotted alongside the results of the former tests and the theoretical results as in Figures 6·21-6·25.

5·22 Analysis of Results.

The results when plotted as in figures 6·21-6·25 show a regular pattern of the variation between air and water discharges. This was apparent in the four larger shafts with the peak air flow values increasing with shaft length. This pattern was not very consistent in the smallest shaft (No. 1) which indicates the unsuitability of the model size for a radical model study.

The results of this series of tests indicate the significance of the shaft length. In shaft no. 5 a reduction of shaft length of 80% indicates a reduction of the peak air flow of 75%, with a similar percentage reduction in length in shaft no. 1, gives rise to a peak air flow reduction of 33%.

5·30 SERIES III TESTS

With the introduction of an Annular Hydraulic Jump in the shaft, the tests conducted in this series, indicate a reduction in the air entrainment as compared to the former tests.

SERIES II TEST RESULTS

Test Code	Shaft length (Ft.)	Head (in ft.) over notch	Water Flow Cusecs	Maximum Air Velocity ft. per min.	Air Flow Cusecs
2·1	12	0·289	0·0130	226	0·0202
		0·307	0·0180	265	0·0237
		0·318	0·0220	283	0·0255
		0·332	0·0274	291	0·0260
		0·335	0·0287	330	0·0295
	9	0·338	0·0300	293	0·0261
		0·326	0·0250	289	0·0258
		0·319	0·0223	271	0·0242
		0·305	0·0175	251	0·0224
		0·307	0·0182	268	0·0239
	6	0·284	0·0115	210	0·0187
		0·305	0·0174	235	0·0210
		0·326	0·0250	267	0·0238
	3	0·286	0·121	197	0·0176
		0·315	0·021	222	0·0198
		0·338	0·030	219	0·0196

Table 5.21

SERIES II TEST RESULTS (contd.)

Test Code	Shaft length (ft.)	Head (in ft.) over notch	Water flow Cusecs	Maximum Air Velocity ft. per min.	Air Flow Cusecs
2·2	12	0·297	0·0150	320	0·0286
		0·340	0·0305	415	0·0370
		0·360	0·0400	465	0·0416
		0·364	0·0425	485	0·0433
	9	0·305	0·0175	330	0·0295
		0·326	0·0250	390	0·0350
		0·359	0·0385	430	0·0386
		0·374	0·0480	465	0·0416
	6	0·310	0·0190	310	0·0275
		0·329	0·0260	350	0·0313
		0·345	0·0330	385	0·0343
		0·362	0·0412	405	0·03616
	3	0·313	0·020	260	0·0230
		0·340	0·031	280	0·0250
		0·365	0·043	285	0·0255

Table 5.22

SERIES II TEST RESULTS (contd.)

Test Code	Shaft length (Ft.)	Head (in ft.) over notch	Water flow Cusecs	Maximum Air Velocity ft. per min.	Air Flow Cusecs
2·3	12	0·280	0·0106	340	0·0300
		0·329	0·0260	505	0·0450
		0·391	0·0580	675	0·0601
		0·437	0·0920	810	0·0720
	9	0·313	0·0200	365	0·0325
		0·349	0·0350	510	0·0452
		0·383	0·0530	610	0·0545
		0·435	0·0901	710	0·0635
	6	0·330	0·028	390	0·0350
		0·345	0·033	470	0·0420
		0·406	0·066	555	0·0495
		0·434	0·089	530	0·0475
	3	0·312	0·0139	280	0·0251
		0·354	0·0370	350	0·0315
		0·401	0·0630	310	0·0275
		0·438	0·0931	240	0·0210

Table 5.23.

SERIES II TEST RESULTS (contd.)

Test Code	Shaft length (Ft.)	Head (in ft.) over notch	Water flow Cusecs	Maximum Air Velocity ft. per min.	Air Flow Cusecs
2.4	12	0·341	0·0311	600	0·0532
		0·387	0·0560	785	0·0699
		0·407	0·0690	935	0·0832
		0·444	0·0981	1010	0·0899
	9	0·326	0·0250	450	0·0399
		0·377	0·0499	675	0·0600
		0·421	0·0793	855	0·0762
		0·445	0·0999	975	0·0867
	6	0·315	0·0210	375	0·0333
		0·350	0·0351	525	0·0466
		0·370	0,0460	575	0·0512
		0·415	0·0750	740	0·0660
	3	0·315	0·0210	315	0·0281
		0·345	0·0330	380	0·0338
		0·387	0·0562	415	0·0369
		0·425	0·0831	390	0·0345

Table 5.24

SERIES II TEST RESULTS (contd.)

T.Test Code	Shaft length (ft.)	Head (in ft.) over notch	Water flow Cusecs	Maximum Air velocity ft. per min.	Air flow Cusecs
2·5	12	0·434	0·090	1605	0·143
		0·522	0·181	2480	0·221
		0·591	0·281	2640	0·235
		0·637	0·360	2910	0·259
		0·678	0·443	3535	0·315
	9	0·457	0·110	1600	0·142
		0·495	0·149	1920	0·171
		0·585	0·270	2175	0·194
		0·659	0·405	2110	0·188
	6	0·434	0·090	1245	0·111
		0·514	0·171	1480	0·132
		0·584	0·269	1400	0·125
		0·617	0·325	1200	0·107
		0·691	0·473	1020	0·091
	3	0·428	0·085	630	0·056
		0·509	0·165	620	0·055
		0·594	0·285	530	0·047
		0·644	0·375	530	0·047
		0·677	0·441	480	0·043

Table 5.25.

5·31 Experimental Observations.

There were many visual observations in this series of tests. Detailed study of air bubble and air pocket motion is undertaken in the next series of tests, where some of these observations will be discussed.

Although this is the first series of tests where the actual air entrainment is visible in the form of bubbles and pockets, it is however, quantitatively the more desirable state.

In addition, the air rejection from the pressure box envisaged the utility of a de-aeration device at the exit of the shaft.

The formation of the annular hydraulic jump under different flow conditions enabled a closer examination of the types of jump and their air entraining properties to be procured. The flow patterns within the jump were observed and resembled those described by Quick (5).

An experimental difficulty which sometimes persisted was in maintaining a constant free fall in the shaft. This was due to the tendency for the air pockets to rise against the flow. These pockets caused an upward motion of the water which elucidates the cause of sudden gushes of water, shooting into the air from some prototypes.

Air and water flow readings were taken at different free falls. The decrease of the free fall with increase of water flow led to the presentation of the results in a non dimensional form. Hence, the Tables 5·31-5·33 describes the variation of air-water ratio and free fall to diameter ratio, which is then plotted in Figure 6·30.

SERIES III TEST RESULTS

Test Code	Head (ft.) over notch	Water Flow (Q_w) Cusecs	Max. Vel. ft. per min.	Air Flow (Q_a) Cusecs	Free Fall (Ft.) H	Q_a/Q_w	H/D
3·1	0·300	0·0160	72	0·0064	12·5	0·400	109·09
	0·312	0·0198	84	0·0075	12·4	0·380	108·21
	0·336	0·0290	121	0·0108	12·3	0·371	107·34
	0·339	0·0303	122	0·0109	12·2	0·360	106·47
	0·281	0·0109	40	0·0035	9·5	0·325	82·90
	0·308	0·0185	66	0·0059	9·4	0·320	82·03
	0·325	0·0245	88	0·0078	9·3	0·319	81·16
	0·334	0·0281	99	0·0088	9·1	0·315	79·41
	0·284	0·0116	34	0·0031	6·5	0·265	56·72
	0·311	0·0195	57	0·0051	6·4	0·261	55·85
	0·330	0·0265	74	0·0066	6·3	0·250	54·98
	0·338	0·0298	83	0·0074	6·2	0·248	54·11
3·2	0·317	0·0215	91	0·0081	12·5	0·379	85·71
	0·332	0·0273	98	0·0087	12·2	0·320	83·65
	0·356	0·0382	130	0·0116	12·2	0·305	83·65
	0·362	0·0413	144	0·0128	12·0	0·310	82·28
	0·323	0·0237	73	0·0065	9·5	0·275	65·14
	0·334	0·0281	86	0·0076	9·2	0·273	63·08
	0·346	0·0334	101	0·0090	9·0	0·270	61·71
	0·364	0·0424	120	0·0106	9·0	0·252	61·71
	0·325	0·0245	62	0·0055	6·5	0·224	44·57
	0·331	0·0269	68	0·0060	6·5	0·224	44·57
	0·347	0·0339	84	0·0075	6·2	0·220	42·51
	0·363	0·0418	100	0·0089	6·2	0·215	42·51

Table 5·31

SERIES III TEST RESULTS (Contd.)

Test Code	Head (ft.) over notch	Water Flow (Qw) Cusecs	Max. Vel. ft. per min	Air Flow (Qa) Cusecs	Free Fall (Ft.) H	Q_a/Q_w	H/D
3·3	0·357	0·0387	145	0·0128	12·5	0·333	66·66
	0·378	0·0502	158	0·0141	12·5	0·280	66·66
	0·411	0·0720	214	0·0191	12·2	0·265	65·06
	0·440	0·0949	276	0·0246	12·0	0·260	63·99
	0·334	0·0281	72	0·0064	9·5	0·228	50·66
	0·359	0·0393	97	0·0086	9·5	0·220	50·66
	0·405	0·0677	167	0·0149	9·2	0·220	49·06
	0·421	0·0795	187	0·0166	9·2	0·210	49·06
	0·337	0·0294	60	0·0054	6·5	0·183	34·66
	0·387	0·0557	109	0·0097	6·2	0·175	33·06
	0·413	0·0734	140	0·0124	6·2	0·170	33·06
	0·443	0·0975	185	0·0165	6·0	0·170	31.99
3·4	0·328	0·0257	100	0·0089	12·5	0·350	54·54
	0·343	0·0320	108	0·0096	12·5	0·301	54·54
	0·361	0·0408	123	0·0110	12·2	0·271	53·23
	0·401	0·0649	171	0·0152	12·0	0·235	52·36
	0·336	0·0290	65	0·0058	9·5	0·200	41·89
	0·372	0·0468	104	0·0094	9·5	0·201	41·89
	0·409	0·0705	154	0·0137	9·2	0·195	40·14
	0·431	0·0874	182	0·0162	9·0	0·186	39·27
	0·339	0·0303	54	0·0047	6·5	0·158	28·36
	0·373	0·0473	80	0·0070	6.5	0·149	28·36
	0·420	0·0787	132	0·0118	6·2	0·150	27·05
	0·438	0·0932	155	0·0137	6·0	0·148	26·18

Table 5·32

SERIES III TEST RESULTS (Contd.)

Test Code	Head (ft.) over notch	Water Flow (Qw) Cusecs	Max. Vel. ft. per min.	Air Flow (Qa) Cusecs	Free Fall (ft.) H	Q_a/Q_w	H/D
3·5	0·446	0·1002	270	0·0240	12·5	0·240	26·08
	0·538	0·2021	385	0·0340	12·0	0·171	25·04
	0·604	0·3023	475	0·0423	11·5	0·140	23·99
	0·636	0·3596	524	0·0467	11·0	0·129	22·95
	0·469	0·1218	150	0·0133	9·5	0·111	19·82
	0·541	0·2062	243	0·0216	9·0	0·105	18·78
	0·601	0·2972	333	0·0297	8·5	0·100	17·73
	0·642	0·3710	395	0·0352	8·0	0·095	16·60
	0·496	0·1504	153	0·0136	6·5	0·091	13·56
	0·533	0·1955	186	0·0166	6·0	0·085	12·52
	0·579	0·2615	235	0·0209	5·5	0·080	11·47
	0·629	0·3465	272	0·0243	5·0	0·071	10·43

Table 5:33

5·32 Analysis of Results.

An attempt was made to determine variation of air flow with water flow for different free falls. This was done, so as to be in uniformity with the previous analysis. However, it was not possible to obtain a consistent relationship due to the variation of free fall with increase of water discharge.

A non-dimensional plot of the ratio of free fall to shaft diameter against the ratio of air flow to water flow displays an uniform variation as presented in figure 6·30. A smooth curve drawn representing Viparelli's (2) relationship as described in section 1·22, shows agreement with the experimental points. Deviation of the experimental points from Viparelli's curve is evident specially at low values and also at high values. This is probably due to the scale effects which persist and is dealt with in detail in Chapter 7. At values of $^{h}/_{D}$ when the free fall h is equal to the length of the shaft, there is a deviation from the curve with a tendency for the ratio $^{h}/_{D}$ to remain constant, in spite of increase in the air-water ratio. This effect was evident in Viparelli's experiments as presented in figure 1·2.

5·40 SERIES IV TESTS

This series of tests were conducted on the four smaller and a detailed study was executed on the 3rd shaft. The behaviour of the air bubbles and the formation of air pockets were carefully observed with a view to deduce empirical relationships as to their idiosynchrasies.

5·41 Experimental Observations.

Although in this series of tests, measurements were not made by very precise instruments, the consistency of the results was encouraging.

The bubble diameters were observed visually to be in the region of 1/8 to $\frac{1}{4}$ inch except when they coalesced to form larger cavities. The bubble speeds were obtained by recording the time taken by a bubble to travel a known distance. The downward motion of the bubbles was dependent on the velocity of the mixture in the shaft, while the rising velocity of the bubbles was consistent when the water was under static conditions.

Three distinct types of flow were evident in the shaft and are classified in the next chapter. The results of the test are as presented in Tables 5·41-5·42. The notations in the Table are as follows:-

h = free fall in ft.

Qw = water flow in cusecs.

Qa = air flow in cusecs.

V = velocity of mixture in ft. per sec.

Q = discharge parameter where $Q = {}^{Qw}/\sqrt{g}d^{5/2}$.

Fr = froude number $V/\sqrt{gd}$.

d = shaft diameter in ft.

q = total flow (Qa + Qw) in cusecs.

Rising velocity measurements of the air bubbles are as in Table 5·43. A statistical analysis of the results is also established in the table.

SERIES IV TEST RESULTS

Test Code	h	Qw	Qa	q	V	Q	Fr
4•1	6	0•0154	0•0036	0•0190	1•84	0•6111	0•9378
		0•0241	0•0058	0•0299	2•74	0•9563	1•4260
		0•0181	0•0042	0•0223	2•16	0•7182	1•1240
		0•0307	0•0072	0•0379	3•67	1•2182	1•9101
	3	0•0052	0•0008	0•0060	0•58	0•2063	0•3030
		0•0154	0•0024	0•0178	1•72	0•6111	0•8980
		0•0201	0•0032	0•0233	2•26	0•7976	1•1150
		0•0285	0•0040	0•0325	3•15	1•1309	1•6400
4•2	9	0•0188	0•0045	0•0233	1•39	0•4086	0•6435
		0•0208	0•0051	0•0259	1•55	0•4522	0•7150
		0•0285	0•0075	0•0360	2•15	0•6195	0•9920
		0•0316	0•0076	0•0392	2•34	0•6869	1•0800
		0•0382	0•0100	0•0482	2•88	0•8304	1•3300
		0•0462	0•0120	0•0582	3•48	1•0040	1•6070
	6	0•0198	0•0030	0•0228	1•36	0•4304	0•6290
		0•0532	0•0116	0•0642	3•84	1•1564	1•7721
		0•0330	0•0060	0•0390	2•33	0•7174	1•0750
		0•0403	0•0077	0•0480	2•87	0•8761	1•3251

Table 5•41

SERIES IV TEST RESULTS (Contd.)

Test Code	h	Qw	Qa	q	V	Q	Fr
4·3	9	0·0435	0·0090	0·0525	1·90	0·5034	0·7733
		0·0642	0·0141	0·0783	2·83	0·7431	1·1520
		0·0850	0·0192	0·1042	3·76	0·9837	1·5301
	6	0·0532	0·0010	0·0542	1·96	0·6157	0·7970
		0·0663	0·0120	0·0783	2·83	0·7673	1·1521
		0·0810	0·0150	0·0962	3·48	0·9375	1·4142
		0·0850	0·0155	0·1005	3·64	1·4039	1·4801
	3	0·0234	0·0028	0·0262	0·95	0·2708	0·3851
		0·0479	0·0056	0·0535	1·94	0·5543	0·7870
		0·0712	0·0085	0·0797	2·88	0·8241	1·1720
		0·1404	0·0168	0·1572	5·69	1·6250	2·3150
4·4	9	0·0249	0·0050	0·0299	0·72	0·1746	0·2660
		0·0451	0·0105	0·0556	1·33	0·3162	0·4890
		0·0691	0·0125	0·0816	1·97	0·4345	0·7250
		0·0874	0·0175	0·1049	2·54	0·6129	0·9350
	5	0·0253	0·0042	0·0295	0·71	0·1774	0·2610
		0·0663	0·0100	0·0763	1·85	0·4649	0·6810
		0·0826	0·0126	0·0952	2·29	0·5792	0·8430
		0·0866	0·0130	0·0996	2·41	0·6072	0·8881

Table 5·42

Rising Velocity of Air Bubbles.

Distance in ft.	Time taken in secs.	Velocity ft. per sec.
5·00	8·1	0·617
5·75	10·0	0·575
5·75	9·0	0·639
5·00	7·6	0·654
2·00	2·5	0·800
2·25	3·0	0·834
2·25	3·0	0·750
2·25	3·3	0·681

From Statistical Analysis.

Mean Velocity = 0·693 ft. per sec.

Standard deviation = 0·0858 ft. per sec.

Coefficient of variation = 12·39 per cent.

Table 5·43.

5·42 Analysis of Results.

The results were analysed on the basis of Froude law. Due to the absence of a theoretical approach, an empirical relationship between Froude Number and the non-dimensional discharge parameter $(Q_w/\sqrt{g}d^{5/2})$ is sought in the analysis. The results are plotted as in Fig. 5·43. A definite linear relationship between the two non-dimensional parameterswas significant. In evaluating the velocity of the air-water mixture, it was necessary to refer to the air discharges from the preceding tests, to consider the total volume of the mixture./

Variation of Froude Number with Discharge

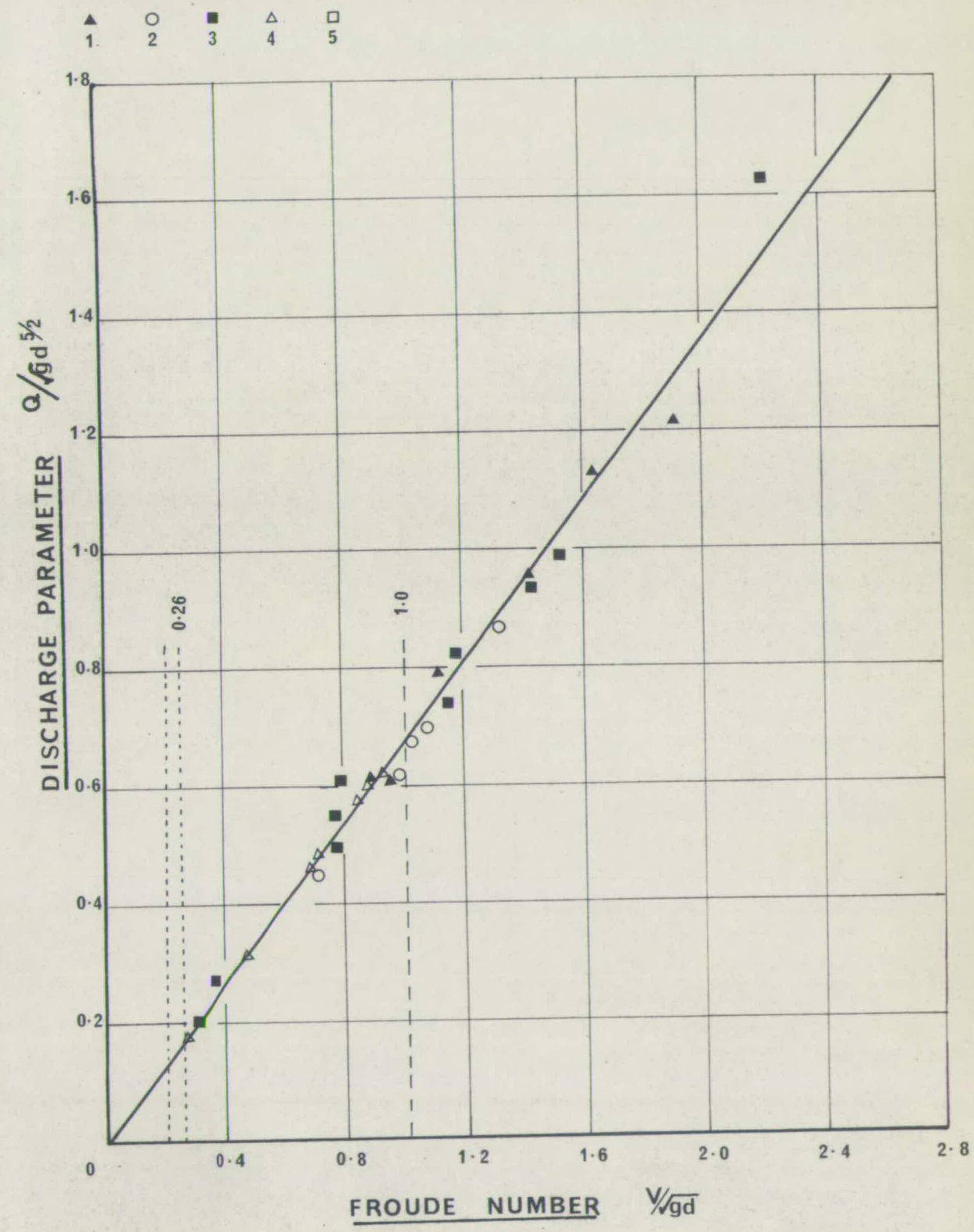

FIG. 5.1

(a) Initial

(b) Intermediate

(c) Final

Plate 5•3 TYPES OF FLOW REGIMES.

mixture.

In order to discuss each of the regimes in detail it may be necessary to define them as Initial, Intermediate and Final regimes. The transition of each regime is distinguished with respect to Froude number. The three types of flow are illustrated in Plates 5·3 (A, B and C).

5·43 Classification of Flow Regimes.

Initial Regime: This regime of flow in the shaft is characterized by the very low velocities and by the absence of the downward motion of air bubbles. From the results in Tables 5·41 and 5·42 it is evident that in the initial regime the velocity of the pipe full flow is less than that of the upward velocity of the bubbles as determined in Table 5·43.

The critical flow at the end of the initial regime indicates that the velocity of the mixture is very nearly the same as the rising velocity of the bubbles and at this flow the bubbles were on the verge of moving downwards. Prior to this flow the bubbles were observed to be stationary for a considerable change of flow. This state may be defined as the transition zone of the initial regime. The value of Froude number demarcating the extent of the initial regime was from zero to 0·26, with the transition zone acting from 0·2 to 0·26. Though the initial regime appears to be the safest, with no air entrainment nor air pocket formation, the transition zone renders unstable conditions which requires caution. Hence the experimental observation not only indicates that the upward rising velocity of the bubbles is attained at the end of the initial regime but also aver that the value of Froude number should be less than/

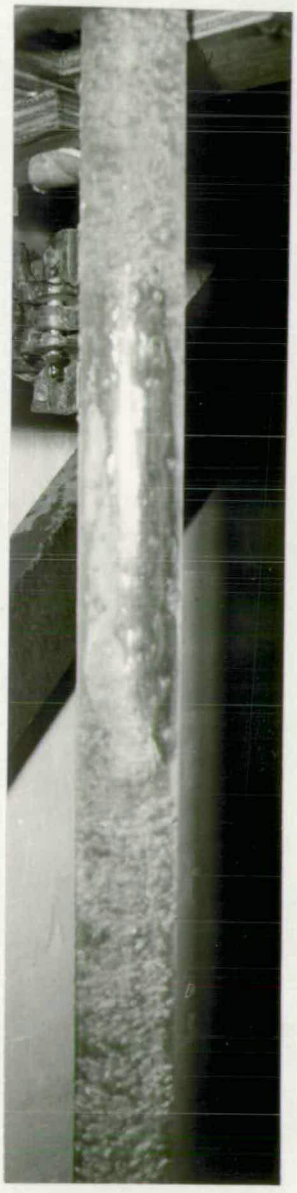

Plate 5·4 TYPICAL AIR POCKET IN THE INTERMEDIATE. REGIME.

be less than 0·20 in this regime to vouchsafe satisfactory performance.

Intermediate Regime: This regime is undoubtedly the most undesirable as its detrimental effects are clearly evident from the experiments.

A typical air pocket formation in this regime is as illustrated in Plate 5·4. The haphazard movement of air pockets both in the direction of the water flow and also against it rendered very unsatisfactory conditions.

The slow velocity of the mixture, induced the bubbles to rise against the flow under gravity, which eventually caused the bubbles to coalesce and form pockets of varying sizes. The diameters of the pockets were almost up to the full diameter of the shaft but their lengths were estimated to vary from 1 inch to about 2 feet. The increase of water flow in the shaft increases the velocity of the mixture which improves the situation. The increase of tunnel head (or decrease of free fall) also improves the conditions due to the resistance offered by a longer column of water, to the air pocket movement. Therefore the increase of water flow and increase of tunnel head improves the impetuous tendencies of the bubble and pocket motion in this region.

The boundaries of the intermediate regime were defined as having values of Froude number 0·26 to 1·0. These limits were identified as the instance when the bubbles commenced to move downwards and as the instance when the air pocket formation was absent.

During this regime of flow, wide pressure fluctuations are imposed at the shaft exit and also gushes of water and air are emitted at the shaft entry.

Final Regime: This regime of flow is completely free from air pockets and contains only air bubbles, travelling downwards with the flow. The latter aspect is the main visual difference from the initial regime. The velocities are high in this regime which accounts for the drag of the air bubbles downstream.

Both from economic aspects and with a view to obtaining satisfactory performance this regime of flow is most desirable, subject to any long term adverse effects resulting from the bubbles.

5·44 Comparison of Flow Regimes.

In postulating a comparison of the regimes, the initial regime having a Froude number less than 0·2 is considered the best, with respect to the air entraining aspects. It may not be economic to always attain such a regime, as large shaft diameters are needed to produce the low velocities.

The intermediate regime is one which should be avoided at all possible instances. The experimental observations of its unsatisfactory performance, indicates its detrimental effects.

The final regime appears to be the most practicable. Since it is necessary to incorporate small diameters to produce high velocities, the ability for such diameters to accomodate the estimated maximum discharge through the shaft should be ensured.

By considering the estimated minimum flow (for the cases when this flow is not equal to zero) or the mean flow, it will be of value to ensure that the value of Froude number remains above 1. This precaution is also necessary if the flow is designed to be in the initial regime, where a change into the transition zone could render adverse effect..

Classification of Regimes

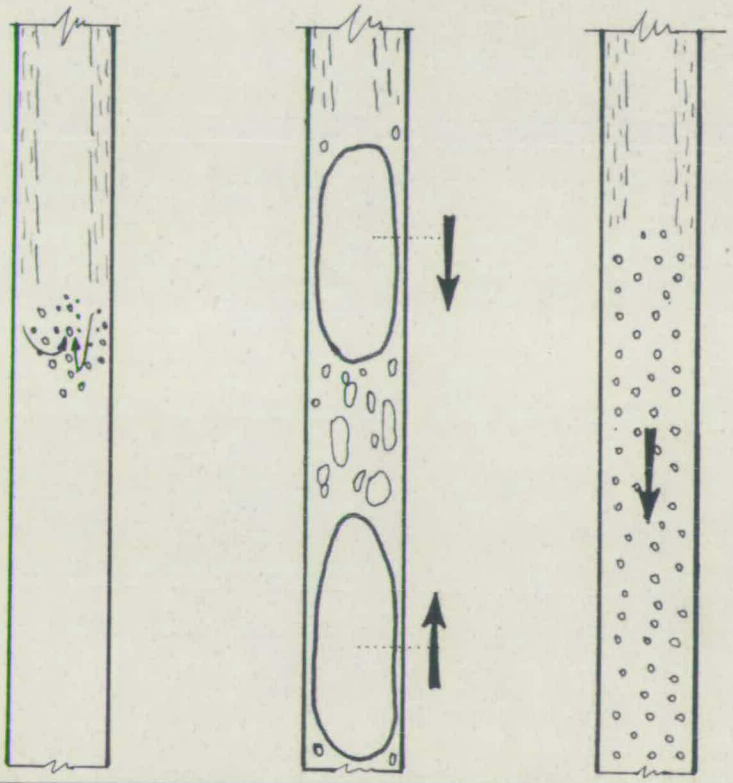

FLOW REGIMES	INITIAL	transition	INTERMEDIATE	FINAL
FROUDE NUMBER		0·20	0·26	1·00

FIG. 5.2

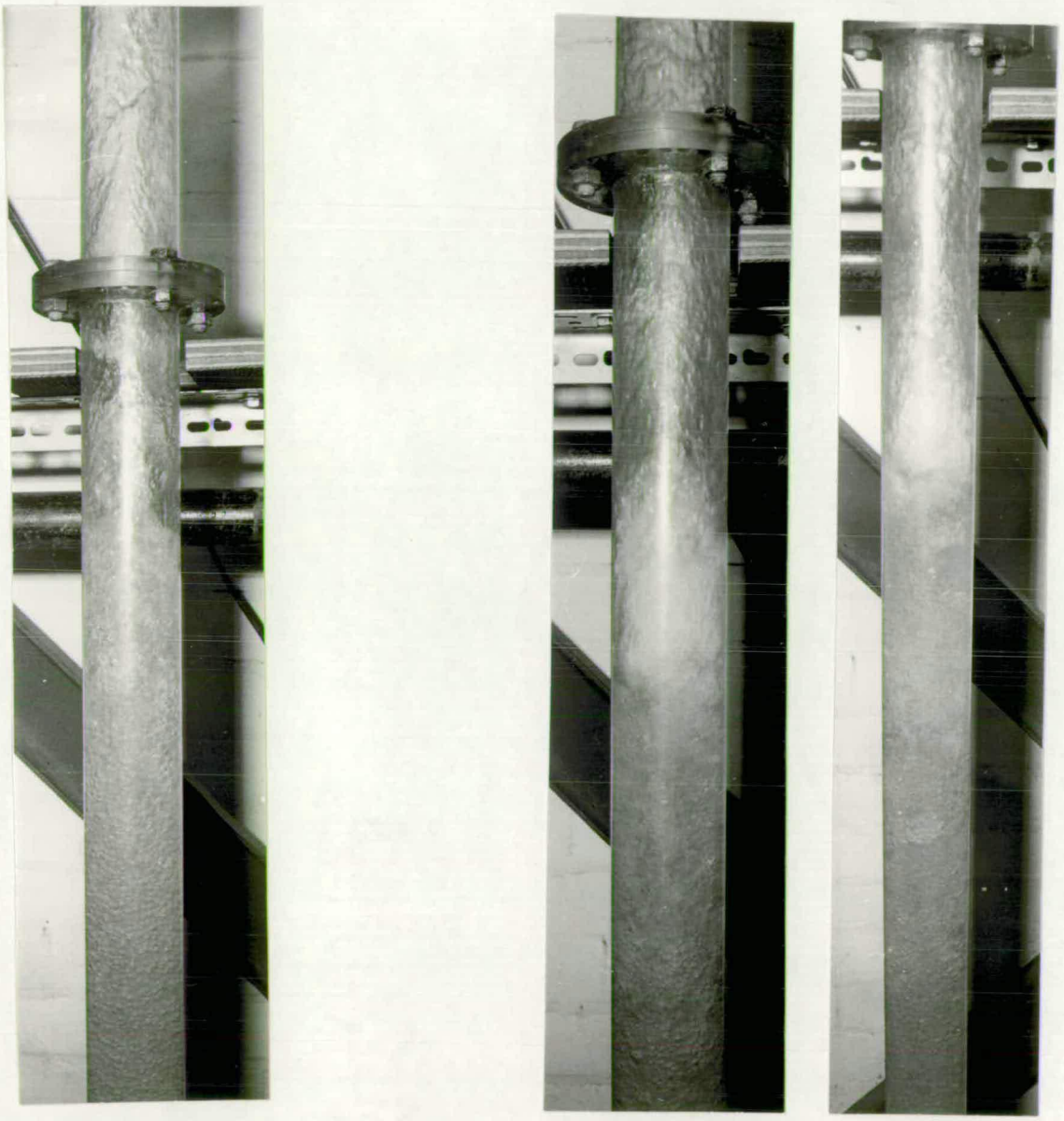

(A) Initial (B) Intermediate (C) Final

Plate 5·5 TYPES OF JUMPS.

The diagram in Figure 5·2 illustrates the three types of regime with respect to Froude number. The Plates 5·5 (A, B and C) represent the three different turbulent states of the annular jump for the three regimes.

5·50 SERIES V TESTS

This series of tests deals with the experimental verifications of two vital theories incorporated in the theoretical analysis. The investigations were carried out on shaft no. 2.

5·51 Variation of Air Core.

The theory illustrated in section 2·11 of Ackers and Crump (6) expressed the variation of the air core diameter with the discharge in a vortex chamber of known geometry.

The experimental observations are as in Table 5·51 and plotted in Figure 6·42 along side the theoretical results.

5·52 Velocity Variation along shaft.

In section 2·12 the theory developed by Dawson and Kalinske (7) on the velocity variation along a shaft length is expressed. In the analysis the presence of a terminating velocity is indicated. The experimental observations were hindered at high velocities due to the entrapping of air in the pitot tube. Therefore the measurements were restricted to low discharges. The experimental results are as presented in Table 5·52 and plotted as in Figure 6·41. The measurements were taken on a comparative basis to verify the constancy of the velocity beyond the 'Terminating Section'.

SERIES V TEST RESULTS

Air Core diameter variation at Throat.

Head (ft.) over notch	Water flow (Cusecs)	Air-core diameter (ins.)	Fractional air core $d = 1{\cdot}75''$
0·253	0·0053	1·576	0·811
0·286	0·0120	1·383	0·685
0·316	0·0210	1·262	0·520
0·357	0·0385	0·348	0·395

Table 5·51.

Velocity Variation along shaft.

Head (ft.) over notch	Water flow (cusecs)	Free fall in ft.				Readings
		10	8	3	1·5	
0·322.	0·0234	13·5	13·0	13·5	13·3	Pitot tube reading in inches.
		8·51	8·34	8·51	8·45	Velocity ft./sec.
0·293	0·0139	10	9·5	9·8	8·8	Pitot tube reading in inches.
		7·46	7·15	7·24	6·85	Velocity ft./sec.

Table 5·52.

5·60 CONCLUSIONS

The scope of the experimental investigations included:

(1) Verification of previous work which has been incorporated in the present study.

(2) Deduction of empirical and semi-empirical relationships, and

(3) Verification of theoretical analysis in the present study.

The latter two aspects are dealt with in a thorough manner, with precise experimental measuring techniques being ensured during most tests.

The correlation of the results with the theoretical analysis is presented in the next chapter and their close agreement endorses the satisfactory nature of the experimentation.

The third series of tests being one dealt with on a purely empirical basis indicates the choice of flow regime which would produce satisfactory working conditions in the shaft. Values of Froude number demarcates the regimes.

While the experimertal investigations aver that the actual air entrainment is dependent on the tunnel head or free fall, they also corroborate that the type of flow regime governs the carriage of the entrained air; hence the water flow and shaft diameter are among the controlling factors.

CHAPTER VI

CORRELATION OF THEORETICAL AND EXPERIMENTAL ANALYSIS

6·00 INTRODUCTION

In two of the earlier chapters, investigations into the air entrainment in vertical shafts have given rise to the need of correlation of the results obtained theoretically and experimentally. Justification of a theory postulated depends a great deal on the experimental evidence and an attempt is made in this chapter to interpret the experimental results with a view to correlate them to the theoretical analysis.

6·10 HYDRAULIC PROPERTIES

The hydraulic properties of the drop shafts derived from procedures recommended by various authors (6), (7) are incorporated in this section. These properties have been the basis for further developments in the analysis and are presented in Figures 6·10-6·15; in which Qw denotes water discharge in cusecs.

Hm - distance to the Terminating Section in feet.

V - velocity in ft. per sec.

Vo - Throat velocity. ft. per sec.

Vm - Terminating velocity. ft. per sec.

f - fractional air core.

6·11 Fractional Air Core.

The method described by Ackers and Crump (6) which is illustrated in Section 2·11 has been utilised and incorporated in a Computer program.

Hydraulic Properties

Model I

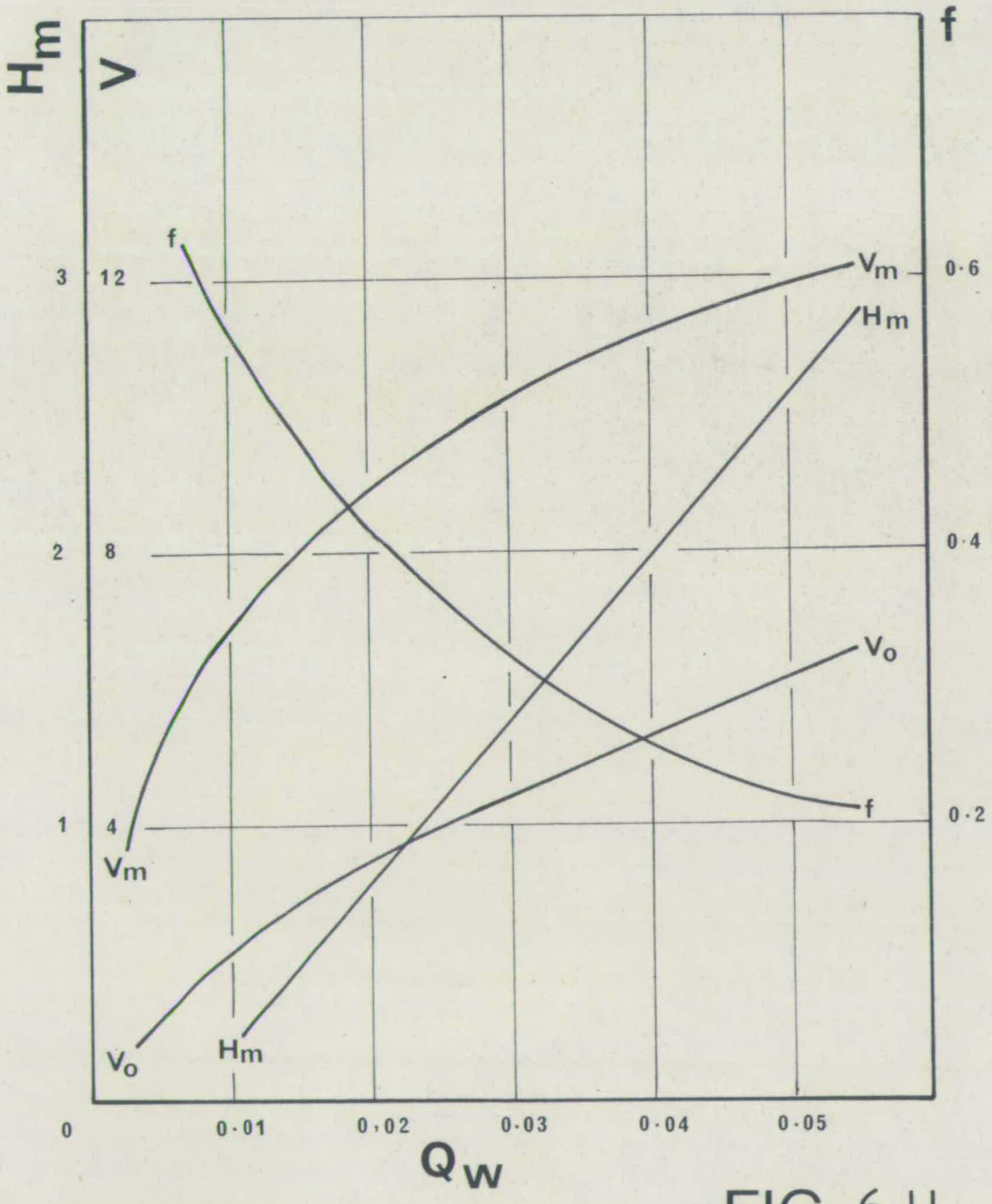

FIG. 6.11

Model II

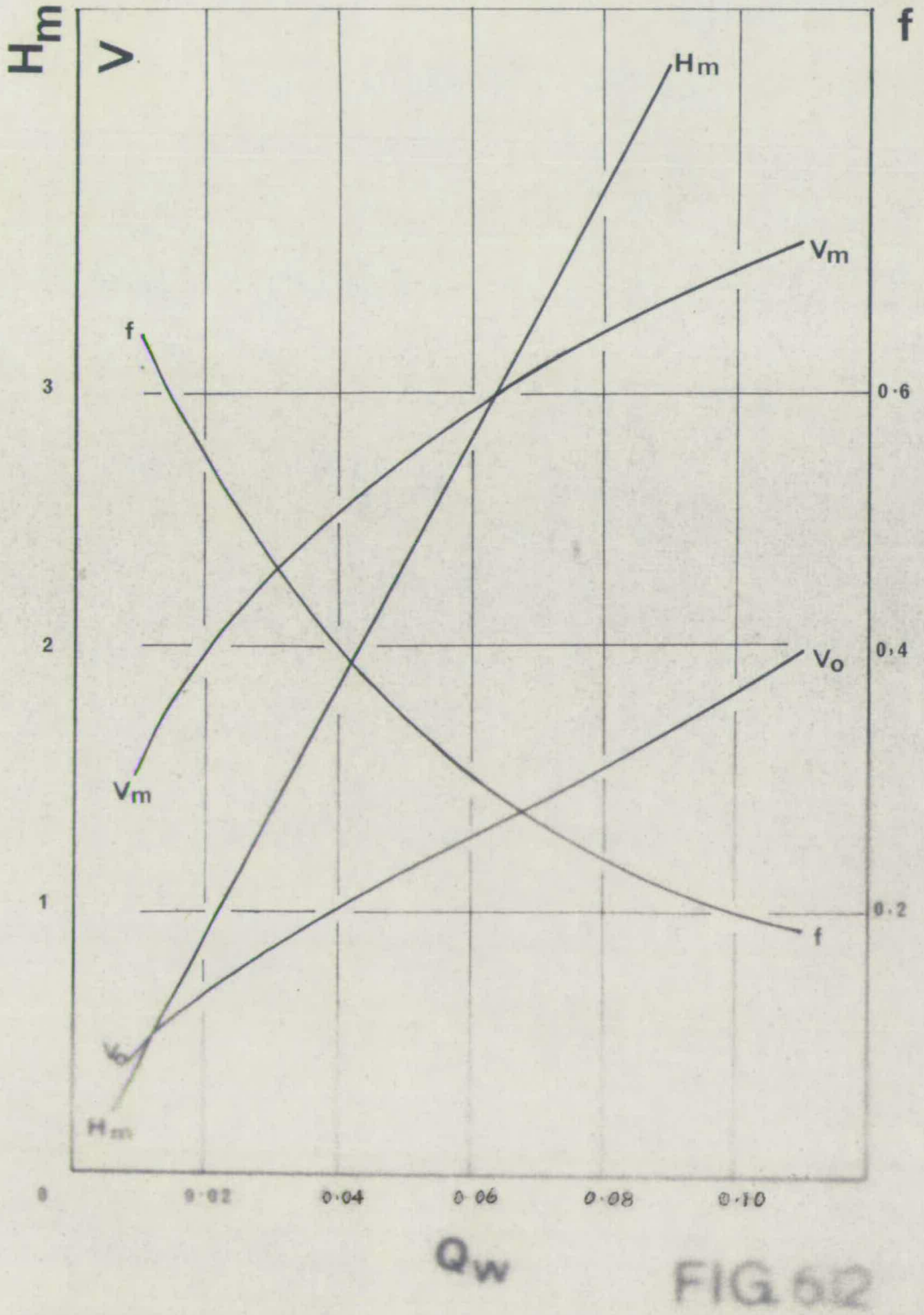

FIG 62

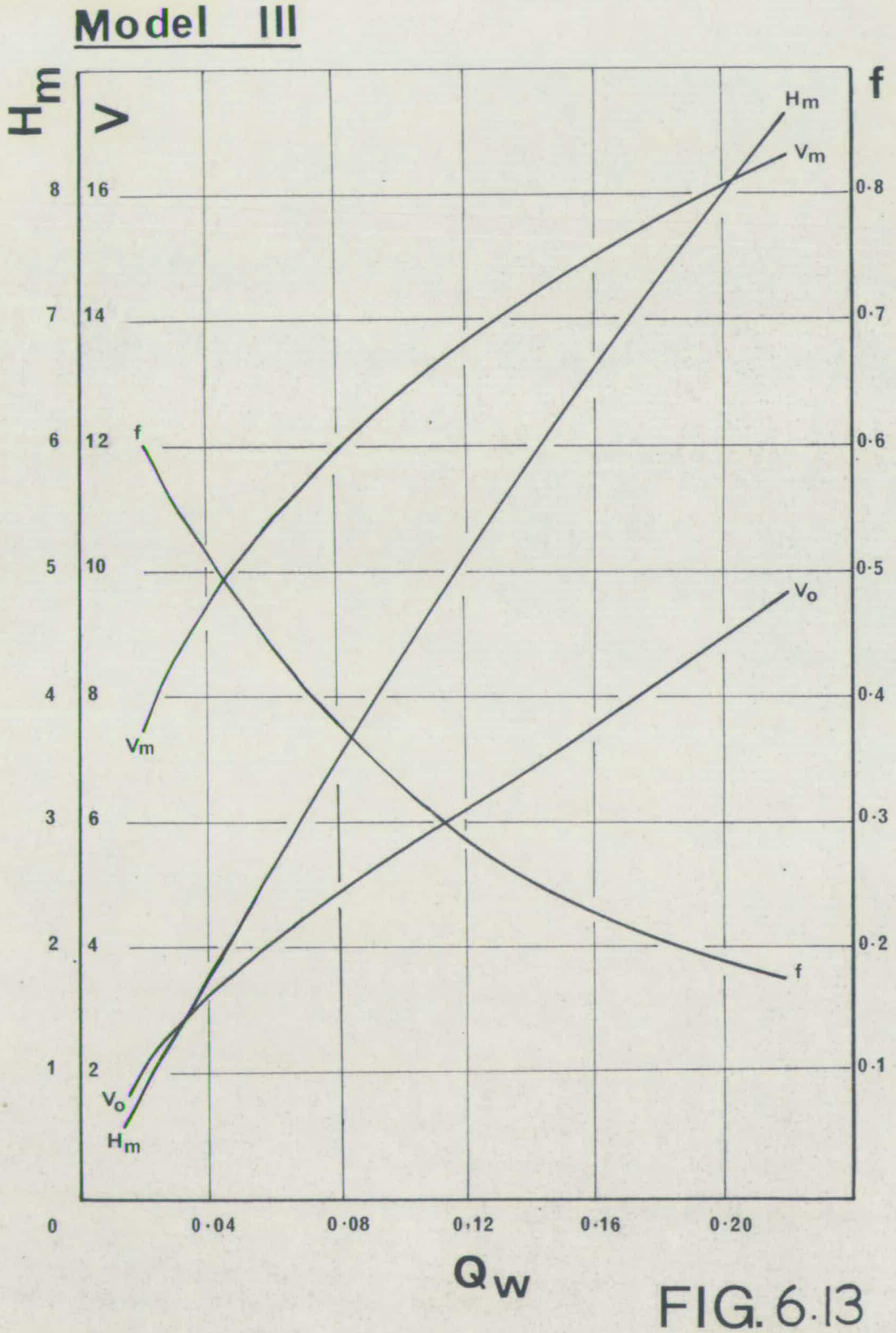
Model III
Hm
V
f
Hm
Vm
Vo
f
Vm
Vo
Hm
8
7
6
5
4
3
2
1
0
16
14
12
10
8
6
4
2
0·8
0·7
0·6
0·5
0·4
0·3
0·2
0·1
0·04
0·08
0·12
0·16
0·20
Qw

FIG. 6.13

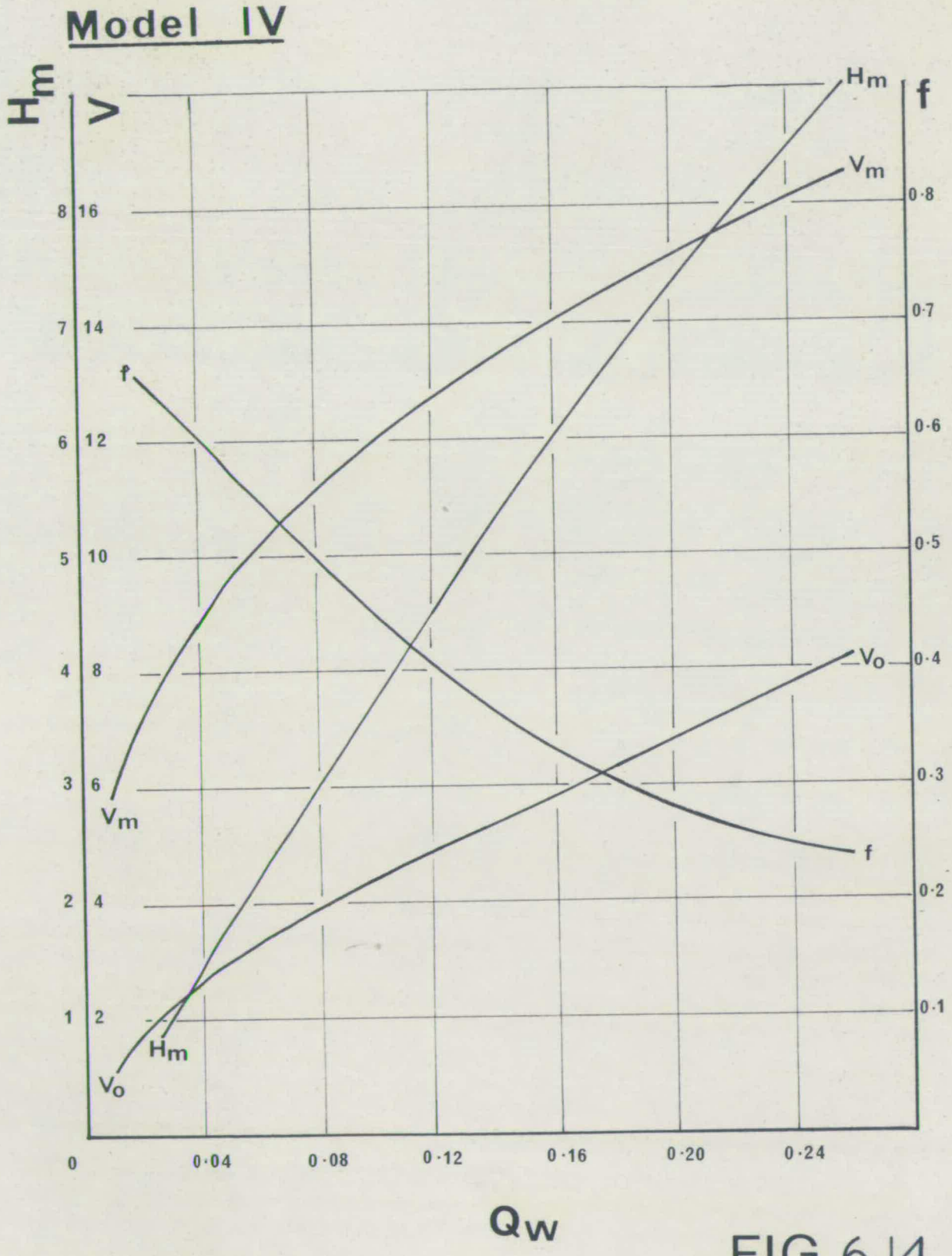
Model IV
Hm
V
f
Hm
Vm
f
Vm
Vo
f
Hm
Vo
8
16
7
14
6
12
5
10
4
8
3
6
2
4
1
2
0
0·8
0·7
0·6
0·5
0·4
0·3
0·2
0·1
0·04
0·08
0·12
0·16
0·20
0·24
Qw

FIG. 6.14

Model V

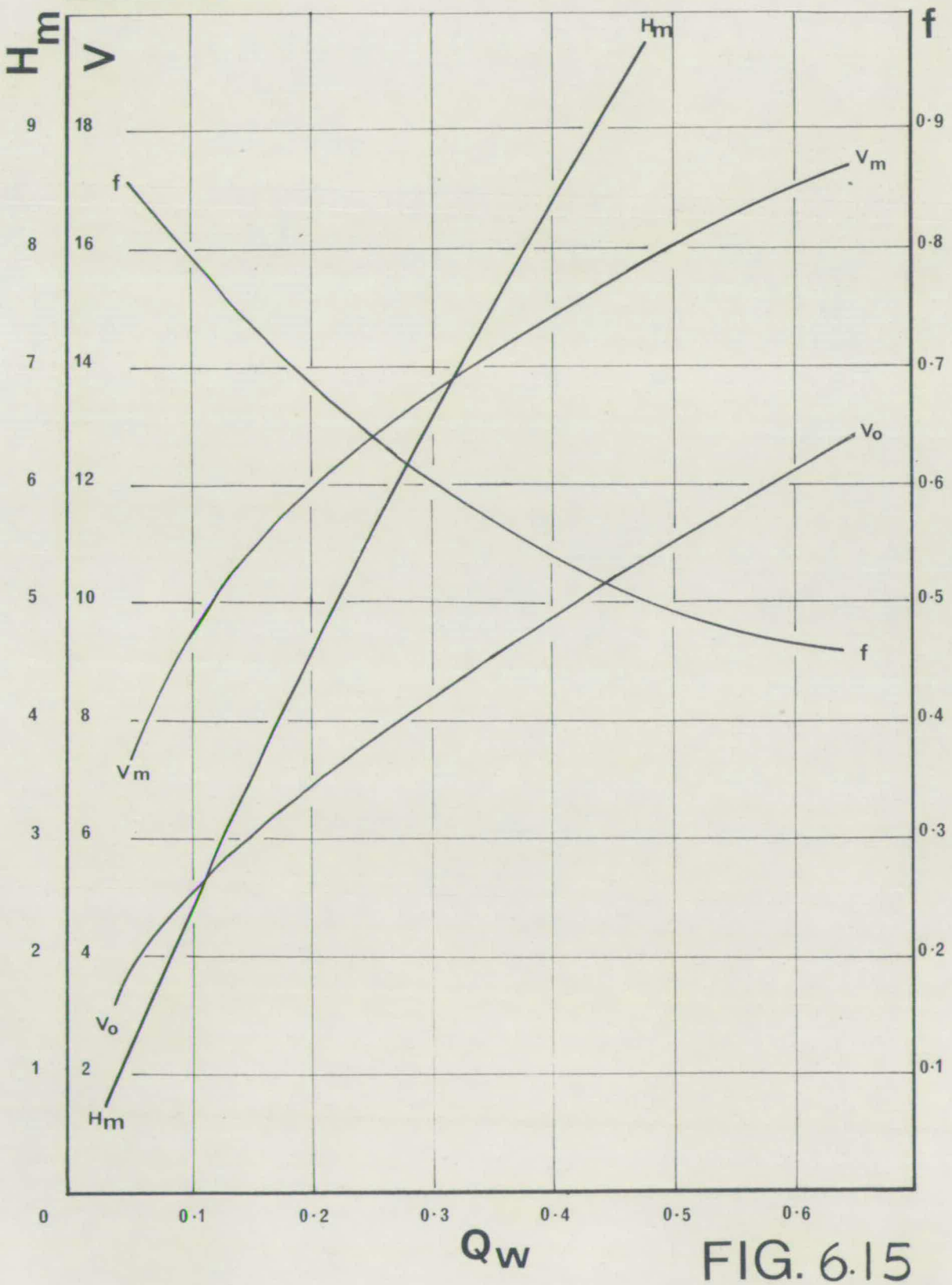

FIG. 6.15

6·12 Terminating Section and Terminating Velocity.

The position of the terminating section for a particular discharge in a drop shaft and also the magnitude of the terminating velocity have been determined according to the analysis presented in Section 2·12.

6·13 Throat Velocity.

The throat velocity which depends on the discharge and the area of the cross section of the annular ring of water at the throat, is also derived and illustrated in the Figures 6·10-6·15.

6·20 DISCUSSION ON THE ANALYSIS WITH FREE FLOW CONDITIONS

This section concerns the test results of series I and II. The former deals with the full shaft length and the latter with progressive reductions of shaft lengths. By considering five different model sizes, it does not only facilitate a wide range of discharge to be considered but also accounts for the effect of diameter which is quite a significant parameter.

The information on Figures 6·20-6·25, are the theoretical curves plotted from the computer aided results of the analysis in Chapter 2 and, also the corresponding experimental points plotted from the results in Chapter 5. It is evident that a regular pattern exists in the results of the four larger models. With increase of water discharge there exists an increase of air discharge up to a peak value, after which, with the increase of water discharge there is a decrease in the air flow.

A peak air flow is significant in the experimental analysis only in Model 5, and also somewhat in model 3. It is not readily evident/

Correlation of Theoretical and Experimental Results; model I

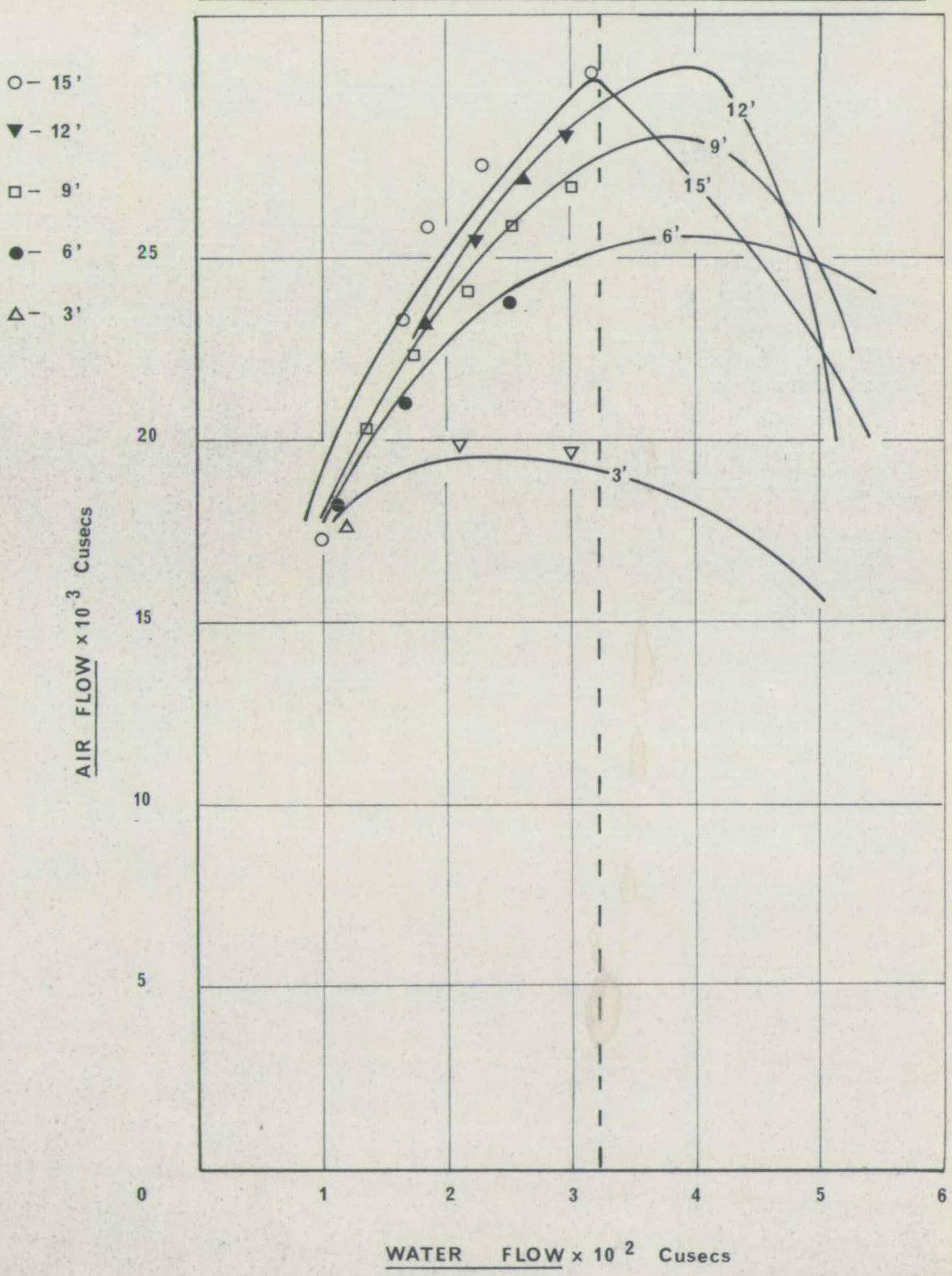

FIG. 6.21

model 2

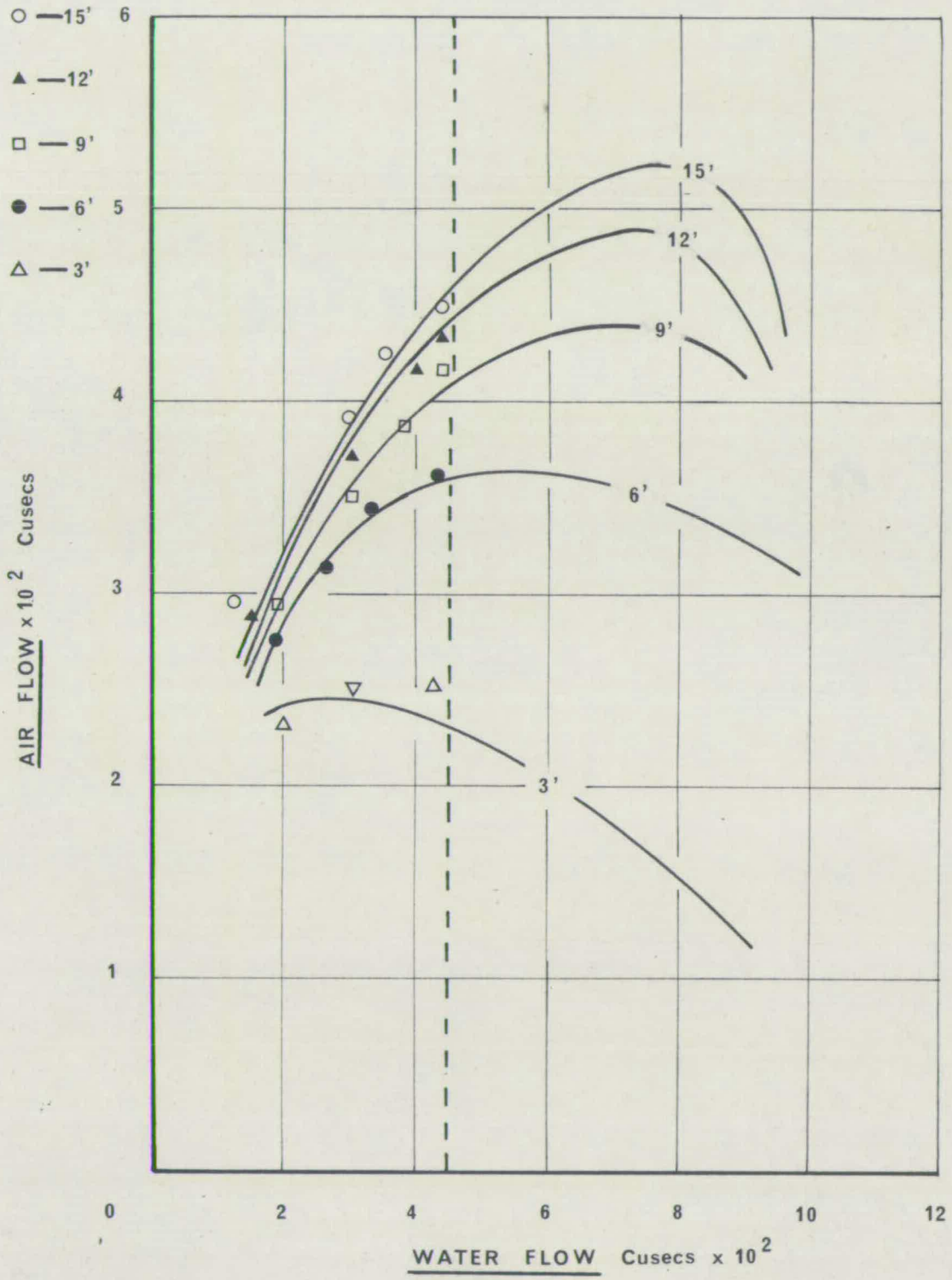

FIG.6·22

model 3

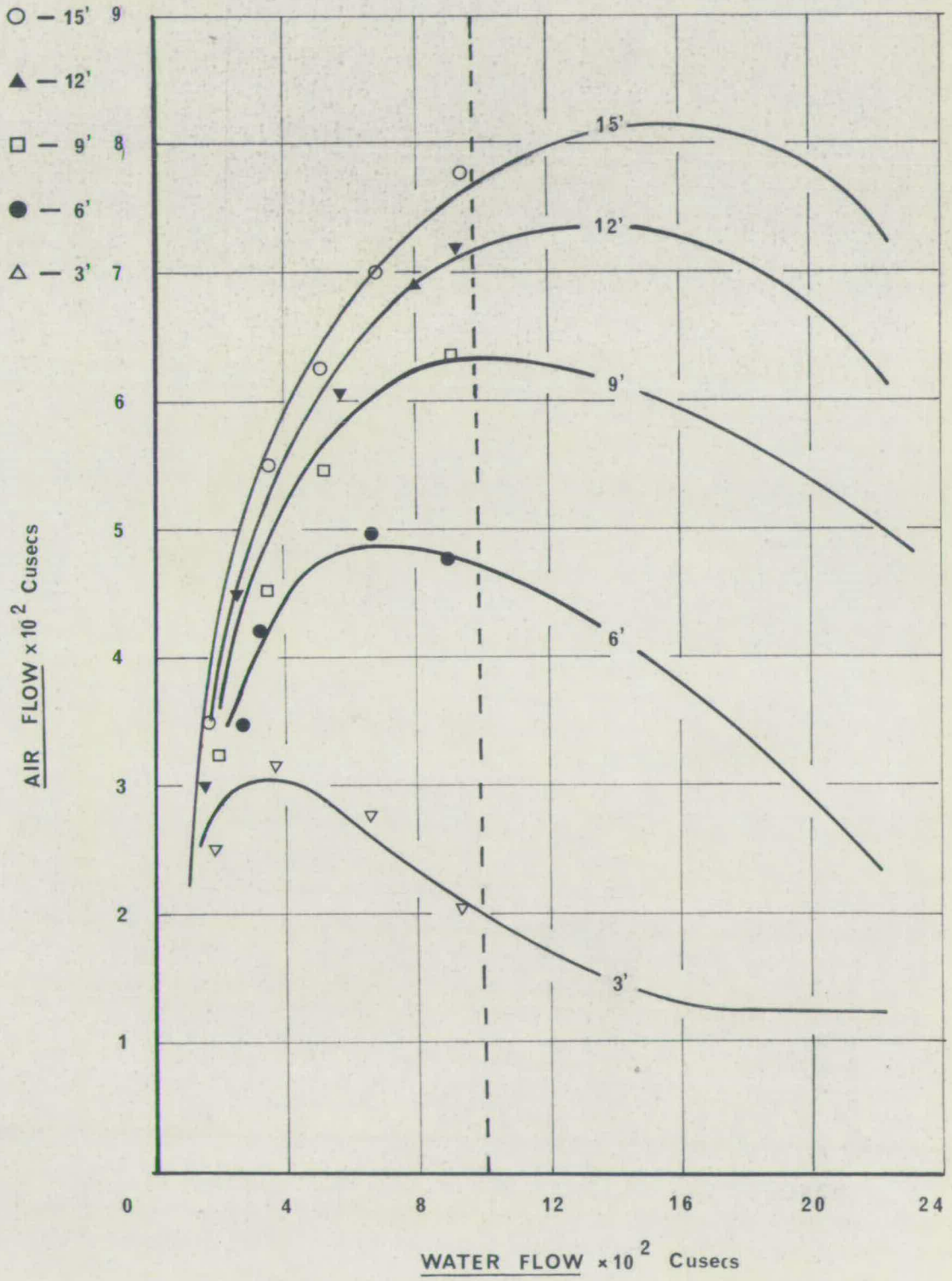

FIG. 6·23

model 4

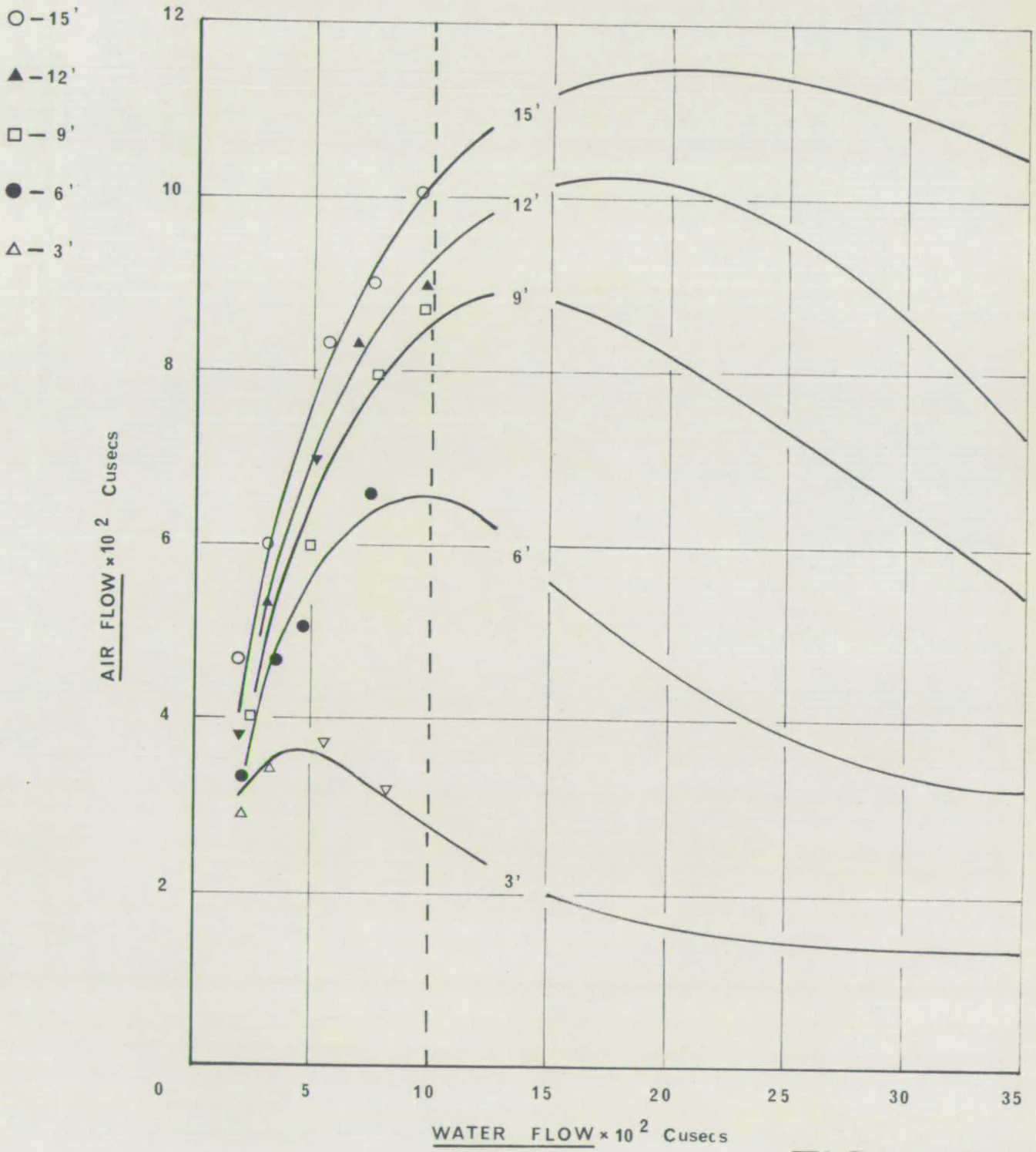

FIG. 6·24

model 5

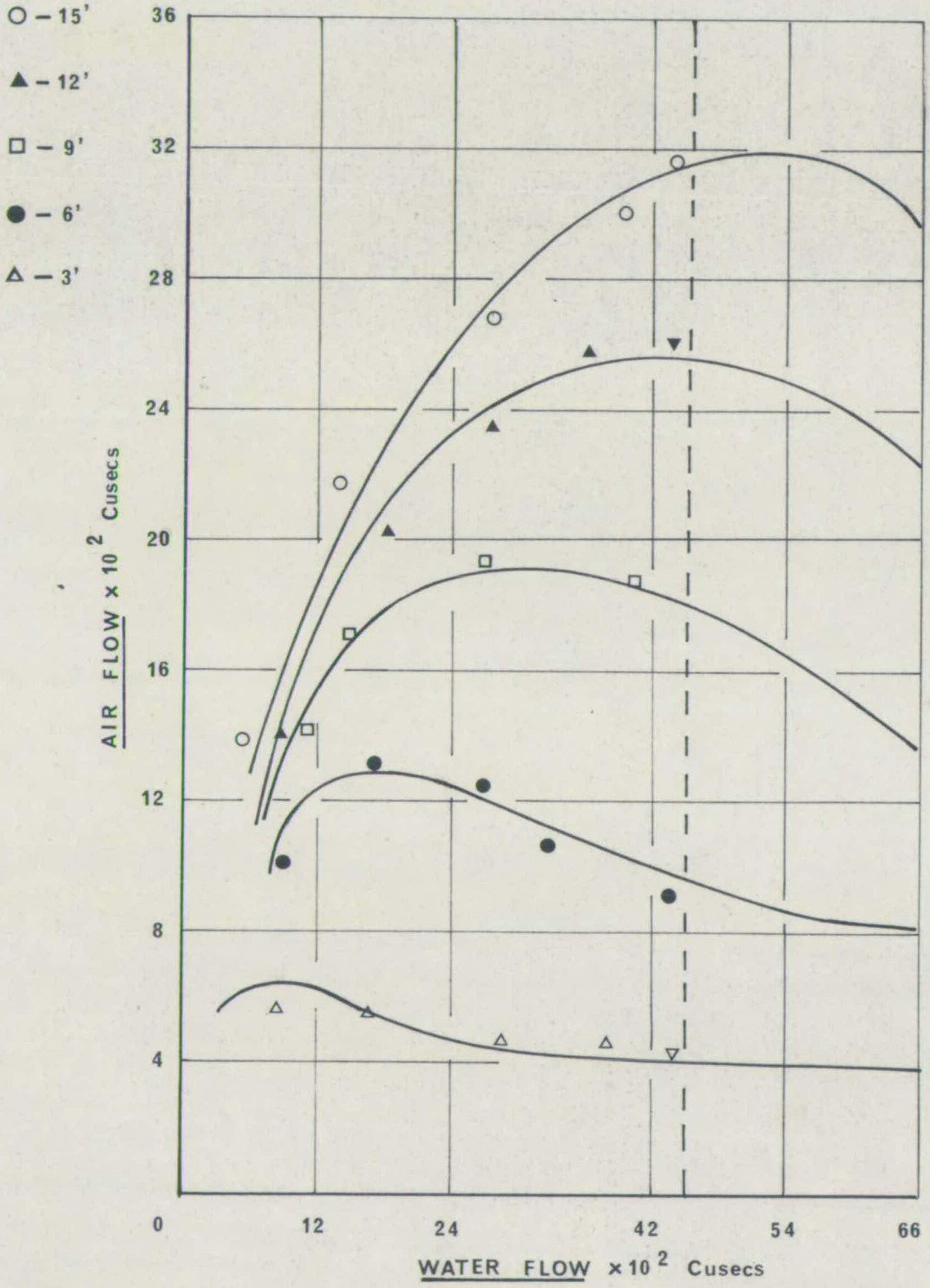

FIG. 6·25

evident in the other models due to inability of providing sufficient water flow in to the models beyond the peak values.

The maximum water flows possible due to the experimental set up, are as indicated by a vertical dotted line on each figure, for the respective models.

Another characteristic feature in the theoretical and experimental analyses observed in the four larger shafts, is the reduction in the peak air discharge with decrease of shaft length. This is, however, due to the reduction in the total volume of air core as described in section 2·13 and is experimentally significant, specially on the smaller shaft lengths.

The regular patterns as mentioned above in the four larger shafts seems to be disrupted in model 1. The irregularity of the distribution of the peak air discharge with respect to shaft length is evident specially on the theoretical curves. It is not readily evident in the experimental results, due to insufficiency of the water discharge in to the chamber. However, it is apparent that overlapping of some of the experimental points and also the irregular nature of the theoretical curves, render the model scale to be unsatisfactory for reliable performance.

Since the theoretical analysis considers each shaft individually, the question of scale effects does not arise in the procedure. Therefore the method of analysis as incorporated in the Computer program (CIE 018/0018 described in 2·22) would render results with respective to individual models. If the results of a particular model investigation is to be utilised for prototype predictions the scale effects/

the scale effects which will be discussed in the next chapter will have to be accounted for.

Two hypotheses assumed in the theoretical analysis are that (i) the maximum air velocity at the throat does not exceed that of the throat water velocity and (ii) rate of air flow into the shaft is equivalent to the increase in volume of the air core within the shaft due to the increase in the vertical velocity.

The close agreement of the experimental points with the theoretical curves justifies the validity of the assumptions.

6·30 DISCUSSION ON THE ANALYSIS WITH AN ANNULAR JUMP

The presence of an annular jump in the shaft changes the entire process of entrainment from the free flow state. The continous flow of air through the central core is disrupted by the jump and the air which is engulfed is the amount which has already been enveloped. This was the basis of the theoretical approach where it was established that the spread of the annular jet surface where the enveloping is occurring, is of a linear form.

The experimental results of the present study as shown in Figure 6·30 conformed very closely to the general equation put forward by Viparelli (2). It is however, suspected that the validity of this equation is in doubt for prototype performances. Hence, the equation is utilised in evaluating the spread of the annular jet, for model sizes whose experimental results conform with the equation. The non-dimensional plot of the air-water ratio against the ratio of free fall to diameter was the best form of presentation of the results. An attempt was made to present the resuls displaying the variation/

Correlation of Experimental results with Viparelli's Relationship

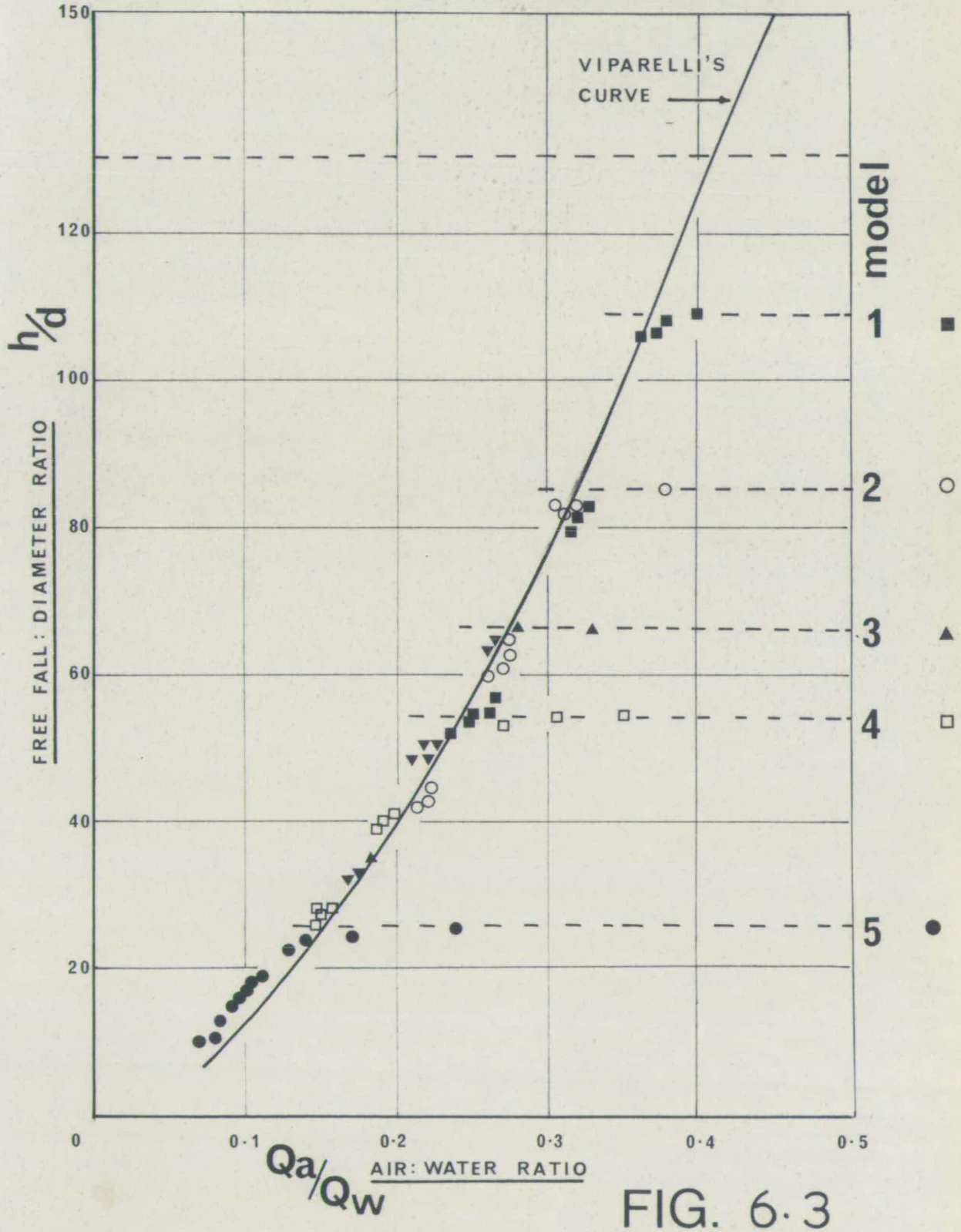

FIG. 6·3

variation of air flow to water flow for each model by considering a series of average free falls. However, this was not possible due to the variation of the free fall which had a considerable effect and could be accounted for only in the non-dimensional plot.

The correlation of the relationships derived by Laushey and Mavis (1) to that of Viparelli's, is illustrated in the Fig. 1·2. The validity of the author's relationship considering the spread of the jet is not readily evident by these tests, as these very tests have been utilized in a way to derive the semi-empirical theory. It however, appears that consideration of the actual cause of air entrainment in the relationship would render confident results in the prototype.

From the series III tests, the advantage of the presence of an annular jump is evident with respect to the reduction in the air-water ratio. However, possible disadvantages arising from the type of flow beyond the jump is illustrated in the next section. A visual comparison of the air entrainment conditions with and without a jump could lead to misconception, as the air which is entrained is not visible in the case of free flow condition, although it is of higher magnitude than with a jump, where the air bubbles and pockets are visible. In the former state the air is in the form of a core, covered all round by the annular ring of water.

6·40 DISCUSSION ON THE FLOW REGIMES

The analysis of the flow regimes has been dealt with in a purely empirical/

empirical manner. A theoretical approach was not attempted since this aspect is not directly related to the air entrainment but rather a consequence of it.

Although, the presence of an annular jump reduces the magnitude of the air-water ratio, conditions beyond the jump could be undesirable. Effects such as gulps of air being blown back and wide ranges of pressure fluctuations at the exit, could be the result of air pocket formation due to the unsuitable flow regime. The net quantity of air flow could be considerably less even during these conditons, but the detrimental effects may be increased. These unstable conditions were evident in the original tests[13] described in Appendix B, where it was decided to have a free flow condition and thereby a larger quantity of air flow than these adverse effects with a lesser quantity of air flow.

Froude's number which has been established as the criterion in classifying the flow regimes is as described in section 5·4, is analogous to its use in defining the type of jump in an open channel. Further investigations into the motion of air bubbles and pockets on a theoretical basis, could lead to more firm conclusions of their performances.

6·50 VERIFICATION OF FORMER THEORIES

A plot of experimental results with the theoretical curves of Dawson and Kalinske are presented in Figure 6·41. The experimental analysis was conducted on a comparative basis, to justify the increase in the vertical velocity along the shaft to a particular depth, after which the velocity to remain constant. This was evident from the tests.

Vertical Velocity Variation

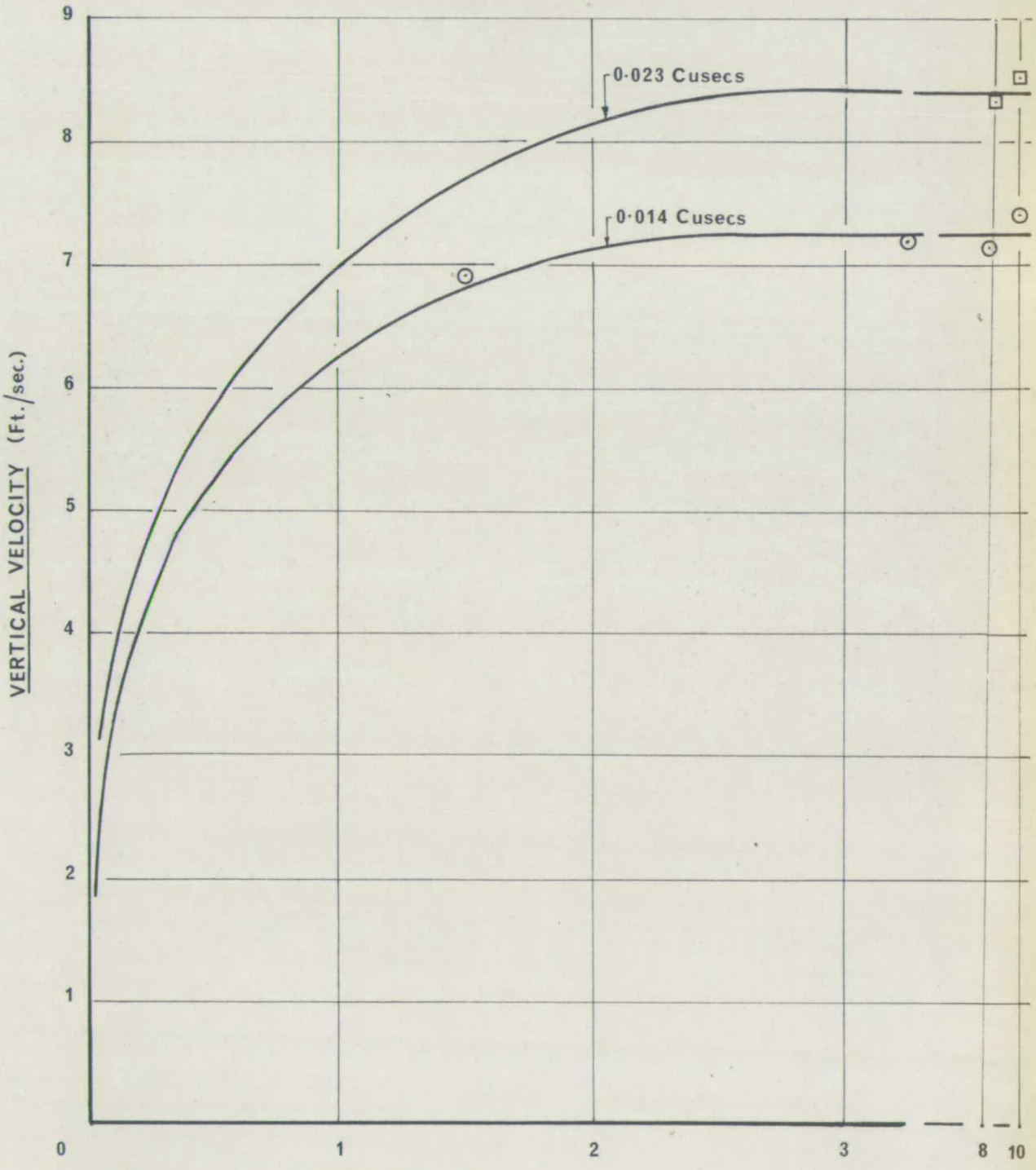

model 3

FIG. 6-41

Variation of Air Core with Water Discharge

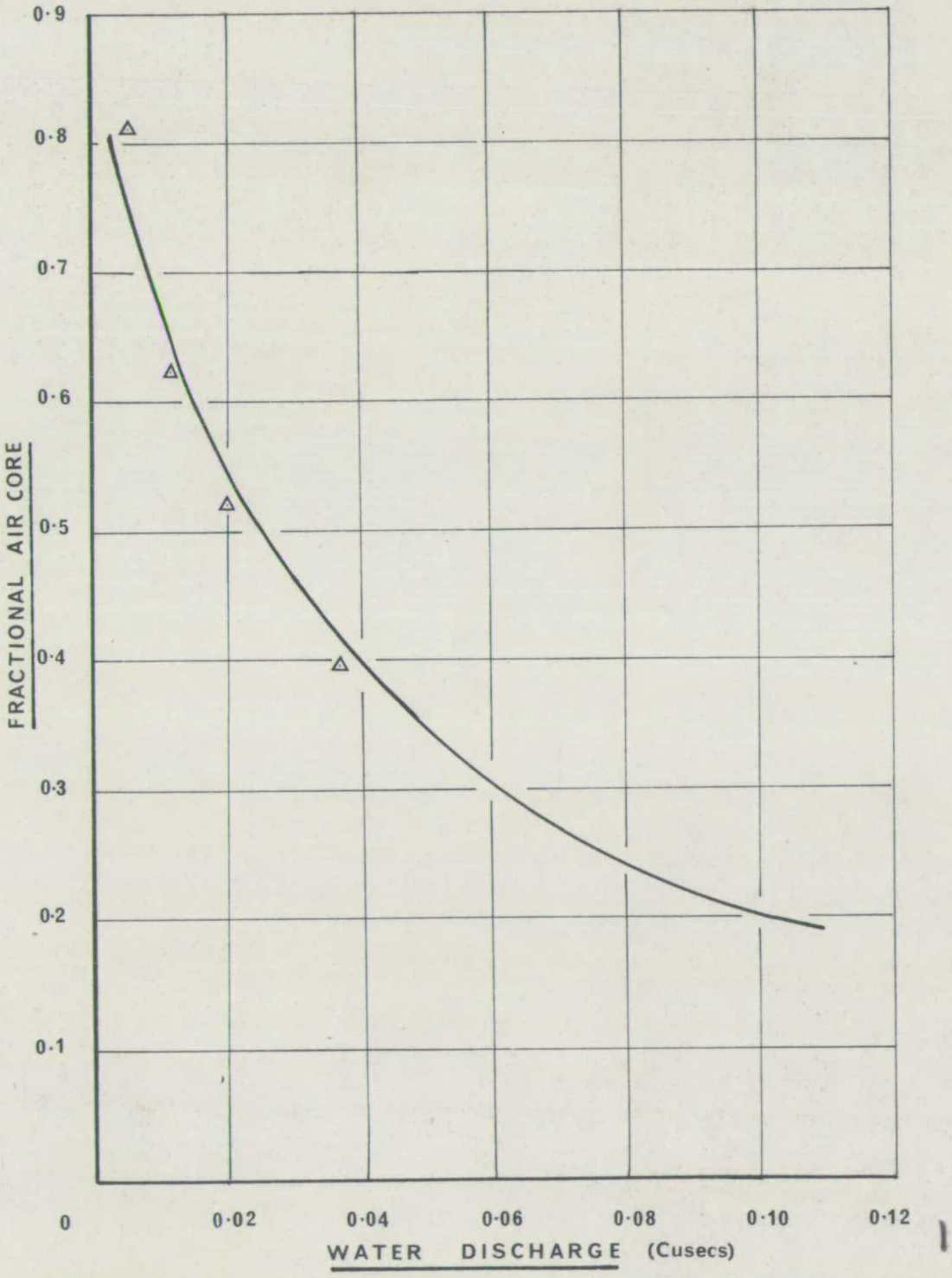

model 2

FIG. 6·42

Air core diameter variation with the water discharge was experimentally verified to be in accordance with Ackers and Crump theory (6) as described in section 2·11. The experimental results are plotted on Fig. 6·42 along side the theoretical curves obtained from the computer analysis. Although there is close agreement of the experimental points with the theory at lower water discharges i.e. large values of fractional air core, there appears to be a possiblity of a deviation. Though this was not possible to be verified due to the lack of water dicharge it seems unlikely that a vortex chamber would be used for fractional air cores less than 0·4.

6·60 CONCLUSIONS

An attempt is made in this chapter to justify experimentally the theoretical analyses incorporated in this study. Correlation has been achieved in most of the cases and any evidence of disparity specially in the early series of tests is due to the unsuitability of the particular model size.

The semi-empirical theory on air entrainment with a jump, is an extension of Viparell's (2) empirical equation and is developed by considering the actual cause of entrainment during such conditions. However, it is not possible to correlate the author's theory with experimentation, unless further large scale or prototype investigations are conducted.

Verification of Ackers and Crump theory indicated possible deviation from their analysis for low values of fractional air core. However, for the range of flows the vortex chambers would normally be used/

be used, the theory correlated satisfactorily with the experimental results.

The increase in vertical velocity along the shaft up to a certain section and thereafter being constant was observed in the experimentation which is in accordance with the theory of Dawson and Kalinske.

CHAPTER VII

SCALE EFFECTS AND PROTOTYPE PREDICTIONS

7·00 INTRODUCTION

It may not be too presumptuous to state that the 'Scale effects' render the greatest hindrance and that estimation of prototype performance is the 'main aim', of any hydraulic model investigation. The question of scale effect is one of the most important matters of concern facing the research worker in this field. Scale effect is merely the conventional expression for possible discrepancies involved in extrapolating the results obtained on models to the full scale. Unless the scale effects are very small or are predetermined experimentally, the results of model tests cannot be applied with confidence to the large scale.

Though Laws of Hydraulic Similarity govern the relationship between model and prototype, a clear understanding of the phenomenon to be investigated is essential, if the results are to be correctly interpreted. Due to the impossibility of achieving simultaneous compliance, in respect of all the laws, the discrepancies in extrapolating to the full scale are inevitable.

As a first step, in reducing scale effect larger models are favoured, but the increase of constructional and operational costs with size, controls the extent of such attempts.

In the present study five scale models are investigated with a view to determining any scalar discrepancies and their magnitudes. The choice/

choice of the five scales as mentioned in Chapter III, and care was taken that prototype hydraulic conditions were maintained even in the smallest scale size. Complete Geometric Similarity between the models was aimed at, except for roughness consideration which was assumed to have very little or no effect on air entrainment properties. For Dynamic Similarity, Froude's Law was considered to be the Criteria.

7·10 FACTORS RESPONSIBLE FOR SCALE EFFECTS

This problem of scale effects which exists ubiquitously in Hydraulic Model Studies is aggravated when more than one fluid is under investigation. Hence, in an investigation of Air Entrainment in water, factors which are responsible for scale effects are in addition to the factors which normally persist. The compressibility of air gives rise to the volumetric flow rate being dependent on the intake pressure.

The inability to obtain perfect hydraulic similarity i.e. to comply with laws of Froude, Reynolds and Weber, would render discrepancies in the extrapolation. At the air-water interface, effects of Surface Tension and viscosity predominate at low discharges. Compliance of the laws of Weber and Reynolds would render major practical difficulties in a large scale experiment of this nature and owing to the significance of gravity predominating above all other factors, Froude's criteria was the basis of the hydraulic similitude. Hence the application of the method of prediction incorporated in this chapter would depend largely for models investigated on Froude's criteria.

The air bubble formation due to impact at the annular jump contributes a possible/

a possible major discrepancy. The size of bubble formed at the jump is independent of the model scale. The increase of model scale may not increase the size of bubble but only increase the magnitude. The ability of a bubble to travel a vertical shaft largely depends on the freedom of movement due to the magnitude of bubbles. Hence an increase of scale virtually restricts this freedom. The investigations conducted in the Hydraulic Research Station (4) indicated a decrease in the total air-water ratio with increase of model scale. They explained this being due to the increased centripetal movement of air bubbles across the higher pressure gradient resulting from greater centrifugal forces in the larger diameter shafts. The question of scale effects primarily arises when predicting prototype performances from model tests. Its disadvantage is also realised when empirical methods are utilised in the design. The latter, could be overcome if the underlying phenomenon is recognised and utilised in the design criteria.

7·20 PROTOTYPE PREDICTION

Considering the two different states where air entrainment would occur in a vertical shaft an attempt is made to postulate a method of prototype prediction for cases where the actual evaluation from the underlying phenomenon is rather laborious.

A theoretical analysis has been developed in this study to evaluate the quantity of air which would be entrained in a drop shaft of known geometry, with a particular water discharge falling freely for the full length. Its evaluation involves a lengthy mathematical manipulation, which could be solved easily only by a computer. Since this facility may not be readily available in all cases, a

Nomogram/

Nomogram has been developed in this chapter. The empirical procedure which has been utilised in producing this graphical analysis, is based on the theoretical results which have been justified by experimental correlation.

In the case of a jump being present in the shaft, the semi-empirical theory developed in this study could be utilised to determine the air-water ratios without much manipulation. Hence, a graphical analysis is not necessary and has not been attempted.

7·30 METHOD OF ANALYSIS

As described in Chapter III the apparatus consists of five shafts of equal lengths. Due to the equality of lengths of the shafts Geometric Similarity is not present with respect to length. To obtain Similarity with respect to length it was necessary to consider one of the shafts to be the true representative length of the prototype, for the purpose of analysis of the scale effects. The largest shaft was assumed to be the scaled length of the prototype and since the model shaft length is 15 ft., the prototype length resulted to be 54·75 feet as the scale of the respective model is $^{1}/_{3.65}$. The effective lengths of the remaining four models were evaluated to be as follows:-

Model No. 1 - 3·59 feet

No. 2 - 4·56 feet

No. 3 - 5·86 feet

No. 4 - 7·16 feet

Hence in this chapter when scale effects are considered on each model, its effective lengths will be taken into account as above, for the purpose/

for the purpose of determining the air-water ratios.

From the theoretical results of the analysis for air entrainment without a jump (as presented in Chapter II and on Figures 6·21-6·25), Table 7·1 is obtained, where six tests flows have been utilised. The water discharges are converted to prototype values so as to maintain a uniformity.

It is evident from the table that the air-water ratio not only varies for each model, but also varies during each test run. Results of each test run when plotted on a logarithmic base indicated that the relationship between the air-water ratio and the model scale was in the form

$$\frac{Qa}{Qw} = a\left(\frac{1}{S}\right)^n \qquad \text{.....7·0}$$

where Qa and Qw are water discharges

$\frac{1}{S}$ is the model scale

a and n are constants

Referring to figure 7·1 where the results of the six test flows are plotted, it is seen that the value of the constants a and n vary with each prototype water discharge. The values of a and n are obtained from figure 7·1 and tabulated in Table 7·2 and plotted in Figure 7·2. Two smooth curves were fitted to the plotted points and the equations fitting the two curves were derived to be as

$$a = 0{\cdot}02187 - \frac{5{\cdot}9577}{Q} + \frac{273{\cdot}9677}{Q^2} - \frac{2275{\cdot}7075}{Q^3} + \frac{2908{\cdot}0333}{Q^4} + \frac{13830{\cdot}0626}{Q^5} \qquad \text{.....7·1}$$

$$\text{and } n = -0{\cdot}5 + 0{\cdot}004Q - 0{\cdot}000065Q^2 \qquad \text{.....7·2}$$

SCALE EFFECTS TEST RESULTS

Unit	Model I	Model II	Model III	Model IV	Model V	Prototype
Scale $^1/S$	$^1/15{\cdot}25$*	$^1/12$	$^1/9{\cdot}34$	$^1/7{\cdot}65$	$^1/3{\cdot}65$	$^1/1$
Discharge Scale $^1/S$	$\frac{1}{909{\cdot}19}$	$\frac{1}{498{\cdot}83}$	$\frac{1}{266{\cdot}60}$	$\frac{1}{161{\cdot}87}$	$\frac{1}{25{\cdot}45}$	$\frac{1}{1}$
Effective length (ft)	3·59	4·56	5·86	7·16	15·00*	54·75
Test Run (1)						
Qw Cusecs	0·005	0·010*	0·018	0·031	0·196	4·98
Qa Cusecs		0·021	0·031	0·049	0·246	
(Q_a/Q_w)		2·1	1·668	1·560	1·254	
Test Run (2)						
Qw Cusecs	0·010*	0·018	0·034	0·056	0·356	9·08
Qa Cusecs	0·018	0·025	0·042	0·062	0·300	
(Q_a/Q_w)	1·800	1·411	1·247	1·098	0·846	
Test Run (3)						
Qw Cusecs	0·015*	0·027	0·051	0·084	0·535	13·62
Qa Cusecs	0·019	0·028	0·046	0·067	0·316	
(Q_a/Q_w)	1·293	1·036	0·905	0·804	0·591	
Test Run (4)						
Qw Cusecs	0·020*	0·036	0·068	0·112	0·713	18·16
Qa Cusecs	0·020	0·029	0·048	0·071		
(Q_a/Q_w)	1·005	0·831	0·705	0·635		
Test Run (5)						
Qw Cusecs	0·033	0·060*	0·112	0·184	1·170	29·92
Qa Cusecs	0·020	0·028	0·044	0·059		
(Q_a/Q_w)	0·621	0·468	0·395	0·322		
Test Run (6)						
Qw Cusecs	0·050*	0·091	0·170	0·281	1·784	45·41
Qa Cusecs	0·017	0·024	0·032	0·026		
(Q_a/Q_w)	0·342	0·259	0·185	0·091		

Table 7·1.

* denotes initially assumed value.

Variation of Air Water Ratio with Model Scale for Prototype Water discharges.

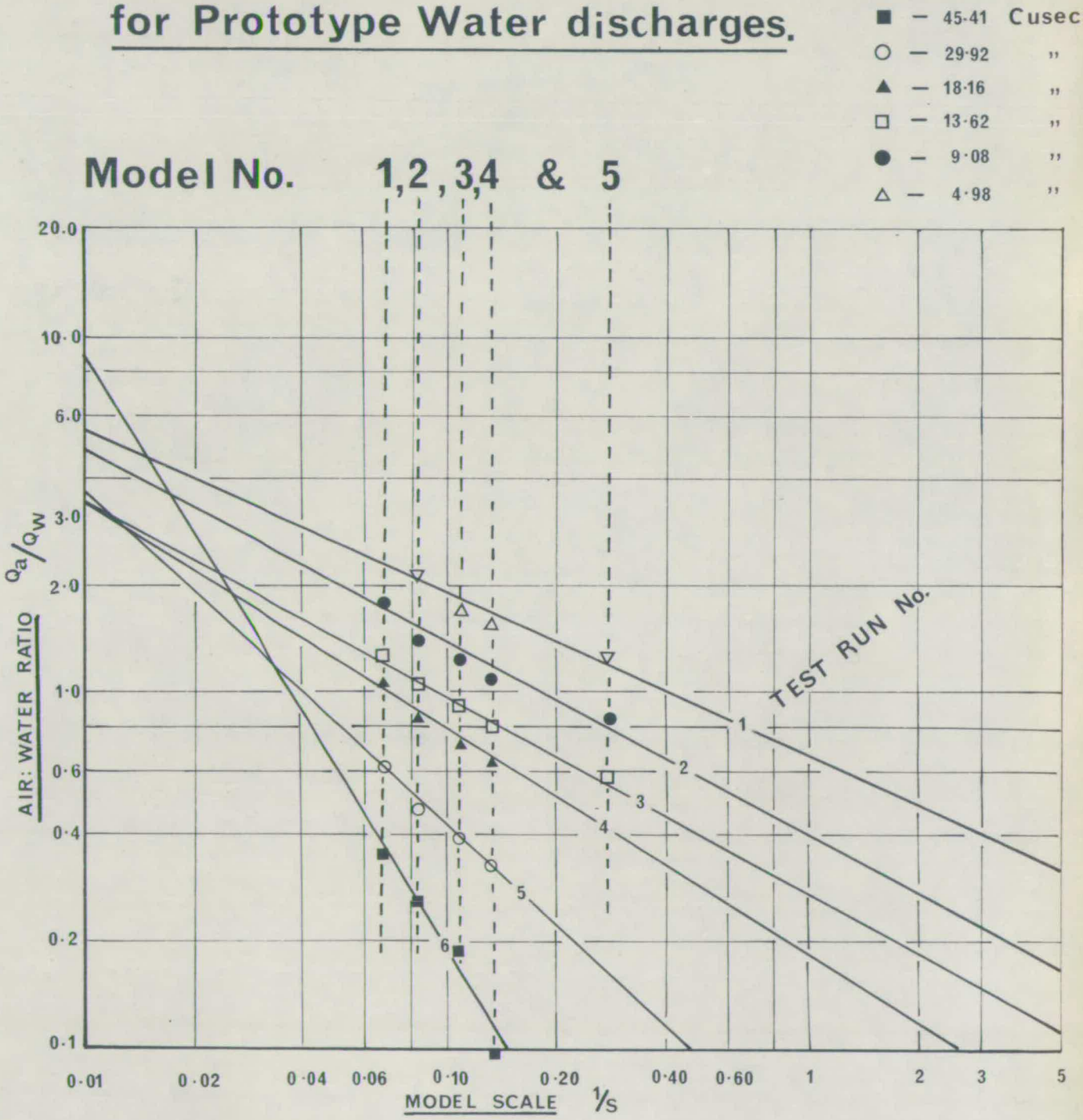

FIG. 7·1

Variation of Scale Constants with Discharge

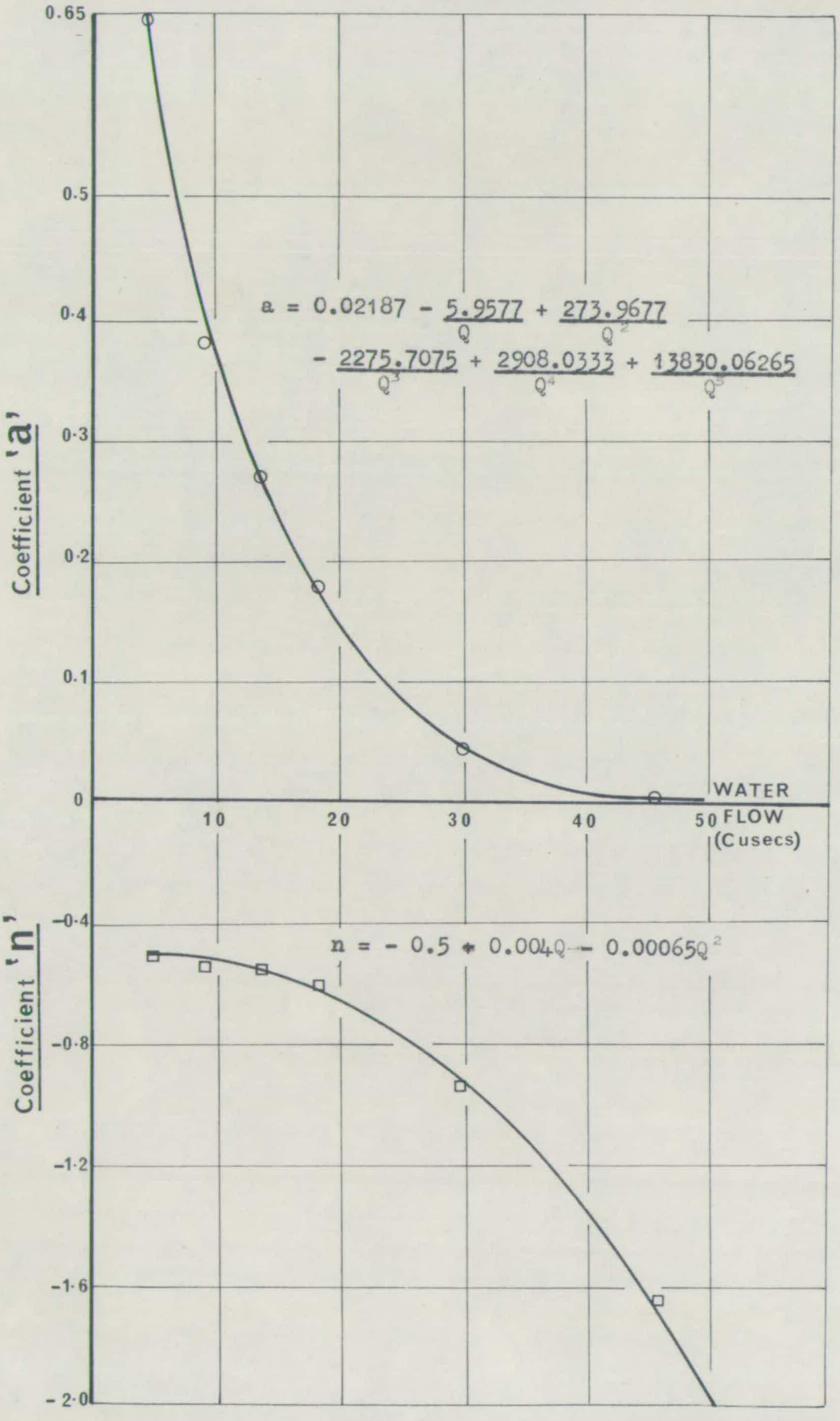

FIG. 7·2

VALUES OF THE SCALE COEFFICIENTS

Test run number	Qw (Proto) Cusecs	n	a
1	4·98	-0·508	0·650
2	9·08	-0·541	0·380
3	13·62	-0·545	0·270
4	18·16	-0·608	0·180
5	29·92	-0·946	0·047
6	45·41	-1·654	0·004

Table 7·2.

7·40 APPLICATION OF THE NOMOGRAM

For any particular prototype water discharge the values of the coefficients a and n could be determined from the equation 7·1 and 7·2. The values of the constants could be substituted in the equation 7·0 with the appropriate scale ($^1/S$) to determine the air-water ratio. Since the evaluation of the constants and thereafter the evaluation of the air-water ratio, requires mathematical manipulation the Nomogram as presented in Figure 7·3 is derived which facilitates the analysis.

Though the variation of the air-water ratio with the model scale is as in equation 7·C, it is necessary to insert an experimental constant k in the equation which would account for any significant effects in the design or in the experimentation. Hence, the general equation will be

$$\frac{Qa}{Qw} = k.\ a\left(\frac{1}{S}\right)^n \qquad \text{.....7·3}$$

NOMOGRAM

RELATING AIR-WATER RATIO TO PROTOTYPE WATER FLOWS FOR DIFFERENT MODEL SIZES

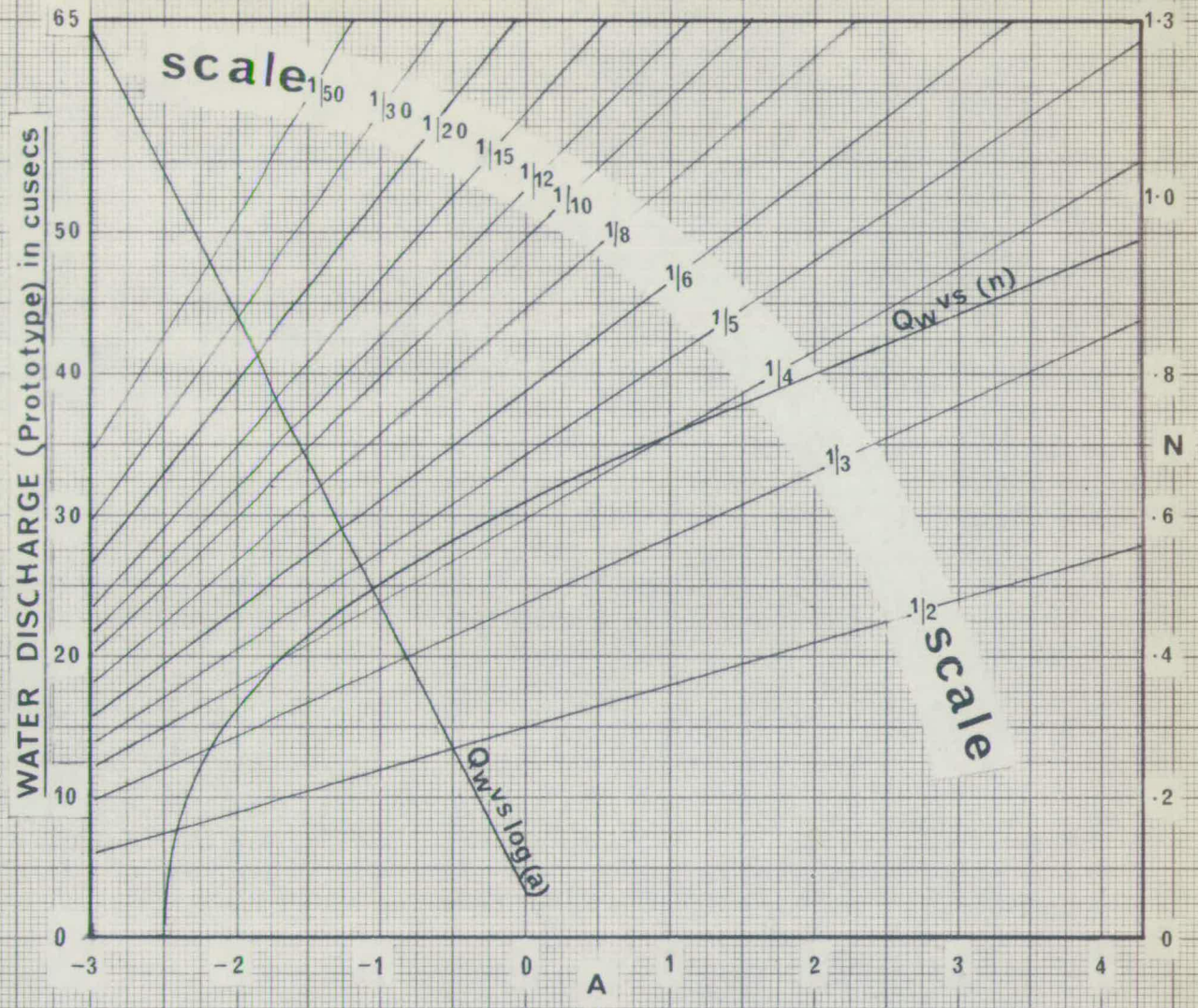

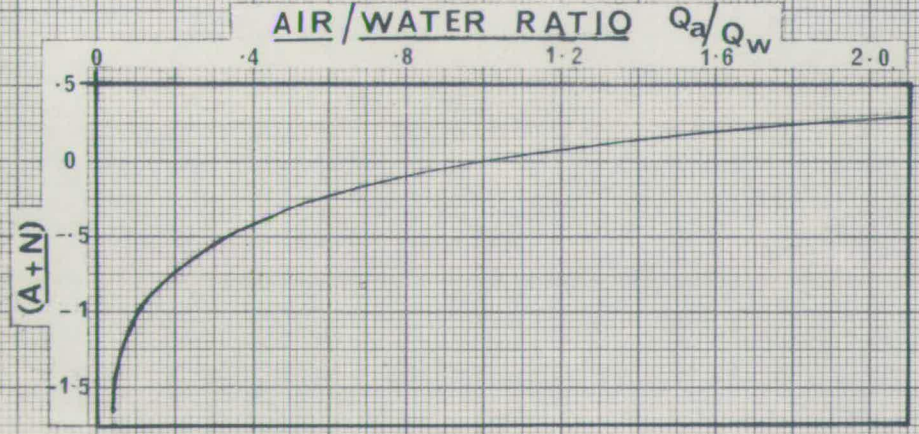

FIG. 7.3

In the application of the nomogram it is first necessary to determine the value of k which would normally be equal to 1, by measuring the air-water ratio on a particular model and also obtaining the value from the nomogram.

Hence $k = \frac{(Q_a/Q_w) \text{ measured}}{(Q_a/Q_w) \text{ nomogram}}$

Knowing the value of k as a correction factor, the air-water ratio of any other model scale or the prototype could be determined. The procedure involved is illustrated below with an example.

Data

Prototype Q_w = 18·16 Cusecs

Scale of model being tested = $^1/12$

Measured $^{Q_a}/_{Q_w}$ = 0·83

Required to know

(a) $^{Q_a}/_{Q_w}$ in a model scale $^1/3$

(b) $^{Q_a}/_{Q_w}$ in the prototype

both under the same prototype discharge.

Method

A horizontal line is drawn across Q_w = 18·16 cusecs till it intersects the graphs Q_w vs(n) and Q_w vs log (a), where the log (a) graph is met, a vertical line is dropped and the value of A noted. Where the original horizontal line intersects with the graph Q_w vs(n), a vertical line is drawn till it reaches a diagonal line representing the scale under consideration. At the intersection with the diagonal line a further horizontal line is drawn to reach the N axis and the value of N then obtained./

obtained. The sum of (A + N) is read on the next graph which would then denote the value of $^{Qa}/_{Qw}$. This value of $^{Qa}/_{Qw}$ corrected by k gives the required value of the air-water ratio.

Results

From graph 7·3a

Reading Qw = 18·16 cusecs; $^{1}/_{S} = {}^{1}/_{12}$;

A = -0·75; N = 0·67;

$\therefore$ A + N = - 0·08

From graph 7·3b

when (A + N) = - 0·08; $\frac{Qa}{Qw} = 0{\cdot}831$

since $k = \frac{(^{Qa}/_{Qw}) \text{ measured}}{(^{Qa}/_{Qw}) \text{ actual}}$

$$k = \frac{0{\cdot}83}{0{\cdot}831} = 0{\cdot}99879$$

Now for a model scale of $^{1}/_{3}$

A = -0·75 and N = 0·3

(A + N) = -0·45 and $\frac{Qa}{Qw} = 0{\cdot}38\ k$

i.e. $\frac{Qa}{Qw} = 0{\cdot}38 \times 0{\cdot}99879 = \underline{\underline{0{\cdot}3795}}$

Also in the prototype, N = 0 and A = -0·75

therefore for (A + N) = -0·75; $^{Qa}/_{Qw} = 0{\cdot}2\ k$

i.e. $^{Qa}/_{Qw} = \underline{\underline{0{\cdot}1996}}$.

7·50 CONCLUSIONS

Although the scale effects occur in the prediction of prototype performance from model tests due to reasons mentioned in this chapter, the ability to estimate their magnitude both theoretically and experimentally, enabled an empirical solution to be derived in the form/

in the form of a Nomogram to account for the discrepancies. The need of this method is specially great for vertical shafts with free flow, as its individual theoretical analysis is rather laboricus.

It may be concluded that the air-water ratio is increased with the decrease of model size. Although this could be considered as an additional factor of safety, it may be uneconomical and also result in unsatisfactory prototype performance with respect to the flow regimes.

CHAPTER VIII

CONCLUSIONS

8·00 INTRODUCTION

The author of a thesis is normally faced with the dilemma of being either complete or compact. The first format could lead to the work being uneven and disjointed because the contributions to some aspects being greater than to others and often being unrelated; the latter would endanger the omission of important peripheral information, which may be indispensable for the extension of the study under consideration.

The growing concern on Air Entrainment in Vertical Shafts led to this investigation.

The results which were postualted and observed, and recommendations deduced from the analyses, are presented in this chapter, so as to suit the individual interests of the reader. (e.g. Theoretician, Experimenter and Model Investigator, Designer and the Research worker).

THEORETICAL CONSIDERATIONS

The consideration of an actual mechanism is necessary in a confident theory and relationships which would overcome scale effects are essential for an empirical analysis.

The theoretical analyses in this study elucidate the process of Air Entrainment in the case of free flow, to be that due to Suction effects; and in the case of a jump in the shaft, the cause being solely the spread of the annular jet.

In the case/

In the case of free flow, the increase in the volumetric air core in the vertical shaft due to the increase in the Vertical Velocity gives rise to negative pressure effects within the shaft, which in turn draws air from the atmosphere. However, the reduction in the throat air core diameter with the increase of water discharge has a controlling effect, which eventually reduces the air flow beyond a particular water discharge.

Although the same process takes place in a shaft with an annular jump, the latter disrupts the free flow of air in the central core. The entrainment occurring under such conditions is solely due to the spread of the annular jet, thus enveloping air along its path of travel and engulfing the air so entrapped at the jump. The spread of the jet was found to be of a linear form and a semi-empirical relationship enables the spread to be evaluated; the spread being dependent on the shaft geometry and the water discharge.

8·20 EXPERIMENTAL CONSIDERATIONS

The experimental analyses of this study were conducted with a view of correlating them to the theoretical results; obtaining further experimental evidence to formulate empirical relationships; and to verify theories of former research work on which the present study is based.

The apparatus which consisted of five geometrically similar models, enabled the effect of scale to be carefully examined. The main experimental techniques constituted of measuring the water discharge over a 'V' notch and the air flow (i) by pressure difference across orifice plates (ii) by a Davimeter (hot wire anemometer principle).

In the Similarity considerations, it is evident that this type of hydraulic problem entails Criteria of Froude, Reynolds and Weber to be accounted for. However, in spite of practical disadvantages, the absence of a fluid to conform to perfect hydraulic similarity led to the choice of the predominating criterion to be procured. This was decided to be as Froude's Law, due to the large gravitational effects acting on this type of vertical flow.

The presence of Surface Tension and Viscous effects at low discharges could give rise to discrepancies due to the non-compliance of Weber and Reynolds laws. These discrepancies together with those mentioned in Chapter VII hinder accurate prototype predictions. The empirical analysis postulated in the form of a Nomogram, (to predict prototype and other model size performances) would be applicable to models investigated on similitude considerations as mentioned.

The results of the experimental analyses support the theoretical approach to the study. The experimentation also revealed a further phenomenon of flow regimes occurring in the shaft beyond the Annular Hydraulic Jump. These flow regimes were classified with respect to Froude's Number, which groups the regimes to be the safest, the most detrimental and the most economical, respectively.

The experimental verifications of former theories though not dealt with very comprehensively, produced convincing results within the limits of the experimental study considered.

8·30 DESIGN CONSIDERATIONS

The results of an investigation of this type are best utilised, if put into practice. A systematic approach to the design of a drop shaft considering air entraining properties seems to be lacking. Hence, it is attempted to provide the designer with the relevant information, which has been procured from the present study.

8·31 Outline of Method.

The main considerations in the design would be the cost and the permissible air content.

The latter aspect for specific purposes is not fully defined. In the case of a drop shaft feeding directly on to a turbine, the air content should be either nil, or least as possible, but in the instance when a shaft is feeding or to a reservoir or an open channel, the air quantity will not be critical. These two cases would establish the limits of the scale.

The cost is greatly governed by the shaft geometry, type of entry and also by any de-aeration devices adopted.

The effects on the dropshaft and its exit would be common to all types of utilization and is necessary to take into consideration in the design.

In the procedure described, although the effect of length will be mentioned this would be a parameter, which would normally be pre-determined by site conditions.

Though, reference to de-aeration aspects will be dealt with later, mention will be made in this section as to the instances, where they are essential.

8·32 Drop shaft feeding to an Open Conduit.

When an open conduit is fed by a drop shaft the ease with which air rejection takes place, lessens the importance on Entrainment.

Diameter

Dependent on the layout there could be a standing column of water in the shaft, in which case the diameter needs to be so designed to ensure that the Froude Number of the flow is above 1, or less than 0·2.

Entry

The entry into the shaft could be that of a simple diversion arrangement and not necessarily producing spiral or radial motion.

Length

The length of shaft is determined by the site layout, or else maintained as short as possible.

De-aeration

A de-aeration device would not be necessary, because of the efficient air rejection properties in an open conduit.

8·33 Drop shaft feeding a Pressure Tunnel.

A drop shaft feeding a pressure tunnel would consist of a static column of water in the lower portion of the shaft equivalent to the pressure head in the tunnel. At the annular hydraulic jump which would be formed under these circumstances, a large quantity of air rejection would occur, nevertheless the drop shaft has to be so designed that conditions beyond the jump are not undesirable.

Length

Once again this factor may be determined by site conditions. Whether the choice/

the choice of length is available or not, it should be ensured that sufficient length is provided for the maximum pressure head in the tunnel.

Diameter

The shaft diameter should be designed considering constructional costs on the one hand, and the flow regimes desired on the other. The flow regime should be decided on from the immediate exit of the pressure tunnel. If the exit feeds directly on to a turbine, the Initial regime should be preferred, as this would eliminate all or most of the air content; and for other cases the Final regime should be sufficient.

When designing for the Initial regime the value of water discharge should be the maximum. This enables that when the maximum value of the Froude Number (i.e. 0·2) is considered the flow regime does not reach the Transition zone nor the Intermediate regime. (See figure 5·2, for the classification).

If the Final flow regime is selected care should be taken that the minimum water discharge would not be so low as to cause the Froude Number to be less than 1 and thereby cause a gradation, to the Intermediate regime. For cases where the estimation of the minimum flow is not feasible, the Initial regime should be adopted.

Entry

The type of entry into the shaft, under this condition, would depend on the flow regime. If the Initial regime is adopted the most efficient type of entry would be a Radial entry; and if the Final regime/

Final regime is the choice, the entry should provide a spiral motion; since the effect of spiral motion decreases at low discharge (1).

De-aeration

The adoption of a de-aeration device would largely depend on the immediate exit from the pressure tunnel.

8·34 Drop shaft feeding a non-pressure tunnel.

Though complete free fall would take place under normal circumstances, the introduction of a constricted exit from the drop shaft would once again lead to a static water column.

During free fall condition, large cavitational effects could occur at the exit, as the air content under this condition would be very high. The design of the various factors would be discussed seperately for the above two instances.

Free Flow

Length

The length of shaft has a great effect on the air content and should be made as small as possible, wherever a choice of length is available.

Entry

It is vital that the entry produces spiral motion, to ensure the annular layer of water adheres to the shaft sides.

Diameter

Consideration of the fractional air core and the fluctuation of the water discharge should determine the shaft diameter. If the flow of water is steady, a smaller diameter which would produce a small fractional air core should be preferred./

This would ensure the air discharge to be beyond its peak value. Care has to be taken in this procedure, that the water discharge does not decrease as this would cause an increase in the Air Entrainment. This pheonomena is as illustrated in Figures 6·21-6·25.

If the intercepted flow into the shaft fluctuates, a larger diameter would be preferable, so that the peak air discharge is avoided. This would require the construction costs to be checked.

The presence of a constriction at the exit in the form of an orifice or nozzle is often preferred because of the advantage of air rejection at the jump. The procedure to be followed in this instance, with respect to flow regime, would be the same as that for a pressure tunnel being fed. However, the orifice or nozzle sizes would have to be determined by estimating the length of standing column required for the wide range of water discharges. When a constriction of this sort is incorporated, the Intermediate regime of flow would produce large adverse effects at the exit, and therefore should be avoided.

De-aeration

If the drop shaft is feeding under free flow conditions, there is a necessity for a de-aeration device to be adopted as the air content would be high. This may be avoided if provision is made for de-aeration along the tunnel in the form of surge shafts or other means.

8·35 Drop shaft feeding directly on to a Turbine.

When a drop shaft feeds a turbine directly, or provides water to an installation where cavitation damage is of great concern, proper design of the shaft is necessary. This would be an appropriate combination of methods already mentioned.

It would be wise to ensure an Initial regime of flow wherever this is possible or to have an efficient de-aeration device in the case of a free flowing shaft.

8·40 RESEARCH CONSIDERATIONS

The investigations carried out in this present study, yield an analytical approach to the problem of Air Entrainment in Vertical Shafts. Though some of the theories developed have been verified in the present study, there are some yet to be confirmed by further investigations.

For the purpose of developing a semi-empirical relationship for Air Entrainment in the case of a jump being present, the very experimental results have been utilised for this purpose. Verification of the theory needs further experimentaion on larger scales and/or Prototype.

As mentioned earlier in 3·00, the models represent scaled sizes of a proposed drop shaft intake scheme. Hence estimation of prototype performance and correlation with the results of the present study would be useful to the future research worker.

Although the actual mechanism of Air Entrainment has been visualised, it is expected that a more theoretical approach would be valuable in the case of a shaft with a jump. The phenomenon of air bubble/

air bubble and pocket motion had resulted in useful data for the designer and firmer conclusions could be arrived at by a thorough theoretical analysis on this topic.

De-aeration aspects have not been dealt with in this study except in the form of certain recommendations in the preceding section. This is due to the wide scope of investigation it would require. An empirical analysis of the study of a de-aeration chamber consisting of baffles has been conducted (4). Also the application of a Vortex chamber as a de-aeration device has been studied (12). Further investigations into this aspect is worthwile as a panacea for air entrainment seems to be far off in the future.

Although an empirical analysis is present l to predict prototype performances a detailed study on this aspect with an analytical approach would be useful to confirm the results.

8·50 THE AUTHOR'S FINAL COMMENTS

The author feels that the present study has opened up the Theoretical approach to the question of Air Entrainment in Vertical Shafts. Although the actual mechanism of the processes has been elucidated, the verification of some of the analyses will require further investigation, specially on prototype performances.

The Nomogram incorporated in the study offers a useful guide in the prediction of model and prototype performances.

The phenomenon observed in the Air Bubble and Pocket Motion leads to valuable information for the designer of drop shafts.

Finally, the Author feels that the practical application of his findings would produce not only efficient, but economic results in the use of Vertical Shafts with Air Entrainment.

APPENDIX A

REFERENCES

1) Laushey L.M. and Mavis F.T. — Air Entrained by water flowing down Vertical Shafts. Proceedings International Association of Hydraulic Research, 1953.

2) Viparelli M. — Les Courants d'air et d'eau dans les puits verticaux. La Houille Blanche, December, 1961.

3) Kalinske A.A. — Hydraulics of Vertical drain and overflow pipes. University of Iowa Studies in Engineering Bulletion No. 26.

4) Hydraulic Research Station — Plover Cove Water Supply Scheme; Report on Hydraulic Model Investigation of a Typical Dropshaft and De-aeration Chamber, Report No. Ex.264, August 1965.

5) Quick M.C. — The Annular Hydraulic Jump, Civil Engineering Vol. 56, 1961.

6) Ackers P. and Crump E. — The Vortex Drop, Proceedings Institution of Civil Engineers, August, 1960.

7) Dawson and Kalinske A.A. — Report on Hydraulics and Pneumatics of Plumbing Drainage Systems. University of Iowa, Bulletin 10, 1937.

8) Binnie A.M. and Hookings G.A. — Laboratory Experiments on Whirlpools. Proceedings Royal Society, Series A, Vol. 194 (1948).

9) Abramovich G.N. — The Theory of Turbulent Jets, M.I.T. Press.

10) Allen J. — Scale Models in Hydraulic Engineering. Longmans, Green and Co. Ltd.

11) Gibson A.H. — The use of models in Hydraulic Engineering. Trnas. Inst. Water Engineers XXXIV.

12) Allen J., Eastwood W. and Taylor G.A. — Scale Model Experiments on High-Head Siphons and Vortex Chambers connected there to. Proc. I.C.E. September 1953.

13) Allen J. and Hendry A.W. — Report on Hydraulic Investigations for the proposed intakes at Whakapapa and Poutu, and the intakes and dropshafts at Okupata and Taurewa. July, 1968.

14) Peterka A.J. — The effect of Entrained Air on Cavitation Pitting. Proc.I.A.H.R. 1953.

15) Marquenet G. — Entrainement d'air par un Ecoulement en Conduite Verticale. Proc.I.A.H.R. 1953.

16) Davies R. — Cavitation in Real Liquids. Proc. of Symposium held at the General Motors Research Laboratories. Michigan 1962.

17) Webber N.B. Fluid Mechanics for Civil Engineers. Spon's Civil Engineering Series.

18) Chanishvili A.G. Air Entrainment and Vertical downward motion of Aerated Flows. Proc. I.A.H.R. 1959.

19) Haindl K. and Sotorink K.V. Quantity of air drawn into a Hydraulic Jump and its measurement by gamma radiation. Proc.I.A.H.R. 1957.

20) Michels V. and Lovely M. Some prototype observations of air entrained flow. Proc.I.A.H.R. 1953.

21) Kalinske A. and Lovely M. Robertson J. Closed condiut flow in Entrainment of Air in flowing water. Trans. A.M.S.C.E. 1943.

22) Haindl K. Hydraulic Jump in Closed Condiuts. Proc. I.A.H.R. 1957.

23) Allcock H.J. and Jones J.R. The Nomogram. 4th Edition, Pitman.

APPENDIX B

GOVERNMENT OF NEW ZEALAND

MINISTRY OF WORKS

TONGARIRO POWER DEVELOPMENT

HYDRAULIC MODEL INVESTIGATIONS ON OKUPATA AND TAUREWA INTAKES AND DROPSHAFTS

SUMMARY

These investigations were carried out jointly and hence reported seperately in the appendix.

Hydraulic tests were carried out on models incorporating each of the intakes and dropshafts, together with a section of the main free-flowing diversion tunnel into which they discharged, with the object of finding methods of avoiding excessive air entrainment in the main tunnel and/or blow-back up the shafts.

Three types of intake were tested for each site, namely (1) a simple drop at the end of the channel leading water from the degraveller, (2) a circular weir at the end of this channel creating radial flow down the dropshaft and (3) a vortex arrangement at the end of the channel giving a large circumferential velocity to the water descending the shaft. This was repeated with orifices of various diameter at the foot of each of the shafts and in each case the amount of air entrainment was observed.

It was found that the best conditions were obtained at the Okupata Intake with a vortex entry to the top of the shaft and a nozzle at the foot/

the foot creating a column of water in the shaft which provided a cushioning effect upon the falling water and which expelled most of the air entrained down the shaft. On the Taurewa shaft, however, no fixed diameter nozzle was capable of producing similar conditions throughout any appreciable range of river flows and the best overall conditions were achieved by leaving the entry to the main tunnel free and creating radial flow conditions at the top of the shaft.

INTRODUCTION

The purpose of these intakes and drop shafts is to divert water from the Okupata and Taurewa Rivers into Lake Roto Aira. The rivers carry a very high sediment load which is to be removed by degravellers before the diverted flows reach the drop shafts. After spilling from the degraveller each diverted flow passes under a stilling baffle and along an open channel leading to the head of the vertical drop shaft.

Preliminary designs considered three alternative flow-entry conditions at the top of the shafts and the presence or absence of throttling orifices at their junctions with the main diversion tunnel, and at the request of Sir Alexander Gibb and Partners, Consulting Engineers to the New Zealand Ministry of Works, hydraulic model investigations of the proposed intakes and drop shafts were undertaken in the Department of Civil Engineering of the University of Edinburgh between December 1966 and December 1967.

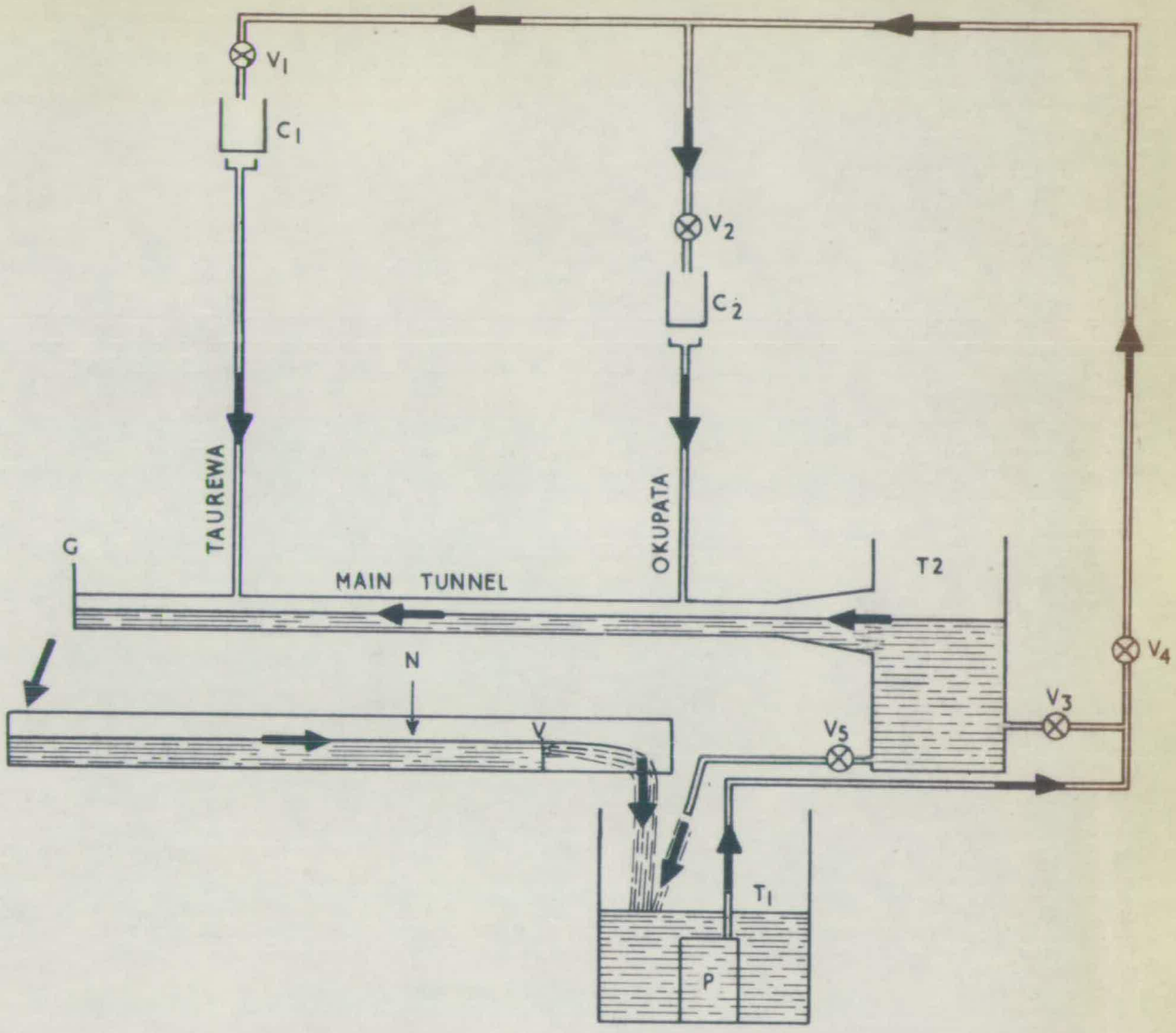

C_1 & C_2 – MEASURING CHAMBERS

V_1 & V_2 – SUPPLY VALVES TO DROPSHAFTS

T_1 – SUMP

T_2 – STILLING TANK

V_3 – SUPPLY VALVES TO TANK T_2

V_4 – CONTROL VALVE FOR DROPSHAFTS

N – NEEDLE GUAGE

G – TAIL GATE

P – PUMP

V – VEE NOTCH

FIG. B.1

TERMS OF REFERENCE

To investigate the performance of the three specified entry conditions to the drop shafts with and without orifices of various diameters at the foot of the shafts and to find means of avoiding excessive air entrainment in the main tunnel and/or blow-back up the shafts.

DESIGN AND CONSTRUCTION OF THE MODEL

The model was designed in accordance with Sir Alexander Gibb and Partners Drawings and was arranged as shown in Figure B·1. To suit laboratory space and the availability of Perspex tubing used to represent the drop shafts and the main tunnel the Okupata Intake and drop shaft were constructed to a scale of 1 : 15·25; the Taurewa Intake and drop shaft to a scale of 1 : 15 and the main tunnel to a scale of 1 : 22·45 resulting from internal tube diameters of 1 $\frac{3}{8}$", 1" and 5$\frac{3}{4}$" respectively.

The water discharge scale in each intake was calculated assuming Froude's Law to be the criterion of similarity as follows:-

Structure	Water Discharge Scale
Okupata intake and drop shaft	1 : $15{\cdot}25^{5/2}$; i.e. 1 : 909
Taurewa	1 : $15^{5/2}$; i.e. 1 : 872
Main Western Diversion Tunnel	1 : $22{\cdot}45^{5/2}$; i.e. 1 : 2388

Throughout the report all dimensions will refer to the full size structures unless otherwise stated.

The concrete work of the intake. was constructed of hardwood and the drop shafts and main tunnel of Perspex. At the intake end of the main tunnel a 4' × 4' × 4' deep metal tank with a converging extension provided smooth entry conditions free from disturbance and/

and air entrainment and an adjustable gate at the downstream end controlled the level in the main tunnel. A valve in a length of pipe between the 4' × 4' × 4'' entry tank and the laboratory sump created a bypass and provided fine adjustment of the flow entering the main tunnel. The water from the main tunnel fell into a tank, containing baffles for energy dissipation, after which it discharged over a calibrated Vee- notch into the laboratory sump.

A suction pump from the sump supplied water to the tank feeding the main tunnel and also to each intake via a cylindrical Perspex measuring tube incorporating several layers of fine wire mesh for tranquil entry conditions, an adjustable constant head overflow device and a calibrated orifice in its base. After falling less than 1" from the orifice the water flowed into the spillway section of the degraveller.

Flows were adjusted by means of valves fitted in the supply and by-pass piping and were measured by noting the heads over the calibrated orifices and the Vee-notch. The relative quantities of air flowing down each shaft were found by means of an uncalibrated vane type aremometer set into a Perspex cylinder of $1\frac{3}{8}$ inches diameter held immediately above the entrance to the shaft.

TEST PROCEDURE - (Figure B·1 refers)

During each test the following procedure was adopted:-

The valve: V_4 was closed and the tail gate G was fully opened: the valve V_5 was fully opened and the needle gauge over the Vee-notch was set to the head corresponding to the total flow required from the main tunnel after which the valve V_5 was half closed. The pump was switche ond and the required flow along the main tunnel/

tunnel was obtained by adjusting valve V_5. The water in the tank T_2 was brought to the required level by balancing the inflow and outflow using valves V_3 and V_5 while the required flow was held constant by continuous checking of the needle gauge measuring the head over the Vee-notch. Further adjustments, if necessary, were carried out by adjusting the tail gate G.

When the required flow in the main tunnel was obtained and the water surface at the mid-point between the drop shafts maintained at the required level, valve V_4 was fully opened. The valves V_1 and V_2 were then adjusted to give the required flows as measured in chambers G_1 and G_2. The uncalibrated vane type anemometer with its extension of 1·375" Perspex pipe was placed just touching the vortex profile and registered a relative measurement of the air entrainment.

Tests were made at maximum diverted flows of 34 cusecs from Okupata and 20 cusecs from Taurewa with flows into the main tunnel of 535, 900 and 1070 cusecs at half, $\frac{3}{4}$ and 99% full depths.

Additional tests were conducted under the above flow conditions with model orifices of diameters 8·5" and $7\frac{5}{8}$" at Okupata, and $3\frac{3}{4}$" - $11\frac{3}{4}$" at $\frac{15}{16}$" intervals at Taurewa.

TEST RESULTS

During the initial tests with no restrictions to the flow at the bottom of the drop shafts a considerable amount of air entrainment was observed in each shaft. Anemometer measurements between shafts and with different entry conditions were:-

Depth of Flow in Main Tunnel	Entry Conditions to Drop Shafts	Relative Air Flow down Drop Shafts. (Volume units/second)	
		Okupata	Taurewa
Full	Free overfall	12·4	28·5
	Radial	15·0	21·2
	Vortex	5·0	29·0
Half full	Free overfall	30·0	30·0
	Radial	24·0	20·5
	Vortex	40·0	36·0

The insertion of nozzles at the junctions of the drop shafts and the main tunnel reduced the air entrainment to less than could be accurately measured by the anemometer, i.e., to less than $\frac{1}{2}$ unit/second, but although the flow down the Okupata shaft was greatly improved, conditions in the Taurewa shaft became very unstable and altogether unsatisfactory with successive volumes of water and air filling the pipe and creating excessive vibration.

At Okupata a nozzle of $7\frac{5}{8}$" diameter created a column of water about 75 feet high which dissipated the energy of the water flowing from above and expelled almost all of the air. The depth of vortex chamber required at the top of the shaft was $4\frac{1}{2}$ feet. No diameter of nozzle however could achieve these conditions at Taurewa; the larger the diameter tested the greater became the lengths of the air pockets entrained with a resulting increase of vibration. To eliminate them entirely required an increase in the depth of the vortex chamber at the top of the shaft to 30 feet.

CONCLUSIONS AND RECOMMENDATIONS

If access for maintenance can be provided to the foot of the Okupata drop shaft then a nozzle $7\frac{5}{8}$" diameter should be provided here and the vortex entry design should be adopted at the top.

In the Taurewa shaft with its very large length: diameter ratio, the radial-entry design with a free exit should be adopted and a steady amount of air entrainment accepted, since any restriction would lead to the danger of instability or choking which would have much more serious consequences.

APPENDIX C

DERIVATION OF EXPRESION FOR VELOCITY - HEIGHT VARIATION FROM EQUATION 2·12 E

$$h = \int_{Vo}^{V} \frac{V dV}{g - ZV^3} \qquad \ldots\ldots\ldots\ldots C1$$

From equation 2·12D

$$\frac{g}{Z} = Vm^3 \qquad \ldots\ldots\ldots\ldots C2$$

$$h = \frac{1}{Z} \int_{Vo}^{V} \frac{V}{Vm^3 - V^3} dV \qquad \ldots\ldots\ldots\ldots C3$$

$$h = \frac{1}{Z} \int_{Vo}^{V} \frac{V dV}{(Vm - V)(Vm^2 + Vm.V + V^2)} \qquad \ldots\ldots\ldots\ldots C4$$

Putting equation C4 into partial fractions

$$h = \frac{1}{Z} \int_{Vo}^{V} \left[\frac{A}{Vm - V} + \frac{BV + C}{Vm^2 + Vm.V + V^2}\right] dV \qquad \ldots\ldots\ldots\ldots C5$$

$$= \frac{1}{Z}\left[\int_{Vo}^{V} \frac{A}{Vm - V} dV + \int_{Vo}^{V} \frac{BV}{Vm^2 + Vm.V + V^2} dV + \int_{Vo}^{V} \frac{C}{Vm^2 + Vm.V + V^2} dV\right] \qquad \ldots\ldots\ldots\ldots C6$$

$$= \frac{1}{Z}\left[\int_{Vo}^{V} \frac{A\, dV}{Vm - V} dV + \int_{V}^{V} \frac{B/2(2V + a)dV}{Vm^2 + Vm.V + V^2} - \int_{Vo}^{V} \frac{Ba/2\, dV}{Vm^2 + Vm.V + V^2} + \int_{Vo}^{V} \frac{C.dV}{Vm^2 + Vm.V + V^2}\right] \qquad \ldots\ldots\ldots\ldots C7$$

$$h = \frac{1}{Z}\left[\int_{Vo}^{V} \frac{A\,dV}{Vm - V} + \int_{Vo}^{V} \frac{B/2(2V + Vm)\,dV}{Vm^2 + Vm.V + V^2} + \int_{Vo}^{V} \frac{(C - Ba/2)\,dV}{(Vm/2 + V)^2 + (\sqrt{3}/2\ V_m)^2}\right] \quad \ldots\ldots\ldots\ldots C8$$

Integrating

$$h = \frac{1}{Z}\left[-A \log_e (Vm - V) + \frac{B}{2} \log_e (V_m^2 + Vm.V + V^2) + (C - B.Vm/2)\frac{2}{\sqrt{3}a} \cdot \tan^{-1} \frac{(Vm/2 + V)}{\frac{\sqrt{3}}{2} Vm}\right]_{Vo}^{V} \quad \ldots\ldots\ldots\ldots C9$$

Since from partial fractions

$$A = \frac{1}{3a} = B \quad \text{and} \quad C = -\frac{1}{3}$$

Substituting

$$h = \frac{1}{6.Z.Vm}\left[-2 \log_e (Vm - V) + \log_e (Vm^2 + Vm.V + V^2)\right]_{Vo}^{V} - \frac{1}{\sqrt{3}.Z.Vm}\left[\tan^{-1} \frac{(Vm/2 + V)}{\sqrt{3}/2 \cdot Vm}\right]_{Vo}^{Vm}$$

$$= \frac{1}{6.Z.Vm}\left[\log_e \frac{(Vm - V)^2 + 3Vm.V}{(Vm - V)^2}\right]_{Vo}^{V} - \frac{1}{\sqrt{3}.Z.Vm}\left[\tan^{-1} \frac{Vm + 2V}{\sqrt{3}.Vm}\right]_{Vo}^{V}$$

Inserting the limits

$$h = \frac{1}{6.Z.Vm}\left[\log_e \left\{1 + \frac{3Vm.V}{(Vm - V)^2}\right\} - \log_e \left\{1 + \frac{3Vm.Vo}{(Vm - Vo)^2}\right\}\right] - \frac{1}{\sqrt{3}.Z.Vm}\left[\arctan \frac{Vm + 2V}{\sqrt{3}.Vm} - \arctan \frac{Vm + 2Vo}{\sqrt{3}.Vm}\right] \quad \ldots\ldots\ldots\ldots C10$$